The power and pitfalls of amino acid carbon stable isotopes for tracing the use and fate of basal resources in food webs

Vane K.[1*] ORCID:0000-0001-8172-7831

Cobain M.R.D.[2,3] ORCID:0000-0003-1701-3986

Larsen T.[4] ORCID:0000-0002-0311-9707

[1] Department for Polar Biological Oceanography, Alfred Wegener Institute for Polar and Marine Research, Bremerhaven, Germany

[2] School of Natural Sciences – Zoology, Trinity College Dublin, the University of Dublin, Ireland

[3] Department of Biological and Environmental Science, University of Jyväskylä, Finland

[4] Department of Archaeology, Max Planck Institute of Geoanthropology, Jena, Germany

* Corresponding author: kim.vane@awi.de

Key words: biotracer; food-web tracing; fingerprints; microbes; patterns; review; spatiotemporal

Abstract

Natural and anthropogenic stressors are spatiotemporally complex, having indirect effects on the composition and biomass of organisms at the base of a food web, and their availability and nutritional quality. Because basal organisms synthesise the biomolecules essential for metazoan growth and survival (i.e. basal resources), understanding the connections between basal resources and consumers across diverse time scales is needed to fully comprehend their impact on food webs. Traditional approaches using bulk stable isotope ratios have provided insight into basal resource use, but lack specificity in identifying multiple basal resources and their transfer through ecosystems. The development of compound-specific stable isotope analyses now allows researchers to trace the trophic transfer of specific biomolecules. This paper provides an overview of the advances and challenges associated with tracing basal resources with carbon stable isotopes in amino acids (δ^{13}C-AA). We develop a conceptual framework for understanding the mechanistic underpinning of δ^{13}C-AA values. Subsequently, formal definitions of associated terminologies that have so far been lacking in the literature are proposed. We empirically highlight the diagnostic ability of the relative offsets between δ^{13}C values of essential amino acids, termed δ^{13}C-EAA patterns. As these offsets remain largely unaltered during trophic transfer and across varying environments, they can be used as fingerprints to trace spatiotemporal shifts in basal resource use within food webs. Given the stable preservation of amino acids in many metazoan tissues, δ^{13}C-EAA fingerprints can provide insights into basal resource use in food webs from geological history through to the contemporary. The added value of non-essential amino acids as metabolic biomarkers are explored and demonstrated in an archaeological context. We provide thorough overviews of the analytical and statistical methodologies involved in making robust inferences in food web studies. The constraints and pitfalls of δ^{13}C-AA data are discussed, such as issues with basal resource specificity, de novo synthesis, and problems with large compilation datasets. Taken together, δ^{13}C-AA values provide a powerful tool for understanding the specific use of basal resources in food webs on various spatiotemporal scales, but careful consideration and characterization of basal resources is necessary to ensure accurate estimations of proportional use.

OVERVIEW

1. Introduction

Food webs are increasingly affected by anthropogenic stressors such as rising CO_2 levels, climate change, biodiversity loss, habitat destruction, and pollution (Hoegh-Guldberg and Bruno 2010, Blanchard et al. 2012, Kędra et al. 2015). These stressors cause a decline in the diversity and biomass of metazoan species within food webs, which in turn threaten the ecosystem services they provide (Verity et al. 2002, Hondorp et al. 2010). Organisms at higher trophic levels rely on a suite of biomolecules - referred to as basal resources - synthesised by primary producers and microbes. Assessing basal resource use across a food web requires careful consideration of intricate spatial and temporal variations (Pauly and Christensen 1995, Bolnick et al. 2003, Moloney et al. 2011, Dall et al. 2012, Raubenheimer et al. 2012, Chidawanyika et al. 2019). Several physiochemical factors determine the timing, location, and magnitude of basal resource production, including natural cycles of environmental phenomena (Eker-Develi et al. 2006, McMeans et al. 2015, Vining et al. 2022). However, anthropogenic stressors can disrupt these cycles and processes leading to far-reaching implications for the dynamics, structure, functioning and stability of food webs (Nakazawa 2015, Svanbäck et al. 2015, Kortsch et al. 2015). Therefore, understanding how different organisms use basal resources across spatiotemporal scales is critical for assessing the vulnerability of species, food webs and entire ecosystems to environmental change.

The primary approach for tracing trophic transfer of carbon from basal organisms involves measuring the relative abundance of carbon stable isotopes within all carbon-containing biomolecules - i.e. bulk - and comparing consumer tissues to their potential basal resources. This is done by measuring the relative abundance of heavy (^{13}C) to light (^{12}C) carbon, normalised to the primary international standard (Vienna Pee Dee Belemnite, VPDB), and expressed as $\delta^{13}C$ per mille (‰) values. In addition to carbon, the isotopic ratios of other elements can provide valuable insights into the ecological and environmental factors influencing the use of basal resources. For instance, the isotope ratios of oxygen can reflect water source and metabolic processes (Soto et al. 2013). Sulphur isotopes can indicate marine versus terrestrial dietary inputs due to the difference in sulphur isotope ratios between marine and terrestrial environments (Yamanaka et al. 2015). Zinc isotopes can provide insights into the nutritional and trophic status of an organism (McCormack et al. 2021), and strontium isotopes can provide information about the geographical origin of food and water, as the ratio of ^{87}Sr to ^{86}Sr varies with geology (Britton et al. 2022). Radiocarbon concentrations (Larsen et al. 2018) and gut content DNA metabarcoding (Casey et al. 2019) can also contribute unique and complementary insights into the use of basal resources. Among

these tracers, $\delta^{13}C$ values are highly suited to trace basal resources because carbon is abundant, ubiquitous, and $\delta^{13}C$ values of basal resources are often habitat or taxon specific. For example, microalgae from benthic and pelagic habitats tend to have distinct $\delta^{13}C$ values (Guiry 2019), and the mode of carbon acquisition, e.g. plants with C_3 and C_4 photosynthetic pathways, likewise result in distinct $\delta^{13}C$ values (O'Leary 1988). However, it is important to note that bulk $\delta^{13}C$ values of basal resource tissues can vary substantially with the environment (Peterson and Fry 1987, Hayes 2001, Tamelander et al. 2009, Casey and Post 2011, Magozzi et al. 2017). This variability can complicate the process of retrospective basal resource reconstruction when isotopic baseline information is unavailable. Moreover, bulk $\delta^{13}C$ values, as only a single tracer, have a limited ability to distinguish between the multitude of basal resources in a given ecosystem. Contributions from microorganisms are frequently underappreciated, largely due to the logistical challenges associated with isolating and sampling them in sufficient quantities from their natural habitats (Casey and Post 2011).

To address the constraints of bulk tissue analysis, researchers increasingly analyse $\delta^{13}C$ values of individual biomolecules (Nielsen et al. 2017, Ruess and Müller-Navarra 2019). However, interpreting $\delta^{13}C$ values of biomolecules is more complex due to many specific biomolecular processes that can cause fractionation and mixing of isotopes. Primary producers and microbes fix (in)organic carbon (e.g., CO_2 or HCO_3^-) into endogenous biomolecules that, once absorbed, can subsequently be incorporated in the tissues of heterotrophs with little or no modification of their carbon skeletons; catabolized for energy; or used in the synthesis of new organic biomolecules (Boecklen et al. 2011). Focusing on individual fatty acids has proven valuable for tracing basal resources to consumers in modern food webs (Burian et al. 2020). Nonetheless, fatty acids are less suitable for past basal resource reconstructions because of their low concentration and degradation in most structural tissues that tend to persist in palaeoecological records (Geigl et al. 2004). Contrastingly, the $\delta^{13}C$ values of the 20 proteinogenic amino acids (AAs) show considerable promise to identify specific basal resources from primary producers to microbial organisms. $\delta^{13}C$-AA values can trace their carbon transfer irrespective of environmental conditions(Larsen et al. 2009, Elliott Smith et al. 2022, Vane et al. 2023). AAs, due to their stability in well-preserved metazoan tissue proteins, serve as powerful spatiotemporal tracers of basal resource use.

Animals can synthesise 11 of the 20 proteinogenic AAs de novo. The non-synthesizable AAs, traditionally termed the essential amino acids (EAAs) (Wu et al. 2014), must be acquired from the diet or supplemented from the gut microflora. For most healthy animals feeding on nutritionally adequate diets the contribution from gut microflora is thought to be minor (Fuller and Reeds, 1998), although such

contributions can play an important role in supplementing the nutrition of detritivores. Since the EAAs are typically routed directly from dietary proteins, their tissue-diet offsets $\delta^{13}C$ values are negligible (McMahon et al. 2010, 2015b, Takizawa et al. 2017, Wang et al. 2019a). For the metazoan-synthesizable AAs (the non-essential amino acids, NEAAs), animals rely both on dietary sources and de novo synthesis. Although NEAAs can be synthesised de novo by animals, almost all of them can be considered conditionally essential, particularly during stages of rapid growth when the rate of utilisation outpaces the rate of synthesis. Regardless of the varying demands for NEAAs across different ontogenetic stages, physiological and metabolic processes in general are constrained without dietary supplementation (Wu 2009, Eisert 2011, Hou et al. 2015).

Lineage-specific pathways and associated carbon fractionation during the synthesis of EAAs in basal organisms contribute to the source diagnostic potential of EAAs to identify and trace basal resource transfer to animal biomass. Broad taxonomic groups such as algae, bacteria, fungi, and vascular plants each have characteristic $\delta^{13}C$-EAA patterns, i.e. the relative differences in $\delta^{13}C$ values among a set of EAAs, that remain largely consistent across variable physical conditions, chemical conditions, and across time (Scott et al. 2006, Larsen et al. 2013, 2015, Lynch et al. 2016, Elliott Smith et al. 2018, 2022, Stahl et al. 2023). Distinct $\delta^{13}C$-EAA patterns among basal organisms have been typically referred to as $\delta^{13}C$-EAA fingerprints (Larsen et al. 2009). Interpreting consumer $\delta^{13}C$ values of the NEAAs ($\delta^{13}C$-NEAA) is more challenging as they can be directly routed from the dietary proteins to consumer tissue or synthesised de novo from various digested dietary macronutrients, i.e., carbohydrates, lipids, and proteins (McMahon et al. 2015b). Despite these caveats, the NEAAs are increasingly used to reconstruct past human diets (Corr et al. 2005, Webb et al. 2017) and understand macronutrient sourcing and routing in aquatic animals (Larsen et al. 2022). AAs, owing to their stability in fossilised materials, like dinosaur eggshells (Zhao et al. 1993) and Pleistocene mollusk shells (Abelson 1954), serve as valuable time capsules. Archives of biogenic carbonates (i.e. coral skeletons, fish otoliths, shells, bones) and other forms of preserved structural tissues hold a vast, yet often untapped potential for retrospective basal resource assessments over thousands of years (Hare et al. 1991, Mora et al. 2018, Tomé et al. 2020, Ma et al. 2021). These assessments could be achieved with $\delta^{13}C$-EAA fingerprints due to their apparent spatiotemporal stability. However, methodological and post-analysis approaches for using $\delta^{13}C$-AA values to estimate basal resource utilisation are diverse and lack standard protocols. Additionally, the use of terminology since the introduction of the concepts of $\delta^{13}C$ patterns and fingerprints over 15 years ago (Scott et al. 2006, Larsen et al. 2009) has been inconsistently applied throughout the literature.

In this review, we provide an in-depth synthesis of the diverse aspects of inferring basal resource AA use by metazoans via the application of carbon isotopes in AAs. While the focus primarily lies on the EAAs, the added value of NEAAs is also explored. We conceptualise AA biosynthesis pathways in basal organisms that determine their respective δ^{13}C-AA values, and explicitly define associated terminology. A glossary of terminology commonly used throughout this review is provided in Table 1. Literature data are compiled from ecological and archaeological studies to explore the extent to which δ^{13}C-EAA patterns can consistently discriminate specific basal resources, the potential mechanisms underlying these patterns, and how δ^{13}C-EAA fingerprints can be characterised. Tilting to a consumer perspective, we detail ways that δ^{13}C-EAA fingerprints can be applied to assess EAA sourcing from pure basal resource origins. Acknowledging the limitations of δ^{13}C-EAA fingerprints, we suggest the inclusion of δ^{13}C-NEAA values alongside baseline δ^{13}C-EAA values in inferring resource use. We also outline the time scales that are represented by different archival faunal tissues, and how their δ^{13}C-AA values are best preserved. As reliable measurements of δ^{13}C-AA values are paramount, we highlight best methodological practices and analytical protocols. We elaborate on the quantitative analyses of δ^{13}C-EAA data used to estimate proportional basal resource use by consumers. Finally, we outline the current application of AA carbon isotopes in food web studies, and contemplate future directions for this field. This review serves as a comprehensive, step-by-step guide on the use of δ^{13}C-AA data, covering everything from sampling and analysis to interpretation. The review aims to support the growing use of this method for tracing EAA flow from basal resources through food webs.

Table 1. Glossary of terms

Term	Definition
Amino acid (AA)	The 20 proteinogenic amino acids
Amino acid carbon skeletons	The core structure of the molecule that remains after the amine (-NH_2) and carboxyl (-COOH) groups, which define the molecule as an amino acid, are removed
Analytical accuracy	The absence of bias in measurements of δ^{13}C-AA values, achieved through calibration to a reference value (section 7.2)
Analytical precision	Consistent measurements of δ^{13}C-AA values over extended time periods on an analytical instrument (section 7.2)

Analytical uncertainty	The variation in individual δ^{13}C-AA values measured in an AA standard during the entire analytical period in which the studied tissue samples are measured, typically reported as standard deviations (section 8.1)
Basal organisms	Primary producers and microbes that have the ability to synthesise suites of biomolecules de novo from externally sourced, simple (in)organic carbon. They are considered to be the base of food webs (section 2.1)
Basal resources	The suites of biomolecules (focusing on the suite of AAs in this review) synthesised de novo by specific basal organisms that are assimilated by consumers as a whole or for components in constructing their own biomass (proteins etc., section 4)
Baseline δ^{13}C-(E)AA values	The measured δ^{13}C values of basal organism tissue (E)AAs that are formed by a combination of external and internal physiochemical processes. These processes include initial δ^{13}C values of external carbon sources (and drivers thereof), internal fractionation by acquisition modes, and individual AA biosynthetic pathways (section 2.1 and Fig. 1). Baseline δ^{13}C-AA values can be produced in natural environments as well as artificial laboratory settings (such as in laboratory controlled cultivation environments), however, only natural baseline δ^{13}C-AA values can be directly used in food web analyses. Defined from a consumer perspective, only EAAs are used for tracing basal resources in a food web as they cannot be synthesised de novo by consumers and have negligible trophic fractionation (see TDF, section 3 intro)
Diazotroph	Bacteria or archaea that are able to fix nitrogen gas (N_2) into biologically more usable forms, e.g. ammonium (NH_4^+, section 3.1)
Essential Amino Acid (EAA)	The nine amino acids (leucine, isoleucine, valine, phenylalanine, threonine, lysine, methionine, tryptophan, and histidine) that cannot be synthesised de novo by metazoans, or consumers in a food web
Error propagation	The enlargement of deviations in measured δ^{13}C-AA values due to errors introduced into analytical processes (section 7.2)
Facultative EAA prototrophs	Organisms that utilise organic carbon sources for biomolecular building blocks to synthesise EAAs de novo, but may also assimilate EAAs from external sources for normal metabolic functioning (section 3.2)
Isotopologues	Molecules with the same chemical formula and bonding arrangement of atoms, but at least one atom has a different number of neutrons than the parent: the same molecule with a different isotopic composition and/or arrangement
Measured δ^{13}C-AA values	The δ^{13}C-AA values that are physically quantified in a sample
Obligate EAA prototrophs	Autotrophs that synthesise the EAAs they need solely from simple inorganic carbon sources through photo- or chemosynthesis (section 3.2)

Retrospective basal resource reconstruction	The estimation of the proportions of basal resources synthesised by specific basal organism groups or clades that are assimilated into consumer tissues during their unique turnover or incorporation periods. As AAs are conserved in well-preserved consumer tissue remains, these estimations can extend over geological, archaeological and historical timescales, complementing contemporary retrospective reconstructions.
Training data set	A compilation of δ^{13}C-EAA values, previously measured external to the current study, to characterise basal resources in a study system (section 4.1)
Trophic Discrimination Factor (TDF)	The isotopic offset between a consumer tissue and the assimilated diet, accounting for the summation of isotopic fractionations of atoms across the various metabolic processes from digestion and uptake through to tissue synthesis. Although typically constrained, TDFs can vary by consumer species, consumer tissue type, physiological status, diet quality, element (e.g. carbon or nitrogen), and biomolecule (for compound-specific isotope analyses)
Under-determined mixing system	A system with a multitude of potential basal resources that can be combined in various proportions yet still result in the same δ^{13}C-EAA patterns (section 8.1). Mathematically, this occurs when the number of basal resources is greater than the number of tracers (data dimensionality: here, number of EAAs) plus one
δ^{13}C-AA data	The overarching term pertaining to measured δ^{13}C-AA values, baseline δ^{13}C-(E)AA values, δ^{13}C-(E)AA patterns and δ^{13}C-EAA fingerprints, and/or δ^{13}C-NEAA values
δ^{13}C-EAA fingerprint	The minimum δ^{13}C-EAA pattern space that is solely occupied by a group or collection of similar basal resource organisms and encompasses the intragroup variability in δ^{13}C-EAA patterns expressed by those organisms (section 3.3)
δ^{13}C-(E)AA pattern	The relative offsets between individual δ^{13}C-(E)AA values in a sample, extracted by centring individual values to the within non-weighted sample mean of measured δ^{13}C-(E)AA values. For basal resources, this can be done for all AAs measured, but is restricted to EAAs for food web studies (section 3). As basal resource δ^{13}C-(E)AA patterns are relatively consistent, they can also be obtained from artificial baseline δ^{13}C-AA values obtained from basal organisms in cultivation. For consumer organisms, the pattern is restricted to centring the set of EAAs only as these are directly routed from the diet with little modification (section 4.1)

2. Factors shaping amino acid δ^{13}C values in basal resources

Organisms can be classified based on their AA metabolism: those that can synthesise all proteinogenic AAs de novo, and those that cannot. The majority of basal organisms are autotrophic and rely on photosynthesis or chemosynthesis to fix inorganic carbon into biomolecules such as amino acids, organic

acids, saccharides, and lipids (i.e. basal resources). However, some basal organisms, such as heterotrophic bacteria and fungi, can harness organic carbon sources for chemical energy and simple biomolecular building blocks. The synthesis of all AAs de novo in basal organisms, regardless of the energy source and mode of carbon acquisition, involves numerous biochemical reactions and movements of molecules that alter the distribution of ^{13}C and ^{12}C. Mass-dependent kinetic isotope fractionations (KIFs) associated with these processes result in stepwise changes in relative isotopic ratios as either lighter or heavier carbon atoms diffuse passively, are actively transported, or react in anabolic and catabolic processes at different rates (Box 1, Fry 2006). The isotopic composition of AAs in basal resource tissues therefore reflects the summation of all stepwise fractionations from the isotopic composition of the initial carbon pool. Here, we conceptualise these mechanisms of AA de novo synthesis on a cellular level for basal organisms and address how biochemical pathways affect the ratios of heavy to light carbon atoms in AA carbon skeletons. In doing so, we propose explicit definitions for $\delta^{13}C$-AA terminology.

2.1. Conceptualising amino acid $\delta^{13}C$ values

The pathways from external sources of (in)organic carbon in the environment to intracellular AA synthesis can be generalised into two broad categories. The first is the collection of processes involved in the uptake and conversion of external carbon to internal pools of common precursor molecules, which we refer to as carbon acquisition. The second is the collection of biochemical reactions, or the biochemical network, which synthesises the specific AAs from the precursor metabolites (Fig. 1). Synthesis pathways among AAs are unique, and therefore comprise different summations of kinetic isotope fractionations (Appendix S1: Figure S1A-B). This contrasts with carbon acquisition where, generally, total isotopic fractionation will be reflected equally across all AAs due to the common pool of carbon. The combined effects of carbon acquisition and AA synthesis will fractionate the stable isotopes of the initial external carbon. Basal organisms can use various forms of external carbon sources, each of which will have its own inherent carbon isotope composition. Rates of diffusion, transport, and chemical reactions depend on various environmental factors, which will cause the isotopic fractionation during carbon acquisition to vary. Furthermore, as the isotopic composition of external carbon sources will also depend on various kinetic processes, the external carbon isotope composition will also vary with

environmental conditions. Taken together, the $\delta^{13}C$ value of an AA in basal resources can therefore be broadly formulated as:

$$\delta^{13}C_{AA} \sim \delta^{13}C_{Ext.} + Env. \times Ext. + Acq. + Env. \times Acq. + Synth_{AA} \quad [1]$$

Where $\delta^{13}C_{AA}$ is given by the $\delta^{13}C$ value of the external carbon source, *Ext.*; plus any modifications to this value due to environmental effects, *Env.,* dependent on the nature of the external carbon source; plus the summed fractionations associated with carbon acquisition, *Acq.*; plus any modifications due to environmental effects on the physiology associated with carbon acquisition fractionation; plus the summed fractionation associated with synthesis pathway, *Synth.,* which is AA specific (visualised in Fig. 1). While environmental gradients may also specifically modify the fractionations associated with each AA synthesis pathway, these relative differences will likely be very small compared to the overall average effect of the environment on physiology, and therefore carbon acquisition (Stahl et al. 2023, Larsen et al. 2015, Fig. 2), represented here as *Env.* x *Acq.*

From [1], the measured $\delta^{13}C$ values of AAs in basal organisms depend upon the carbon source, the environment and their phylogeny (via their fixation and synthesis pathways, see section 2.2. below). This aligns with the concept of multiple isotopic baselines in bulk stable isotope approaches, that characterise the base of the food web contextualised with in situ environmental conditions for different production sources (e.g. Docmac et al. 2017, Søreide et al. 2006). We therefore define measured $\delta^{13}C$-AA values in basal organisms as baseline $\delta^{13}C$-AA values.

If we consider the fractionations attributable to AA biosynthesis only as relative differences (i.e. $Synth_{AA}$ averages to zero) then they can be regarded as a relative ordination centred on their mean value. We denote this relative ordination of $Synth_{AA}$ specifically as *(1|AA)* as in Fig. 1. Conceptually, this means any non-zero average fractionation across AA biosynthesis pathways will be incorporated as part of the acquisition term. This has the advantage however that we can now consider the collection of AA biosynthesis fractionations as a relative ordination that is imposed onto an average baseline bulk (protein) stable isotope value within the basal resource:

$$Average\ \delta^{13}C_{AA} = \frac{1}{n}\sum_{i=1}^{n} \delta^{13}C_{AA} \sim \delta^{13}C_{Ext.} + Env. \times Ext. + Acq. + Env. \times Acq. \quad [2]$$

where *n* is the number of AAs. It follows that the ordination can be determined as:

$$(1|AA) \;=\; Baseline\;\delta^{13}C_{AA} \;-\; Average\;\delta^{13}C_{AA} \;=\; \delta^{13}C_{AA} \;-\; \frac{1}{n}\sum_{i=1}^{n}\;\delta^{13}C_{AA} \qquad [3]$$

In this equation, the offset for each AA is simply the mean-centred δ^{13}C-AA value (the non-weighted, within-sample average δ^{13}C-AA value) subtracted from individual baseline δ^{13}C-AA values of the basal organism, which we define as the $\delta^{13}C_{AA}$ pattern. Expressing δ^{13}C-AA patterns via mean-centring has been the standard approach introduced by Larsen et al. (2009, denoted as $\delta^{13}C_{N}$). However, an important constraint in this method is that changes in the suite of AAs considered will result in changes in the absolute, although not the relative, offsets in the expressed δ^{13}C-AA pattern. Therefore for direct comparisons between datasets, the same suite of measured AAs is required. Recentring to the within-sample mean is not the only way to represent the δ^{13}C-AA pattern: the ordination can also be expressed, for example, by centring data to the δ^{13}C value of one specified AA. However, centring data to only a single AA will mean the expressed δ^{13}C-AA pattern will be sensitive to variations in that particular AA (e.g., analytical deviations and natural variations in fractionation).

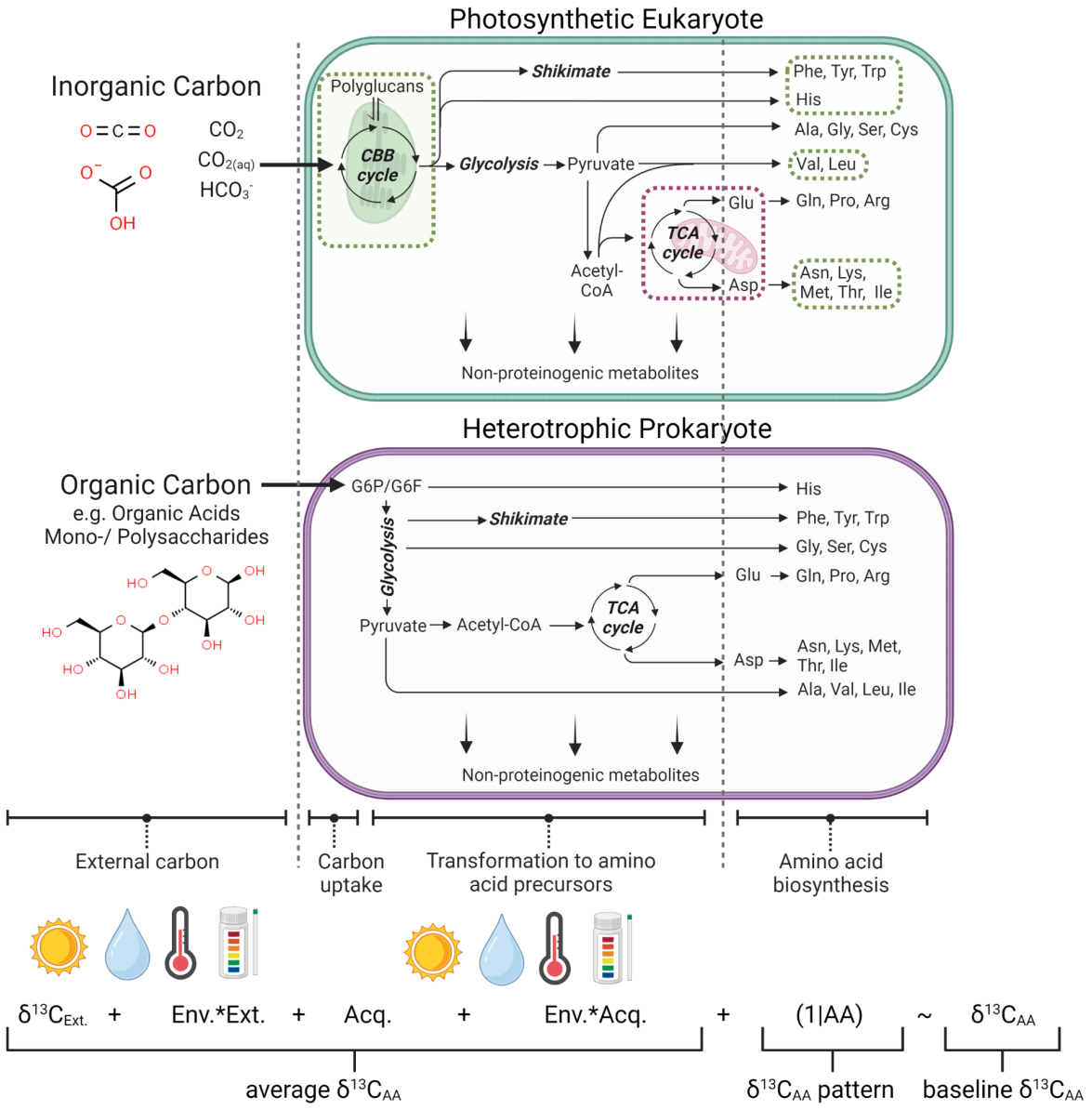

Figure 1. Schematic representation of the sources, processes, and environmental effects that contribute to the $\delta^{13}C$ values of AAs in photosynthetic eukaryotes and heterotrophic prokaryotes. In this paper, AA production from these basal organisms are denoted as basal resources. Within the eukaryotic cell, membrane bound organelles are signified by rectangles with dashed lines: the rounded red rectangle signifies the mitochondrion, and the green rectangles signify plastids including the chloroplast. The remaining cell lumen is the cytosol. The metabolic pathways are summarised based on Chen et al. (2018), and Gupta and Gupta (2021). Detailed metabolic networks are provided in Figs. S1A-B. Abbreviations: Ala, alanine; Asn, asparagine; Asp, Asparagine; CBB, Calvin-Benson-Bassham; Cys, cysteine; F6P, Fructose-6 phosphate; G6P, Glucose-6 phosphate; Gly, glycine; Gln, glutamine; Glu, glutamic acid; His, histidine; Ile, isoleucine; Leu. leucine, Lys, lysine; Met, methionine; Phe,

phenylalanine; Pro, proline; Ser, serine; TCA, Tricarboxylic acid; Trp, tryptophan; Tyr, tyrosine; Val, valine. The illustration was created with BioRender.com.

2.2. Isotope fractionation in metabolic networks

As outlined above, measured δ^{13}C-AA values of basal resources will be broadly determined by external carbon sources and their acquisition, mixing and isotopic fractionation of carbon isotopes in precursor molecules, and AA biosynthesis pathways (Fig. 1). Many of these different processes and reaction steps are highlighted in Box 1, which shows a hypothetical biochemical network where reactants and products are continuously added, removed, and isotopically altered due to unidirectional KIFs. During biochemical reactions and transport, resultant δ^{13}C values of biomolecules are determined by two factors. The first is the flow rates (*f*) of reactant replenishment and product removal. The second is the kinetic isotopic effect (ε), where the fractionation factor is equal to the ratio of the isotope-specific rate constants. While real-world biochemical networks are far more complex than the schematic representation in Box 1, appreciation of the broad mechanisms determining δ^{13}C-AA values can help to develop testable hypotheses and elucidate the potential of δ^{13}C-AA patterns for identifying basal resources.

On a cellular level, ε is associated with differing enzyme and protein structures that modulate the various biochemical reactions and facilitate active and passive transport of metabolites in and out of the cell. Therefore, carbon fractionation along AA biosynthetic pathways should vary among major phylogenetic lineages because different synthesis pathways have evolved to fulfil unique metabolic needs. These different pathways will be modulated by different enzymes resulting in variable cumulative fractionations. Generally, the most biochemically expensive AA pathways involving multiple biosynthetic steps are expected to be evolutionarily conserved. For example, tryptophane, which is one of the most biochemically complex AAs, involves homologous enzymes across the three domains of life (KEGG PATHWAY 2013). In contrast, the comparatively simpler lysine has two different anabolic routes. One is the diaminopimelic acid pathway used by algae, plants, most bacteria, and some fungi and archaea, and the other is the α-aminoadipic acid pathway used by most fungi, some algae and archaea (Velasco et al. 2002). AAs with lineage-specific anabolic routes such as lysine are more likely to be informative of biosynthetic origins (Larsen et al. 2009). Interestingly however, even if AA biosynthetic pathways have similar steps across phylogenetic lineages, fractionations may still change due to modifications of the enzymes and metabolic branching points involved.

Asynchronous flow rates (*f*) of metabolites can also lead to fluctuating $\delta^{13}C$ values of AAs. In Box 1, this is highlighted by the two chemically similar branched pathway reactions. One reaction occurs within the original cell while the other takes place outside the cell following reactant transport. Similarly, internal compartmentalization within eukaryotic cells may result in separate pools of reactants with different $\delta^{13}C$ values (Hayes 2001). Proteinogenic AAs, as well as being used to build proteins, have multiple non-proteinogenic roles. These include precursors for lineage-specific signalling molecules, energy-yielding substrates, and metabolites that are also likely to affect carbon fractionation (Appendix S1: Figure S1A-C). Significant systematic differences in flow rates across phylogeny due to varying metabolic demands of AAs (or intermediates in their synthesis pathways) in basal organisms may therefore result in different fractionations during AA biosynthesis. Some metabolic pathways are lineage specific. For example, the synthesis of alkaloids, a group of compounds found almost exclusively in terrestrial plants, relies on several nitrogenous precursors such as phenylalanine, lysine, and histidine (Aniszewski 2007). In comparison, algae have very low concentrations of flavonoids and alkaloids (Davies et al. 2020, Güven et al. 2010). Biosynthesis of phenylpropanoids, which serve as the backbone of lignan and flavonoid biosynthesis in land plants, uses phenylalanine as a precursor while lignin cannot be synthesised by algae except some Rhodophyta (red algae) (Martone et al. 2009). Macroalgae, including Rhodophyta, Chlorophyta (green algae) and Ochrophyta (class Phaeophyceae, brown algae), produce a range of compounds not found in land plants. Examples are the mycosporine-like amino acids that, like the aromatic AAs phenylalanine and tyrosine, are biosynthesised in the shikimate pathway (Llewellyn et al. 2020). A range of microorganisms from heterotrophic bacteria and cyanobacteria to fungi also produce these mycosporine-like amino acids (Geraldes and Pinto 2021). Bacteria possess a pure monomeric protein array covering their surface, the S-layer, often involving dedicated secretion systems, that may also represent significant downstream demands of particular AAs, altering synthesis flow rates (Silhavy et al. 2010, Fagan and Fairweather 2014).

The relative importance of enzyme mediated KIFs compared to differential flow rates in AA biosynthesis pathways in underpinning $\delta^{13}C$-AA values, and therefore basal resource $\delta^{13}C$-AA patterns, is currently unclear. While it may seem initially that ε will heavily constrain $\delta^{13}C$-AA patterns due to genetic limitations, large differences in flow rates due to varying down-stream demands of AAs could potentially explain the majority of variation in $\delta^{13}C$-AA patterns. The $\delta^{13}C$-AA patterns should therefore reflect both genetic constraints and phenotypic expressions. Therefore, $\delta^{13}C$-AA patterns have the potential of high specificity across the diversity of basal organisms inhabiting varying environments. Baseline $\delta^{13}C$-AA values will not only reflect the drivers of $\delta^{13}C$-AA patterns, but also impose the variability due to the

environment and its interactions with biology on the distribution of heavy to light carbon isotopes in AAs.

Box 1 Isotopic mixing and fractionation

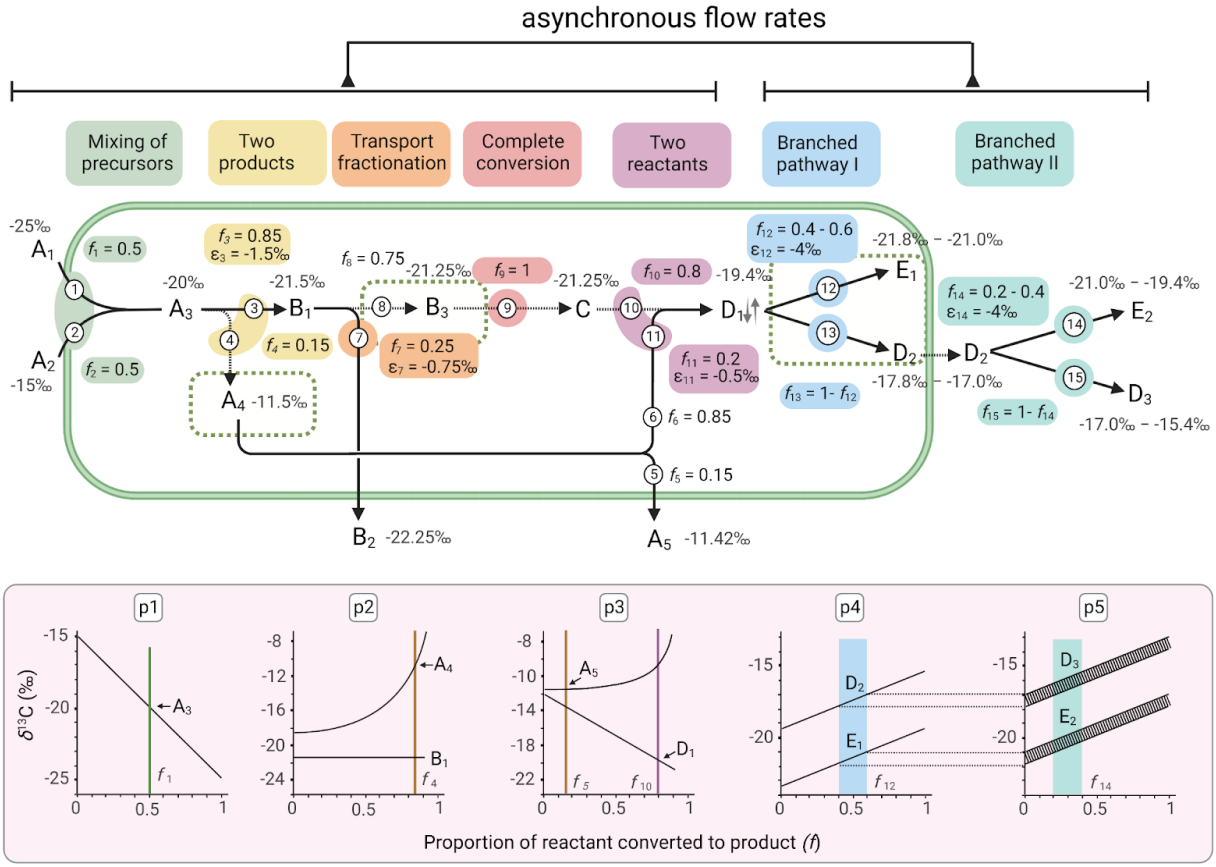

Simplified model of isotopic mixing and fractionation in a series of hypothetical reactions in a eukaryotic cell with organelles (rounded rectangles with broken line borders). Capital letters signify particular compounds, and the subscript numbers indicate compound subpools. Movement and reaction of compounds are indicated by numbered arrows, with broken line arrows indicating that there were no isotopic effects associated with the reaction or movement. In the line plots, stable isotope values of carbon ($\delta^{13}C$) are shown as a function of the relative flow (f_x) of a transfer or reaction and associated fractionation (ε_x). Subplots below their associated reaction step highlight how changing flow rates will influence the resultant $\delta^{13}C$ values, with vertical lines and columns indicating the flow rates indicated in the main plot. The first products to enter the hypothetical biochemical network are the two isotopologues A_1 and A_2 (molecules that differ only in their isotopic composition) that mix to form the isotopologue A_3, whose $\delta^{13}C$ value is determined by the relative proportion of A_1 and A_2 (p1). A_3, is then

converted to B_1 in a reaction that fractionates against the heavier isotope by 1.5‰. To maintain mass balance, the remaining A_3 that is transported to another cell compartment is enriched by 8.5‰. The greater the flow rate from A_3 to B_1 the greater the ^{13}C enrichment of A_4 (p2). The final fate of isotopologue A_4 is twofold: One fraction is converted into product D_1 and the other fraction, A_5, is transported out of the cell. Although there is no transport fractionation here, A_5 becomes slightly depleted relative to A_4 because the reaction that uses A_4 to form D_1 fractionates against the heavier isotope (p3). In some cases, physical transport is associated with isotope effects as illustrated by the transport of intracellular B_1 to extracellular B_2. In the case of passive transport, fractionation is caused by mass dependent diffusion, while fractionation during active transport can be caused by cell membrane transporters. Here, transport of B_1 to extracellular B_2 fractionates against the heavier isotope by 0.75‰. When there is a complete conversion of a reactant to a product, in this case B_3 to C, the isotope composition of both reactant and product must match each other. Varying metabolic flux patterns (i.e. reactions are not maintained at steady state) will result in shifts in the isotopic values of both reactants and products. The dynamic flux patterns for the pathways on the left (reactions 1-11) and right (reactions 12-15) sides differ from one another resulting in the D_1 pool expanding and contracting. In the downstream branched pathway I with D_1 as a precursor, the isotopic values of E_1 and the residual pool D_2 are affected by varying flow rates and isotopic fractionation associated with reaction 12 (p4). When the residual pool D_2 is transported out of the cell, it becomes a precursor for similar reactions to that of the previous branched pathway. In this hypothetical example, the isotopologues E_2 and D_3 are more ^{13}C enriched compared to E_1 and D_2 respectively, because of the isotopic fractionation associated with reaction 12 (p4 & p5). The illustration was inspired by Hayes (2001) and Hobbie and Werner (2004), and created with BioRender.com.

3. Discriminating basal resources with $\delta^{13}C$-EAA fingerprints

The use of basal resources by metazoans in a food web is most reliably traced with the EAAs because they cannot be biosynthesised de novo by metazoans. The nine canonical EAAs (leucine, isoleucine, valine, phenylalanine, threonine, lysine, methionine, tryptophan, and histidine) are valuable indicators of the basal resources that sustain a food web because the measured $\delta^{13}C$-EAA values in consumer tissues reflect those of the basal resources, as the carbon skeletons of EAAs are conserved through trophic transfers (McMahon et al. 2010, 2015b, Liu et al. 2018, Wang et al. 2019a). By mean-centring the baseline $\delta^{13}C$-EAA values in basal organisms, we obtain consistent $\delta^{13}C$-EAA patterns that can be traced into the food web (Fig. 2). The ability to trace and distinguish basal resources using $\delta^{13}C$-EAA patterns is dependent on measuring the same group of EAAs in both the basal resource and the metazoan tissues. However, there are analytical limitations such as sample amount, protein content, relative EAA

composition, retrieval from tissues (in case of tryptophan degradation during acid hydrolysis), and detection limits that impose barriers on the number of δ^{13}C-EAA values that can be measured for a given tissue sample. It is advisable to measure as many EAAs as possible because it increases the potential discriminatory power of δ^{13}C-EAA patterns. Initially, unique and consistent basal resource δ^{13}C-EAA patterns for a given large taxonomic grouping (bacteria, plant, microalgae) that were distinct from another were termed a δ^{13}C-EAA fingerprint (Fig. 3, Larsen et al. 2009). More than a decade after the term δ^{13}C-EAA fingerprint was introduced by Larsen et al. (2009), the specificity and sensitivity of δ^{13}C-EAA fingerprints separating basal resources at different taxonomic levels remains largely unknown. In this section, we collate published δ^{13}C-EAA data of basal resources to investigate how δ^{13}C-EAA patterns can help us identify basal resources. We further reflect on the possible underlying mechanisms that cause δ^{13}C-EAA patterns, building on our conceptualisation in section 2, i.e. fractionation associated with EAA biosynthesis versus their down-stream demand in metabolic networks (Appendix S1: Figure S1A-B). Lastly, we refine the definition of what constitutes δ^{13}C-EAA fingerprints, and discuss the optimal characterisation of δ^{13}C-EAA patterns.

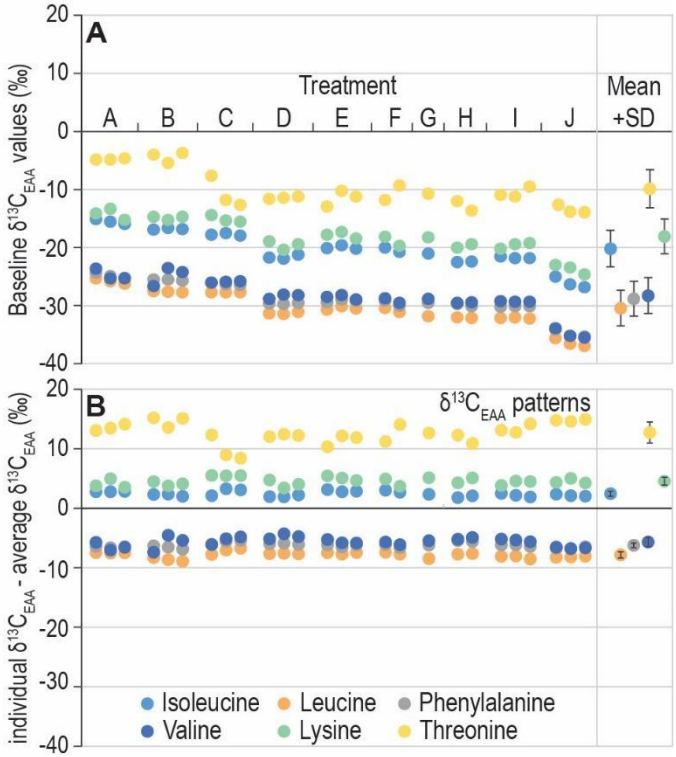

Figure 2. Example of baseline δ^{13}C-EAA values (A) of isoleucine, valine, leucine, lysine, phenylalanine, and threonine in marine diatom *Thalassiosira weissflogii* cultured under different physical conditions by Larsen et al. (2015). By mean-centring the baseline δ^{13}C values within a sample, the δ^{13}C-EAA patterns are obtained (B). Different

treatments used were A) 27°C, B) 18°C, C) High pH, D) Control, E) UV filter, F) No UV filter, G) Low irradiance, H) High irradiance, I) Low pH, J) Low salinity. The mean and standard deviation (SD) of all individual δ^{13}C-EAA values (baseline and mean-centred) are given in the right hand box to indicate their variation in baseline δ^{13}C-EAA values and δ^{13}C-EAA patterns.

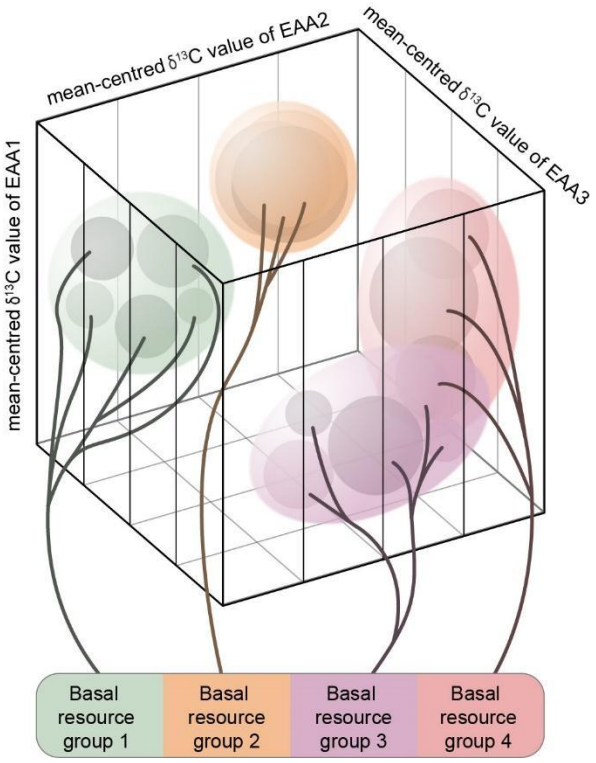

Figure 3. A schematic illustration of the discrimination in basal resources with the δ^{13}C-EAA fingerprint concept. Basal resources are separated into defined groups a priori, typically based on the phylogenetic relatedness and/or the ecological functioning of the measured basal organisms within the studied ecosystem. Mean-centred δ^{13}C values of EAAs define the δ^{13}C-EAA pattern space of the basal resources, with dimensions equal to the number of EAAs (3 shown for illustrative purposes). A basal resource group is considered to have a δ^{13}C-EAA fingerprint when that group solely occupies its δ^{13}C-EAA pattern space, e.g. basal resource groups 1 and 2. The specificity of the δ^{13}C-EAA fingerprint can be high if subgroups of the basal resource (illustrated by branches) occupy unique spaces within their overall basal resource group fingerprint, demonstrated by basal resource group 1. Conversely, the δ^{13}C-EAA fingerprint is considered unique only for the group as a whole if subgroups show overlap within the δ^{13}C-EAA pattern space that they occupy, e.g. basal resource group 2. δ^{13}C-EAA patterns cannot be considered δ^{13}C-EAA fingerprints if basal resource groups exhibit overlap in the δ^{13}C-EAA pattern space that they occupy, as shown by basal resource groups 3 and 4.

3.1. The diagnostic potential of δ^{13}C-EAA patterns among basal resources

By shedding light on the mechanisms that underlie variations in δ^{13}C-EAA patterns, we can gain a better understanding of how to characterise basal resources in specific ecosystems. Here, we evaluate the diagnostic potential of basal resource δ^{13}C-EAA patterns by compiling δ^{13}C-EAA values of isoleucine, leucine, phenylalanine, threonine, and valine measured in 20 ecological and archaeological studies (Fig. 4A-D, see Appendix S2 for compilation criteria). Using linear discriminant analysis (LDA), we explore the ability of δ^{13}C-EAA patterns to distinguish among and within large taxonomic groupings based on previously observed distinctions and their co-occurrence in ecosystems relevant to consumers. It is worth noting that currently, there is no correction for interlaboratory differences of measured δ^{13}C-EAA values. However, our analyses demonstrate that δ^{13}C-EAA patterns can broadly distinguish among heterotrophic bacteria, eukaryotic phytoplankton, and terrestrial plants across ecosystems. The overlap between bacteria and plants is the smallest with a median overlap of 0.08, while the overlap between bacteria and phytoplankton is the greatest with a median overlap of 0.38 (Fig. 4A). Additionally, there are distinguishable patterns among other broad groups, such as fungi versus phytoplankton (median overlap of 0.23; Fig. S2B). Discrimination between heterotrophic bacteria and macrophytes is relatively weak due to the extensive variability that exists in the δ^{13}C-EAA patterns within each of these groups (median overlap of 0.49; Appendix S2: Figure S2C). Within phytoplankton, we observe separation between freshwater and marine phytoplankton (median overlap of 0.36, Fig. 4B) that span two kingdoms, Chromista and Plantae. Within the monophyletic group cyanobacteria, δ^{13}C-EAA patterns are much more variable for diazotrophic species (those that can fix nitrogen), compared to non-diazotrophic cyanobacteria, whose δ^{13}C-EAA patterns occupy only a small subset of the cyanobacteria δ^{13}C-EAA pattern space (Fig. 4B, McMahon et al. 2015). Within aquatic macrophytes, observed differences in δ^{13}C-EAA patterns can be linked to phylogenetic clades (Fig. 4C). Seagrasses (Plantae phylum Tracheophyta) showed minimal overlap with the three macroalgal clades (median overlaps of 0.12, 0.23 and 0.06 with brown, red and green algae respectively). While brown macroalgae (Phaeophyta in the Chromista kingdom) and red macroalgae (Plantae phylum Rhodophyta) also appear to separate (median overlap 0.35), green macroalgae (Plantae phylum Chlorophyta) occupy the overlapping intermediate δ^{13}C-EAA pattern space between the two (median overlaps of 0.52 and 0.68 respectively; Fig. 4C). The δ^{13}C-EAA patterns of the monophyletic red macroalgae (Plantae phylum Rhodophyta) express greater intragroup variation compared to other macrophyte groups (Fig. 4C). This increased variation could be

attributed to the larger species diversity in the data compilation for Rhodophytes. Land plant δ^{13}C-EAA patterns (Plantae phylum Tracheophyta) do not discriminate on their C_3 or C_4 photosynthetic carbon fixation systems (median overlap of 0.91, Fig. 4D). However, limited observations suggest potential separation for CAM plants, here solely represented by two cacti species, *Cylindropuntia* sp. and *Opuntia* sp., from a single study (median overlaps of 0.32 and 0.25 with C3 and C4 plants respectively, Fig. 4D). This is unexpected as CAM physiology affects only the carbon acquisition, and therefore conceptually should only influence the baseline δ^{13}C-EAA values, not the carbon fractionation during AA biosynthetic pathways (section 2). Yet, we also observe that some individual C_3 plants express similar patterns to those of the CAM species (Fig. 4D). Further multivariate modelling of vascular plant δ^{13}C-EAA data reveals that, overall, approximately 50% of the variation in δ^{13}C-EAA patterns can be attributed to phylogeny (Appendix S3: Figure S3A-B) and further, the cacti CAM plants closely align with two other arid adapted C_3 plant (sub)families, Agavoideae and Zygophyllaceae (represented by *Yucca elata* and *Larrea tridentata* respectively, see S3 for details). In some studies, even finer distinctions in δ^{13}C-EAA pattern distinctions have been observed between organs of individual plants, i.e. roots, seeds, and leaves (Lynch et al. 2011, Larsen et al. 2016b, Jarman et al. 2017) as well as among marine phytoplankton clades (Larsen et al. 2020, Vane et al. 2023, Stahl et al. 2023).

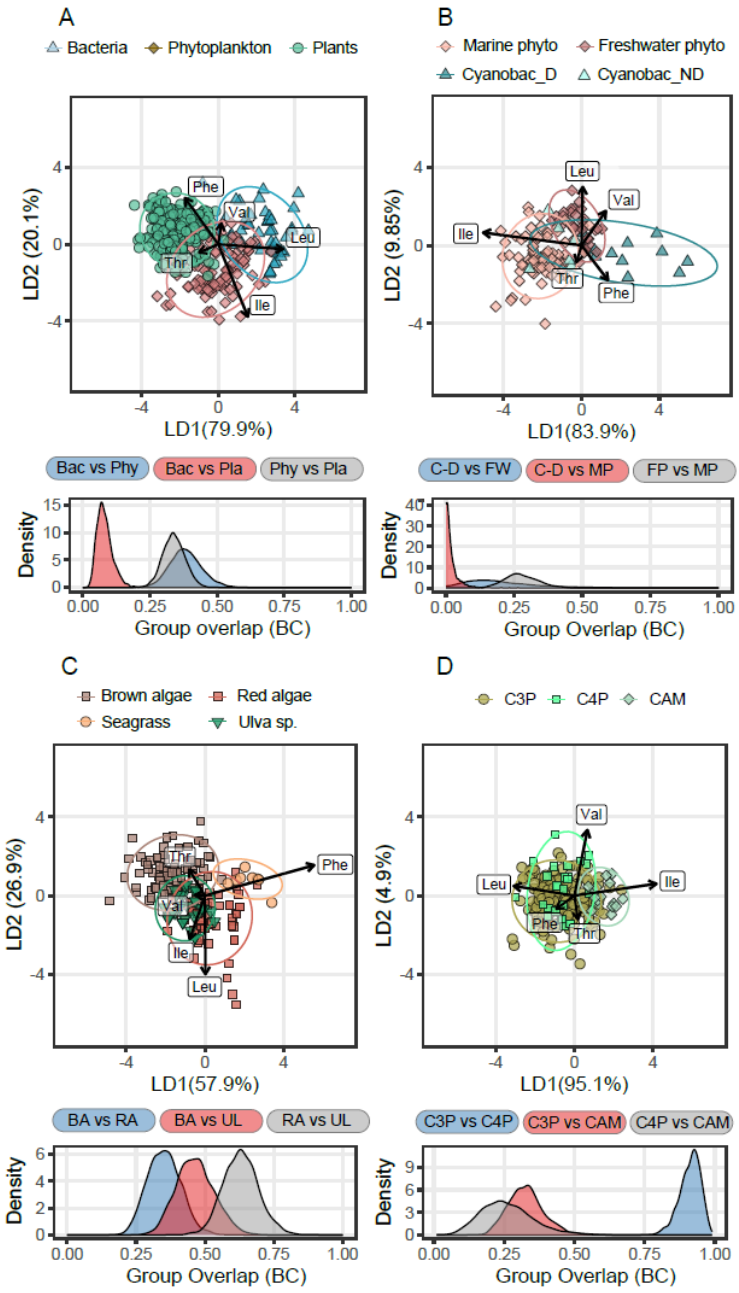

Figure 4. Linear discriminant (LD) analysis of basal resources based on mean-centred δ^{13}C-EAA values compiled from the literature. Upper subplot panel: LD scores for individual samples, with distinct symbols denoting each group. Lower subplot panel: posterior distributions of group pair overlaps, quantified by the Bhattacharyya coefficients (BC, see supplementary S2)., for group pairs represented as density scores, indicating the degree of overlap in LD scores between groups (0 = no overlap, 1 = identical distributions). EAAs considered: leucine (Leu), isoleucine (Ile), valine (Val), threonine (Thr), and phenylalanine (Phe). Each subplot features the following taxa: A) Heterotrophic bacteria, plants, and phytoplankton; B) Freshwater phytoplankton, marine phytoplankton, diazotrophic cyanobacteria (Cyanobac_D), and non-diazotrophic cyanobacteria (Cyanobac_ND, predicted group); C)

Brown macroalgae, red macroalgae, green macroalgae (represented by Ulva sp.), and seagrasses; D) C3 plants, C4 plants, and CAM plants, containing the two cacti species *Cylindropuntia* sp. and *Opuntia* sp. For visual clarity, LD weighting coefficients for each independent variable were multiplied by 8. See sample identities, classifications, and literature sources and BC values see Appendix S2.

Based on the available evidence, separation in δ^{13}C-EAA patterns can be attributed to both phylogeny and phenotypic factors (section 2.2). As highlighted, many δ^{13}C-EAA pattern distinctions are not based on phylogeny but other factors that affect phenotype such as biomes e.g. freshwater vs. marine, tissue type, and diazotrophy. Further insight into the potential drivers behind these separations may be deduced from the specific EAA weightings in the LDAs of the compiled δ^{13}C-EAA patterns (Fig 4A-D). We observe that predominantly higher mean-centred phenylalanine δ^{13}C values discriminate terrestrial plant δ^{13}C-EAA patterns from those of bacteria and phytoplankton (Fig. 4A). The same occurs for seagrasses, the only flowering plant in the marine environment that are also distinguished from freshwater/marine phytoplankton and other macrophytes with phenylalanine (Fig 4C, Appendix S2: Figure S2A). Phenylalanine is a precursor for lignin, a structural organic polymer providing rigidity in vascular plant cells, typically concentrated in wood and bark (Labeeuw et al. 2015). As highlighted in section 2, significant downstream demand for an EAA can produce a ^{13}C enriched EAA carbon skeleton. Associated extracellular transport of the EAA can preferentially incorporate the lighter ^{12}C EAA carbon skeletons into the polymer leaving a ^{13}C enriched EAA pool to be incorporated into proteins. Lignin is known to be relatively deplete in ^{13}C compared to other major biomolecules in vascular plant tissues (Benner et al. 1987). Varying concentrations of lignin produced in a photoautotrophic organism (Klap et al. 2000, Pempkowiak 2020) or its organs could therefore affect phenylalanine δ^{13}C values in proteins (e.g. enzymes, hydrolyzable structural tissues that include the complete EAA molecular structures) that draw from the same phenylalanine pool as for lignin polymers. These hydrolysable biomolecules that include AA are the ones measured for δ^{13}C-EAA values, not the lignin itself, which is not susceptible to acid hydrolysis and does not include complete phenylalanine carbon skeletons. Lignin has been measured in a few red macroalgae (Martone et al. 2009, Espiñeira et al. 2011), and could offer an explanation why some rhodophyte δ^{13}C-EAA patterns align more closely to those of seagrasses compared to other algal clades (Fig. 4C). However, the rhodophytes in our compilation have not been described for lignin content in the literature. It is possible that differences in δ^{13}C-EAA patterns between plant organs could be explained by the fact that phenylalanine is an important precursor to flavonols (Lepiniec et al. 2006), which are produced and accumulated in most seeds and grains. However, this hypothesis requires

further testing to confirm its validity. It is interesting to note that our analysis of compiled δ^{13}C-EAA data for the vascular plant phylum showed that mean-centred δ^{13}C phenylalanine values contribute minimally to variations in δ^{13}C-EAA patterns with respect to phylogeny (Appendix S3: Figure S3B). Observed within-plant groupings were based on mean-centred isoleucine, leucine, and threonine δ^{13}C values that clustered plant species that exhibit significant structural adaptations to arid habitats.

Thus, we propose that consistent and substantial non-proteinogenic demands for specific EAAs (or their intermediates along individual EAA synthesis pathways) that vary between basal organism groups contribute to differential carbon isotope fractionation observed in EAAs. If the biosynthesis of these polymers is a spatiotemporally consistent phenotypic characteristic of a particular basal organism, it can result in δ^{13}C-EAA patterns that are distinguishable from those of other basal organisms. This contrasts with smaller, variable, and stochastic EAA demands in response to short-term environmental fluctuations (e.g. plant defence, thermal stress responses). Further, we speculate such downstream demands may substantially influence relative fractionation patterns compared to variable carbon fractionation by different synthesis pathways and enzyme structures between basal organism clades. This deduction is supported by observations that many enzymes along with their corresponding transcription genes involved in the de novo biosynthesis pathways of EAAs are relatively conserved among photoautotrophic basal organisms such as vascular plants, macroalgae, and eukaryotic microalgae (Appendix S1: Figure S1A, Richards et al. 2006, Prigent et al. 2014).

3.2. Considerations for the δ^{13}C-EAA patterns of facultative prototrophs

Organisms that have the ability to synthesise EAAs de novo (termed EAA prototrophs), i.e. the basal resources in the context of this review, can be split into two distinct functional groups based on their metabolism. The first are the obligate EAA prototrophs, which are the autotrophs that synthesise the EAAs they need from simple inorganic carbon sources through photo- or chemosynthesis. The second group we term the facultative EAA prototrophs, which are organisms that utilise (in)organic carbon sources for biomolecular building blocks to synthesise EAAs de novo, but may also assimilate EAAs from external sources for normal metabolic functioning. This group contains the heterotrophic bacteria and fungi that drive biochemical decomposition (or saprotrophs), and mixotrophic organisms, such as some algal protists, that can both photosynthesise to fix inorganic carbon and take up external organic matter. Obtaining δ^{13}C-EAA data from facultative EAA prototrophs is generally more difficult than from obligate

EAA prototrophs due to the additional effort required for isolating, characterising, and cultivating Archaea, bacteria and fungi, as compared to sampling, characterising, and, if necessary, cultivating algae and plants. Many microbial species are unculturable or have complex growth requirements that limit their isolation and characterization (Parks et al. 2020). Our compiled δ^{13}C-EAA data for bacteria and fungi were predominantly from cultures grown on an AA-free single organic carbon source. This is done to ensure that the EAAs in the harvested biomass are derived from the organisms' biosynthetic pathways and not from the culturing substrate (Larsen et al 2009). However, this creates a bias relative to typical in situ δ^{13}C-EAA patterns because a culture medium cannot mimic natural growth environments. Some bacteria and fungi lack the specific metabolic pathways necessary to synthesise some or all their AAs and must obtain them from the environment or their host organism, making them metabolically dependent on external AA sources (Hosie and Poole 2001, Heizer et al. 2006, Yamaguchi et al. 2017, Price et al 2018, McCarthy and Walsh 2018). For the specific set of EAAs that they cannot synthesise, these organisms are auxotrophic (the term for the incapability of synthesis). For many other microbes that possess the necessary membrane transport proteins, assimilating AAs opportunistically from the external environment is energetically efficient compared to synthesising them de novo (Morrissey et al. 2023). The presence of external EAAs in biomass of facultative EAA prototrophs presents a challenge for δ^{13}C-EAA data, particularly their interpretation: their underlying δ^{13}C-EAA patterns from de novo synthesis being potentially skewed by the assimilation of EAAs synthesised by other, likely photosynthetic, basal organisms.

The degree to which facultative EAA prototrophs may incorporate external EAAs to build biomass is not well understood (Martin-Perez and Villén 2015, Price et al. 2018). Genetic factors and associated phenotypes are necessary for them to compete for and assimilate dissolved organic carbon substrates such as AAs (Dang et al. 2022). According to a recent study, saprophytic bacteria that assimilate polymeric substrates like cellulose do not assimilate significant amounts of simple dissolved organic carbon substrates such as glucose and AAs, as opposed to rhizosphere-associated bacteria (Dang et al. 2022). Fungi are similarly specialised in breaking down large insoluble polymers through exoenzyme secretion, producing smaller constituents (Algora Gallardo et al. 2021, Batista García et al. 2016, Ruiz-Dueñas et al. 2021). These saprotrophic fungi are expected to have higher bulk δ^{13}C values than their substrate (Pollierer et al. 2020, Gebauer and Taylor 1999), due to respiration of ^{13}C-light CO_2 or uptake of ^{13}C-enriched complex polymers. Pollierer et al. (2020) found however that saprotrophic fungi and their litter substrate had similar δ^{13}C values of phenylalanine. While this does not provide conclusive evidence of direct phenylalanine incorporation into biomass, it is noteworthy that ectomycorrhizal fungi,

which receive simple carbon compounds from their plant host, did not exhibit such an overlap. Yeast cultured on high AA content assimilated leucine and valine into their biomass, which affected the yeasts' δ^{13}C-EAA patterns, indicating that external AA uptake rates are specific to each AA (Arsenault et al. 2022a). Dissolved AAs in soils and aquatic environments are typically found in low concentrations of 0.01-50 µM and 1-10 µM/L, respectively (Lytle and Perdue 1981, Kielland 1994). If the turnover rate is equally low, it suggests that under most conditions, heterotrophic bacteria and fungi are unlikely to incorporate enough free EAAs into tissue for growth and to significantly alter their δ^{13}C-EAA patterns. Further, when in free forms in aquatic matrices, hydrophobic EAAs (valine, isoleucine, leucine, methionine, phenylalanine) are likely to be less bioavailable than more hydrophilic or partially hydrophobic EAAs (histidine, threonine, lysine) (Brio 2006).

The synthesis of AAs in heterotrophic bacteria involves various carbon sources and intermediates, including glucose, pyruvate, oxaloacetate, alpha-ketoglutarate, succinyl-CoA, acetyl-CoA, and hexose-phosphates (a simplified overview of the metabolic network is given in Fig. 1B, for a more complete metabolic network, see Fig. S1B). Besides the direct assimilation of EAAs, as discussed above, other classes of biomolecules can enter the metabolic network for AA synthesis. Fatty acids, a product of lipid digestion, can be broken down via β-oxidation to produce acetyl-CoA and other intermediates that can then be used in central metabolism to synthesise the carbon skeleton of e.g. leucine (Jimenez-Diaz et al. 2017). Keto acids, such as alpha-ketoglutarate, which are formed from the deamination or transamination of AAs, can be converted into the carbon skeletons of other AAs via transamination into glutamate, which is then decarboxylated into the TCA intermediate oxaloacetate via the GABA shunt (Feehily and Karatzas 2013). The breakdown of various organic carbon sources can result in intermediates that enter central metabolism at different points, which may explain why Pollierer et al. (2020) found that ectomycorrhizal and saprophytic fungi have different δ^{13}C-EAA patterns. Scott et al. (2006) observed distinct δ^{13}C-EAA patterns in acetate-metabolising bacteria compared to other heterotrophic archaea and bacteria, as well as autotrophic bacteria. Part of the difference can be attributed to organic acids converting to acetyl-CoA. Within the domain Archaea, methanotrophs can use different carbon assimilation pathways depending on the environmental conditions. Takano et al. (2018) found that anaerobic archaea forming methanotrophic mats in cold methane seeps rely on both dissolved inorganic carbon and methane for their carbon. When these archaea convert ^{13}C depleted methane to intermediates such as pyruvate and acetyl-CoA, their AAs become gradually more ^{13}C depleted during biosynthesis with each step of biosynthesis that elongates AA carbon skeletons. Short-chain AAs like glycine and alanine have less negative ^{13}C values (δ^{13}C values between -80 and

-100‰) than long-chain AAs like isoleucine and leucine ($\delta^{13}C$ values between -110 and -120‰). Leucine also serves as a precursor for isoprenoid lipids, which are also extremely ^{13}C depleted. The study also showed that the $\delta^{13}C$-EAA patterns differed between functional groups of methanotrophs.

Regarding our compilation of $\delta^{13}C$-AA data obtained from the biomass of facultative EAA prototrophs, we can exclude the possibility that external EAA acquisition substantially contributed to the variability in $\delta^{13}C$-EAA patterns as they were predominantly cultivated on AA free media. Despite other potential sources of variability such as analytical uncertainties compounded by aggregating $\delta^{13}C$-EAA data from multiple labs and studies, our findings demonstrate that both heterotrophic bacteria and fungi exhibit distinct $\delta^{13}C$-EAA patterns compared to algae and vascular plants (as seen in Figure 5A+B and Appendix Ss: Figure S2A,B). These distinctions are likely due to the varying EAA biosynthetic pathways and metabolic demands dominating the $\delta^{13}C$-EAA patterns among these major taxa, as discussed in section 2. Our analysis distinguishes heterotrophic and photosynthetic microbial groups, but also reveals substantial intragroup variability, particularly in heterotrophic bacteria. Although the pathways for synthesising EAAs are considered conserved in bacteria due to their vital role, they generally have higher degree of genomic variation compared to the other major domains (D'Souza et al. 2014, Price et al. 2018). For example, bacteria have different pathways for synthesising many of the EAAs used for $\delta^{13}C$-EAA fingerprinting such as isoleucine, leucine, lysine, phenylalanine, threonine, and valine (D'Mello 2017). Variability in bacterial $\delta^{13}C$-EAA patterns may also stem from the synthesis of non-EAA products, which affects metabolic flux patterns and isotopic values of EAA precursor molecules as conceptualised in Box 1. Since the domain Bacteria encompasses a wide range of phenotypic and genotypic diversity, considering heterotrophic bacteria as a single, homogeneous group in terms of $\delta^{13}C$-EAA fingerprints is likely a gross simplification. Compared to bacteria, fungi have larger genomes but a lower degree of genomic diversity (Nayfach et al. 2021)**.** Many of the fungal biosynthetic EAA pathways are also found in bacteria with the exception of the α-aminoadipate pathway of lysine, which is fungi specific except for the bacterial genus Thermus (Jastrzębowska and Gabriel 2015). However, the intracellular chemical compartmentalization found in eukaryotes may result in more complex isotopic fractionations compared to prokaryotes (section 2), contributing to the divergent $\delta^{13}C$-EAA patterns between fungi and bacteria (Fig. S2C). Differences in the types and proportions of biomolecules both between and within the domains, potentially affecting branch points related to EAA biosynthesis, may also contribute to differing $\delta^{13}C$-EAA patterns (Hayes 2001).

While most bacterial and fungal EAA prototrophs are wholly dependent on external organic carbon sources, other facultative EAA prototrophs can use both autotrophy and heterotrophy to acquire carbon. Termed mixotrophy, these facultative EAA prototrophs occur in many algal groups, free-living protozoa and green plants (Matantseva and Skarlato 2013, Selosse and Roy 2009). Therefore, incorporation of externally synthesised AAs influencing $\delta^{13}C$ patterns is an issue not only for Archaea, heterotrophic bacteria and fungi. Mixotrophic protists that both photosynthesise and ingest prey by phagocytosis have long been recognised, including representatives in ciliates, flagellates, foraminifera and radiolaria (Stoecker et al. 2009, Jones 2000, Sanders 1991). These mixotrophic protists play important roles in planktonic food webs across the global oceans (Stoecker et al. 2017, Faure et al 2019) and lake ecosystems (Waibel et al. 2019). Two-way exchanges of carbon-containing biomass between green plants and mycorrhizal fungi have been evidenced, leading to the suggestion that mixotrophy may be wide spread across the vascular plant phyla (Selosse et al. 2016, Firmin et al. 2022, Giesemann and Gebauer 2022), beyond the limited cases of carnivory and hemi-parasitism (Selosse and Roy 2009, Schmidt et al. 2013). More generally, mixotrophic strategies may be far more common in traditionally viewed autotrophic species than is appreciated, due to the absorption of simple organic compounds (Selosse et al. 2017). The implications of mixotrophy for $\delta^{13}C$-EAA patterns is currently unclear as the identity of biomolecular exchanges and their metabolic fate is typically unknown (Ward 2019). The grand écart hypothesis proposes that mixotrophic strategies in light limiting environments, such as shaded forest canopies or poorly lit waters that typically coincide with increasing nutrients, exist primarily for carbon uptake (Selosse et al. 2017). This contrasts with the more traditional view that mixotrophic strategies, such as plant carnivory or phagocytosis in late plankton bloom succession, evolved to supplement nitrogen and phosphorus in nutrient poor environments. However, the uptake of heterotrophic carbon sources by autotrophs may not result in its assimilation into their tissues, if such sources are preferentially used for other metabolic purposes. External organic carbon may be used to fuel respiration under stressful conditions as inferred from increased oxidation rates of diatoms grown in the dark with various exogenous carbon compounds (Tuchman et al. 2006). Heterotrophic carbon assimilation should have a minimal effect on $\delta^{13}C$-EAA patterns if the carbon is first transformed into common carbon precursors for AA biosynthesis (section 2). Potential shifts in $\delta^{13}C$-EAA patterns should only arise if there are EAAs directly assimilated and incorporated into tissues, or if AA specific intermediates are introduced into biosynthetic pathways (metabolic shunting, Appendix S1: Figure S1A,B). Assimilation of fungal derived carbon has been evidenced isotopically in plants (Bolin et al. 2017), although whether this specifically includes EAAs cannot be elucidated from the bulk isotope approaches employed. However,

labelling experiments have demonstrated that various microalgal species can take up exogenous AAs, which are then assimilated into their own proteins (Rivkin and Putt 1987). Therefore, high environmental AA availability may not only affect δ^{13}C-EAA patterns in heterotrophic microorganisms, but also in other, mixotrophic, basal organisms.

3.3. From δ^{13}C-EAA patterns to fingerprints

The variety of phylogenetic and ecological factors that can influence δ^{13}C-EAA patterns prompts the question of how to define the δ^{13}C-EAA pattern space for a given basal resource. The concept of a "fingerprint" for δ^{13}C-EAA patterns, as introduced by Larsen et al. (2009) to differentiate between bacterial, fungal, and plant EAA biosynthesis, has since been applied to a wider range of contexts (e.g. Larsen et al. 2012, Arthur et al. 2014, Yun et al. 2022). However, there is still a notable lack of a formal definition of a δ^{13}C-EAA fingerprint. This has likely contributed to variations in the construction and interpretation of "δ^{13}C-EAA fingerprints", such as the use of measured rather than mean-centred δ^{13}C-EAA values (e.g. Besser et al. 2022), or referring to consumer δ^{13}C-EAA patterns as "fingerprints" (e.g. McMahon and Newsome 2019). To maintain clarity and reflecting on the original purpose of δ^{13}C-EAA fingerprints, which was to trace different basal resources and their contributions of proteinaceous carbon to consumer tissues (Larsen et al. 2009), we explicitly define a "δ^{13}C-EAA fingerprint" as:

"*the minimum δ^{13}C-EAA pattern space that is solely occupied by a group or collection of similar basal organisms and encompasses the intragroup variability in δ^{13}C-EAA patterns expressed by those organisms.*"

where the δ^{13}C-EAA pattern and basal resource organisms are as defined in section 2. Here, the 'uniqueness' characteristic of fingerprints is qualified by sole occupancy, which offers an explicit and unambiguous mechanism for determining whether δ^{13}C-EAA pattern space is unique. By limiting it to the minimum occupied space, arbitrary overlaps between basal resources can be excluded. However, it is worth noting that the sole occupancy of a δ^{13}C-EAA pattern space by one group is comparative, and therefore depends on the presence or absence of other basal resource groups in an ecosystem (shown in Fig 3, basal resource groups 3 & 4) or its relevance to the consumer (section 4.1). A priori understanding of a consumer's ecology and the ecosystem that it inhabits underpin which basal resource δ^{13}C-EAA patterns will be defined as δ^{13}C-EAA fingerprints. Therefore, being considered a δ^{13}C-EAA fingerprint will

be study and context specific, and may change between studies that include the same basal resource group(s).

To define groups of similar basal organisms, a flexible framework is needed to accommodate the variety of studies using δ^{13}C-EAA approaches. Phylogenetically closer organisms are expected to express more similar δ^{13}C-EAA patterns due to genetic constraints associated with AA biosynthesis, as we observed in broad basal resource groups (Fig. 4). Yet adaptations to particular environments can lead to similar patterns among phylogenetically distant groups (see Appendix S3). Our compilation showed that mean-centred δ^{13}C values of phenylalanine separates plants from most other basal resource groups, but variation is noticeable at individual and family levels (Appendix S3: Figure S3A,B). Phenotypic expressions associated with adaptations to particular environments can imprint over broad phylogeny as disparate groups converge in their δ^{13}C-EAA patterns. For example, families highly adapted to arid environments show greater similarity in their δ^{13}C-EAA patterns than phylogenetically closer families lacking highly specialised water uptake and retention mechanisms (Appendix S3: Figure S3A). Additionally, variation in δ^{13}C-EAA patterns occurs across varying levels of biological organisation, and these differences may be driven by different EAAs. While phenylalanine separated plants from other broad basal resource groups, it contributed little to within phyla distinction in plants. In contrast threonine contributed little to broad basal resource group separation in δ^{13}C-EAA patterns (Fig. 4), yet varies across plant families and is the most variable EAA at the individual level (Appendix S3: Figure S3A,B). These observations suggest that δ^{13}C-EAA patterns have the potential to express higher specificity than is typically acknowledged when applied in the literature, where data are often grouped from multiple studies into broad basal resource categories (Arthur et al. 2014, Ayayee et al. 2015, 2016a,b, McMahon et al. 2015a, Rowe et al. 2019, Macartney et al. 2020, Wall et al. 2021, Pollierer and Scheu 2021, Arsenault et al. 2022b, Stubbs et al. 2022). Empirical work conducted over the past decade has provided valuable phenomenological insights, however, we propose the development of a conceptual framework focused on the metabolic functioning of organisms (as commenced in section 2) to facilitate greater prediction of δ^{13}C-EAA pattern structures of basal resources across environments. This aspiration for a greater mechanistic understanding would complement the current conservative approach that requires in situ measurement of basal resources on a study by study basis to avoid erroneous inferences.

3.4. Optimal characterisation of δ^{13}C-EAA fingerprints

To make fine-scaled distinctions with δ^{13}C-EAA fingerprints, well-defined sampling protocols and δ^{13}C-EAA measurements with minimal analytical error are essential (section 7). Basal resource samples should accurately represent the taxonomic group under investigation in the system of study. This precludes composite samples such as particulate organic matter filtrates, microalgal and bacterial mats, or partially degraded materials (detritus). Such composites may contain faeces, degraded organic matter, bacteria etc., and therefore are inaccurate representations of pure basal resources. Further, composites average over a diversity of clades or species, which may or may not be suitable to the specific study. Tissue samples of specialist primary consumers (e.g. zooplankton or specialised herbivorous fish) are often used as a surrogate for specific basal resource δ^{13}C-EAA fingerprints (e.g. Skinner et al. 2021). However, sole dependency of a primary consumer on one specific basal resource is unlikely due to incidental ingestion and digestion of other sources (e.g. functionally similar basal resources, detritus, associated bacteria and meiofauna in macroalgal turfs, Nicholson and Clements 2023). Prior to in situ sampling, systematic characterisation of δ^{13}C-EAA fingerprints in singularly cultured basal organisms would be optimal to establish to what extent basal resources can be subdivided into clades with similar functionality or divergence if not already known. Field collected samples with a high concentration of a particular species or clade can then be analysed for verification, as some basal resources might display different δ^{13}C-EAA fingerprints in situ compared to cultures. For example, δ^{13}C-EAA patterns of the sub-ice algae *Melosira arctica* growing in long-chained strands in its natural under-ice habitat significantly differed from their cultivated form where they grow in singular cell suspension (Vane et al. 2023). Secondly, the extent to which unique δ^{13}C-EAA fingerprints can be characterised depends on the number of EAAs measured as including more EAAs increases the potential to discriminate between different basal resources. The number of EAAs that can be measured depends on the analytical sensitivity of the instrument as well as the EAA concentrations in consumer tissue types. In most proteinaceous soft tissues 6-7 EAAs can be measured, but this is reduced in mineralised tissues such as biogenic calcites due to lower EAA concentrations (e.g. methionine and lysine, McMahon et al. 2018, Vokhshoori et al. 2022).

Directly visualising whether $\delta^{13}C_{EAA}$ patterns of select basal resource groups are distinct is not feasible due to the high dimensionality of the data. However, sole occupancy is a requirement in order for a δ^{13}C-EAA pattern space to be considered a fingerprint for a basal resource group (section 3.3, Fig. 3). Multiple pairwise biplots of mean-centred δ^{13}C-EAA values subset higher dimensional data that can be visualised, however results in significant information loss and are difficult to interpret holistically. Dimension reduction approaches that can be used to visualise δ^{13}C-EAA patterns include principal

component analysis (PCA) and linear discriminant analysis (LDA), which recast the data to fewer variables whilst minimising information loss. However, the two approaches differ in what information they optimally retain. PCA maximises total variation across the dataset onto fewer, uncorrelated axes regardless of data groups. LDA meanwhile maximises the differences between groups while minimising intragroup variability to optimally separate groups, providing linear, uncorrelated discriminants (although they may not be geometrically orthogonal in the original variable space in contrast with PCA). While it may seem that LDA is more appropriate to identify distinctions between δ^{13}C-EAA patterns, it is worth noting that when sample sizes are small, as is often the case with δ^{13}C-EAA data, PCA can outperform LDA in separating groups and is less sensitive to input data (Martínez et al. 2001; for a comparison of the two approaches, see section 5.3). While visual inspection of δ^{13}C-EAA patterns can be fruitful, it remains a subjective approach to discerning distinctions. Objectively discerning distinctions between δ^{13}C-EAA patterns requires the use of statistical measures to quantify the degree of overlap or closeness between basal resource groups. One such general measure is the Bhattacharya coefficient (BC, Bhattacharyya 1946, see Fig. 3 and Appendix S2), which quantifies the similarity of two multivariate probability distributions on a scale between 0 and 1, and therefore can be applied directly to the multivariate δ^{13}C-EAA patterns or transformed data (e.g. following PCA/LDA). Quantifying δ^{13}C-EAA pattern distinctions not only improves statistical clarity for defining δ^{13}C-EAA fingerprints, but will also facilitate more direct comparisons between studies that, for example, measure different suites of EAAs.

4. Tracing basal resources from a consumer perspective

The application of δ^{13}C-EAA fingerprints comes with many advantages for tracing carbon from basal resources to consumers. Due to the consistency of δ^{13}C-EAA patterns in natural and cultivation environments, a wide array of basal resource groups including microbes can be traced, and potentially to specific clades. The high number of individual EAA tracers enables the characterisation of many basal resources simultaneously. However, the application of δ^{13}C-EAA fingerprints depends on the appropriateness for the research question regarding the consumer. Estimates of basal resource use across large taxonomic groups (such as plants, bacteria, and microalgae) requires coarser δ^{13}C-EAA fingerprints, than more specific questions on basal resource use. For example distinguishing between microalgae clades requires the use of finer scale taxonomic δ^{13}C-EAA fingerprints. From the hypothesised mechanisms driving δ^{13}C-EAA fingerprints (section 3.1), and spatially varying availability of basal organisms, it is likely that they are specific to the regional ecosystem in which they occur and cannot be

generalised across broad basal resource groups due to their phylogenetic and phenotypic variations (section 3.3). Inferences surrounding basal resource use become more complicated for consumers that partially acquire EAAs biosynthesized by (endo)symbionts and the use of δ^{13}C-EAA fingerprints in such cases is still relatively understudied. In this section, we therefore review and discuss the myriad of ways that δ^{13}C-EAA patterns and fingerprints can be applied to infer basal resource use or EAA sources by consumers.

4.1. Applying δ^{13}C-EAA fingerprints in ecological studies

As organisms consume basal resources either directly or indirectly through their prey, they assimilate the δ^{13}C-EAA patterns of those basal resources into their own tissues. By mean-centring the measured δ^{13}C-EAA values in consumer tissues (which are in effect a mixture of baseline δ^{13}C-EAA values from consumed basal resources), the δ^{13}C-EAA patterns in consumer tissues are obtained. In the simplest case, a specialised consumer that wholly depends on a single basal resource would have a tissue δ^{13}C-EAA pattern identical to that of the basal resource due to the negligible changes in δ^{13}C-EAA values during trophic transfer of EAAs (often referred to as a trophic discrimination factor - TDF). However, if this consumer started to incorporate a second basal resource with a separate δ^{13}C-EAA fingerprint, then its own tissue δ^{13}C-EAA pattern would become a mixture, or weighted average, of the two basal resource fingerprints. While estimating proportional basal resource use may seem relatively simple with only two resources, real world trophic systems can be highly complex. There are a multitude of potential basal resources within ecosystems, various combinations of which could result in similar δ^{13}C-EAA patterns in consumer tissues (referred to as an underdetermined mixing system; Parnell et al. 2010). Reconstructing basal resource use by the studied consumers thus requires the characterisation of relevant basal resource δ^{13}C-EAA patterns. Prior knowledge on the dietary niche of the organism and the extent of the distinction in basal resource δ^{13}C-EAA patterns determine the specificity with which basal resource use can be quantified. The variation in the basal resource δ^{13}C-EAA fingerprints then has to be evaluated together with the consumer tissue δ^{13}C-EAA patterns to assess whether the consumers do not fall outside of the basal resources (e.g. with biplots and, or PCA/LDAs). When consumer tissues are outliers this can indicate that a basal resource is missing or that a basal resource group's variation is insufficiently characterised either due to low replication or due to incomplete sampling of consumer-relevant basal resource clades. However, different analytical methods, carbon fractionations during treatment protocols of consumer and basal resource tissues, or deviations during isotopic measurements can lead

to offsets between consumer and basal resource (section 7). These considerations are important prerequisites to obtain reliable quantifications of the proportional basal resource by the consumer (section 8).

Relatively simple questions regarding the relative use of aquatic versus terrestrial basal resources by a consumer have been commonly addressed using both bulk and AA stable isotope approaches. The δ^{13}C-EAA patterns of terrestrial plants and aquatic microalgae are distinct globally (Fig. 4A), show less within-group variation than their bulk or baseline δ^{13}C-EAA values, and therefore are excellent tracers for quantification of their use by consumers (Larsen et al. 2013). While the distinction between the δ^{13}C-EAA fingerprints of these two large basal resource taxa is highly consistent (Larsen et al. 2013, Liew et al. 2019), the intragroup variation is likely to be specific to the ecosystem in which the consumer resides.

Most ecological questions revolve around estimating the proportional use of multiple potential basal resources by a consumer, including bacteria, microalgae, and macroalgae. In such studies, it has become common practice to use training data sets, or basal resource δ^{13}C-EAA values characterised in other studies such as Larsen et al. (2013) and McMahon et al. (2016). Training data is often combined with additional basal resources δ^{13}C-EAA patterns measured from the ecosystem of interest to infer basal resource use of the studied consumers (e.g. Arthur et al. 2014, Ayayee et al. 2015, Rowe et al. 2019, Macartney et al. 2020, Wall et al. 2021, Arsenault et al. 2022b, Stubbs et al. 2022). The extensive use of training data stems from the main assumption that basal resource δ^{13}C-EAA patterns are highly conservative and representative of similar basal resources across all ecosystems. While the evidence suggests δ^{13}C-EAA patterns are highly consistent, the assumption of δ^{13}C-EAA patterns being representative across various ecosystems is unlikely to be true at broad taxonomic scales. As discussed in section 3, the variation within δ^{13}C-EAA patterns of large basal resource taxa such as microalgae and bacteria can be attributed to finer distinctions in phylogeny and associated with phenotypic structural components. δ^{13}C-EAA fingerprints even occur between plant structures such as seeds, roots, and leaves and therefore exact sampling of plant organs that are ingested by the consumer is necessary. Generic training data may therefore not include the specific variations in δ^{13}C-EAA patterns in the particular ecosystem in which the studied consumer resides. Additionally, the use of general training data can add significant additional variation that is not pertinent to the specific ecosystem. Using training data sets can lead to poor discrimination between basal resources (Liew et al. 2019, Macartney et al. 2020, Phillips et al. 2020, Stubbs et al. 2022) and may not reflect the true underlying basal resource δ^{13}C-EAA patterns

space against which the consumer δ^{13}C-EAA patterns are compared (Philips et al. 2020, Macartney et al. 2020). The use of training data further requires inter-laboratory calibration of the δ^{13}C-EAA values by measuring identical reference tissue materials in each facility to correct for potential analytical offsets (Arthur et al. 2014). As laboratories have different analytical protocols and errors that are not yet well-constrained, corrections with calibration post-hoc can lead to greater uncertainties in the δ^{13}C-EAA values that should be accounted for (see section 8.2). In the absence of reference materials and δ^{13}C-EAA patterns that are directly related to the diet and ecosystem of the studied consumer, studies should ideally characterise their own relevant basal resource δ^{13}C-EAA fingerprints to make reliable inferences on basal resource use.

Some consumers are known to rely on only a few related or one basal resource taxa as for example in marine open water food webs that are mainly fueled by phytoplankton. It is increasingly apparent that such basal resources can be distinguished into finer clades within a taxa such as different clades of phytoplankton (Vane et al. 2023, Stahl et al. 2023), more detailed inferences on their use by consumers can be made. These basal resource δ^{13}C-EAA fingerprints discriminate over a relatively smaller isotopic space (i.e. basal resource group 1 in Fig. 1, Vane et al. 2023). Such detailed basal resource discriminations provide opportunities for detailed inferences on specific basal resource use by consumers on spatiotemporal scales. Shifts in diazotrophic and non-diazotrophic cyanobacteria, eukaryotic microalgae, and heterotrophic bacteria were observed over a 1000 years by analysing δ^{13}C-EAA patterns in subsequent growth rings of proteinaceous deep-sea corals (McMahon et al. 2015a). Significantly different δ^{13}C-EAA patterns in planktivorous fish caught across different locations in the Baltic Sea indicated the use of different marine microalgae clades (Larsen et al. 2020). In the Arctic Ocean, δ^{13}C-EAA patterns in zooplankton and planktivorous fish showed a larger variation than the δ^{13}C-EAA patterns characterised in early spring particular organic matter consisting mainly of diatoms. This indicated that other microalgae clades occurring earlier in the season might not have characterised and explained the additional variation in the consumer tissues (Vane et al. 2023). While potentially powerful, researchers need to consider if such fine-scale basal resource distinctions no longer inform about the ecological processes of interest in relation to the consumer. For example, distinguishing between various clades within phytoplankton will not be informative when phytoplankton make only a minor contribution to the consumer biomass. Similarly, if the spatiotemporal variability in availability of specific basal resources is high compared to consumer tissue integration times and movement patterns, such as during phytoplankton bloom progressions, then fine scale distinctions are unlikely to be observed within the consumers as they average over that resource specificity. However, more studies characterising δ^{13}C-EAA

fingerprints in microalgae, cyanobacteria and marine bacteria clades are required to identify the extent of discrimination. This could then be a powerful method to trace the potential finer changes in basal resource use by consumers that can occur with climate change and other anthropogenic alterations to ecosystems around the world.

4.2. Tracing EAA sources in consumers with (endo)symbiotic relationships

For some consumers, the amount of EAAs obtained from their diet is insufficient to directly meet their physiological demands. Endosymbionts that are able to biosynthesise EAAs can meet this shortfall for host consumers and therefore facilitate the specialisation on nutrient-poor diets, opening previously inaccessible ecological niches. A classic example is that of aphids and other plant sap feeding insects that rely on endosymbiotic gut bacteria synthesising EAAs that are missing in their sugar dominated diets (Akman Gündüz and Douglas 2009). Symbiotic bacteria occurring in the gut of the host often, but not always, possess the full set of genes for EAA synthesis (Neis et al. 2015, Portune et al. 2016), and are common occurrence in detrital consumers, such as earthworms, springtails, Diptera, sesarmid crabs, and oribatid mites. The hosts typically subsist on nutrient-deficient diets such as detrital matter or woody plant materials (Ayayee et al. 2015, 2016b) from which symbionts digest complex polymers and synthesise EAAs that are passed to their host. The EAA contribution of gut symbionts can be variable however due to changing dietary availability or digestibility. In enchytraeids, a family of oligochaetes, increasing indigestible fibre content in the diet resulted in increased symbiont EAA supplementation, but also led to decreased growth (Larsen et al. 2016a). Changes in EAA provisioning by gut microbes are proposed to be associated with the changes in microbiome composition and metabolic rate (Ayayee et al. 2020).

In the marine environment, many corals, molluscs, and sponges are mixotrophic holobionts: in addition to heterotrophic particle capture, the animal hosts rely on a complex community of symbiotic photoautotrophs and heterotrophs for their nutrition to varying degrees (Skinner et al. 2022, Pita et al. 2018). In corals these can include endosymbionts, typically dinoflagellates of the clade Symbiodiniaceae hosted within the coral tissue (Skinner et al. 2022); diverse endolithic microbiomes on and within their carbonate skeleton, including microalgae, fungi, and bacteria (Pernice et al. 2020); and potentially microorganisms associated with epidermal and gastrodermal mucus (Fox et al. 2019, Kwong et al. 2019). Coupled $\delta^{13}C_{AA}$ values between coral hosts and their endosymbionts suggests that endosymbiotic algae

play a major role in the biosynthesis and provisioning of AAs to their hosts, despite evidence that cnidaria may have the potential to synthesise some EAAs directly (Ferrier-Pagès et al. 2021 and references therein). Transfer of photoassimilates has also been shown to occur between endolithic symbionts and the overlying coral host tissues (Schlichter et al. 1995, Fine and Loya 2002). It should be recognised however that biochemical roles of holobiont symbioses are not restricted to just AA synthesis: rapid fixation and transfer (within 15 minutes) of inorganic carbon in seawater by endosymbionts is facilitated by intracellular storage structures including lipid droplets and glycogen granules in both the photoautotrophs and host tissues (Kopp et al. 2015). Approximately 50% of newly fixed carbon is respired by the holobiont as a whole within 48 hrs (Tremblay et al. 2012), therefore coral symbionts play a considerable role in provisioning high-energy biomolecules to fuel holobiont metabolism. Highly variable host-symbiont interactions add further complexity when considering EAA contributions of symbionts to host tissues, which can be related to in situ light levels (Wall et al. 2021), depth or resource availability (Macartney et al. 2020), and therefore specific to microhabitats and host species. Observed seasonality in holobiont microbiome compositions implies not only spatial, but temporal variability in potential symbiont functioning, including the capacity for EAA provisioning (e.g. Sharp et al. 2017, Glasl et al. 2020).

Identifying and quantifying the EAA sources that contribute to host consumer tissues in the presence of symbionts will ultimately depend on the ability to characterise and distinguish symbiotic basal resources from those obtained through the diet. This could potentially be assessed by characterising symbiont δ^{13}C-EAA patterns across various host systems. The δ^{13}C-EAA patterns in endosymbiotic dinoflagellates separated by repeated centrifugation from coral tissue have been observed to be distinct from the surrounding particulate organic matter, a proxy for phytoplankton (Fox et al. 2019, Wall et al. 2021). Recent work indicates that the δ^{13}C-EAA patterns of Symbiodiniaceae may be distinctive from other free living dinoflagellates (Stahl et al. 2023). Baseline δ^{13}C-EAA values often vary between the symbionts and coral tissue but whether this translates to differing δ^{13}C-EAA patterns is unclear (Martinez et al. 2020, 2021, Ferrier-Pagès et al. 2021). Although sponge microbial symbionts have not been successfully cultivated (Pita et al. 2018), sponge tissue and their assumed symbiotic microbes have been separated through size fractionation in the tropical sponge *Mycale grandis* (Shih et al. 2020). Gut microbial δ^{13}C-EAA patterns have not been characterised even though potential model organisms exist, e.g. *Drosophila*, from which they can be readily cultivated (Erkosar et al. 2013). Currently, general bacterial δ^{13}C-EAA patterns from data compilations consisting mostly of terrestrial bacteria are used in identifications of gut microbial EAA supplementation due to perceived similarities with consumer tissue

δ^{13}C-EAA patterns (Arthur et al. 2014). These findings are supported by offsets in δ^{13}C-EAA values between consumer tissue and their diet observed in some controlled feeding studies that are interpreted as gut microbial EAA supplementation (Newsome et al. 2011, 2020). However, such observed offsets may be a result of particular tissue pretreatments leading to bias (see section 7.1 and Fig. 8). Bacterial δ^{13}C-EAA patterns are highly variable (Fig. 4, section 3.1) and those of gut bacteria are potentially distinctive, therefore utilising training datasets of (terrestrial) bacteria δ^{13}C-EAA patterns could lead to false inferences on host EAA sourcing.

As symbionts are typically hosted in diverse communities, the optimal characterisation of symbiont δ^{13}C-EAA patterns will likely be difficult beyond isolating single symbiont species cultures. Yet, determining symbiont EAA provisioning will require extensive characterisation of symbiont δ^{13}C-EAA patterns to capture the variation between symbiont species. Accurately reconstructing symbiont δ^{13}C-EAA values retrospectively from the offsets between δ^{13}C-EAA values of diet and consumer tissues (Larsen et al. 2016b, Newsome et al. 2020) requires prior knowledge of proportional contributions of symbionts to consumer tissues, which are currently lacking. Despite high potential, future studies will require a good understanding of the spatiotemporal host-symbiont dynamics when assessing the potential of acquiring distinctive symbiont δ^{13}C-EAA fingerprints.

5. Beyond δ^{13}C-EAA fingerprinting

In some instances, basal resources of interest may not exhibit distinct δ^{13}C-EAA patterns, especially when phylogenetically similar resources are spatially or ecologically separated (e.g., underwood versus canopy vegetation or sea-ice microalgae versus pelagic phytoplankton) (de la Vega et al. 2019, Tejada et al. 2020). Moreover, even when basal organisms are phylogenetically similar or identical, their macronutrient content may differ, such as in leaves compared to tubers (Jarman et al. 2017). Thus, relying solely on δ^{13}C-EAA patterns may not adequately resolve multiple protein sources for cosmopolitan omnivores (Larsen et al. 2022). In such cases, researchers can employ additional tracers to gain further insights into the environment in which the consumer lived (see Introduction). However, additional insights into resource use may also be gleaned from the dataset already at hand, namely δ^{13}C-NEAA values in conjunction with baseline δ^{13}C-EAA values. The argument can be made that baseline δ^{13}C-EAA values are more informative than bulk δ^{13}C values because the EAAs are synthesised exclusively by basal organisms as opposed to bulk carbon (Hobbie et al., 2017). In this section, we will explore the

potential of using the full range of δ^{13}C-AA data, particularly δ^{13}C-NEAA and baseline δ^{13}C-EAA baseline values, to provide complimentary dietary insights applicable across spatiotemporal scales.

5.1. Factors affecting δ^{13}C-NEAA values in animals

δ^{13}C-NEAA data has been underutilised in ecological studies, likely due to animals' de novo NEAA synthesis and the subsequent reduction in diagnostic potential compared to δ^{13}C-EAA patterns (Larsen et al. 2009). NEAAs include alanine, glycine, and serine synthesised in the glycolytic pathway; asparagine and glutamine synthesised in the TCA cycle; aspartate derived from asparagine; glutamate, proline, and hydroxyproline derived from glutamine; tyrosine derived from phenylalanine; and cysteine derived from serine (Fig. 1C). Since animals can synthesise NEAAs de novo, they are likely to reflect adaptive or physiological responses to resource changes (Fig. 5). Consumer δ^{13}C-NEAA values can be conceptually thought of as a mixture of two sources: the de novo synthesised NEAAs and those directly sourced from the diet. Factors influencing the δ^{13}C-NEAA values during de novo synthesis will reflect those discussed in section 2 (eq. 1), whereas those directly routed into tissues will reflect the isotopic values of those in the diet. The carbon used for NEAA synthesis comes from different macronutrients, each with their own isotopic composition, associated catabolic processes, and proportional contribution to NEAA biosynthesis (see Fig. 5 for graphical conceptualisation and Appendix S1: Figure S1C for detailed metabolic network). For example, lipid moieties and short-chain fatty acids are ^{13}C depleted relative to proteins and carbohydrates (Deniro and Epstein 1977, Melzer and Schmidt 1987, Weber et al. 1997). While directly routed NEAAs will have δ^{13}C values that reflect those of the diet, substantial downstream processing of NEAAs, particularly in the splanchnic tissues, e.g. the tissues of the organs in the abdominal cavity such as liver, stomach, small/large intestine, pancreas, spleen, and kidney, may cause some fractionation (Caut et al. 2009, Larsen et al. 2022a). Responses to changes in diet quality may also be AA specific as macronutrients enter different parts of the overall central metabolic network. For example, alanine metabolism is particularly responsive to carbohydrate but not protein intake, whereas glycine metabolism appears to be responsive to dietary protein levels (Yu et al. 1985).

As mentioned, dietary AAs may undergo fractionation during their catabolic processing in the splanchnic tissue, but also within the microbiome of the abdominal cavity. Some NEAAs are used for oxidative fuel in the mucous membrane or as building blocks for other metabolites (Burrin and Stoll 2009). However, a lack of these NEAAs or caloric restrictions in general can lead to increased catabolism of certain EAAs,

making them unavailable for the formation of structural tissues (Neis et al. 2015). In humans, between 20% to 50% of dietary EAAs such as leucine, lysine, and phenylalanine are retained in the abdominal cavity, but retention can reach 90% for threonine (Hoerr et al. 1991, Biolo et al. 1992, Matthews et al. 1993, Van Goudoever et al. 2000, Schaart et al. 2005). Retention rates of dietary NEAAs is typically higher, with glutamate and aspartate being almost completely retained in splanchnic tissues (Battezzati et al. 1995, Reeds et al. 1996, Stoll and Burrin 2006, Riedijk et al. 2007), making them unavailable for tissue formation elsewhere in the body. The retention of alanine in splanchnic tissue is around 70%, but little of its carbon skeletons are used for new protein synthesis (Battezzati et al. 1999). Compared to alanine, dietary glycine has a higher proportion routed towards the formation of new proteins and metabolites such as glutathione, a powerful antioxidant, and bile acids, which are essential for digestion and fat absorption (Jourdan et al. 2011). Around 40% of dietary proline is retained in the splanchnic tissues, making it a crucial amino acid for overall protein synthesis (Dabrowski et al. 2005, Wu et al. 2008). However, it is challenging to determine if dietary NEAAs are metabolised during digestion, or used as building blocks in tissue proteins (Battezzati et al. 1999, Dai et al. 2012). Once dietary NEAAs enter the liver, the central organ for AA degradation and syntheses, they are utilised for protein building and as precursors for non-proteinogenic metabolites (Fig. 5). If dietary NEAAs are in excess, they are converted into fat, which can be catabolized into glycogen when needed. While the ratio of dietary NEAAs incorporated versus those synthesised de novo in proteinogenic tissues often remains unclear due to varying catabolic rates and metabolic demands, it is feasible to make reasonably precise estimates in collagenous tissues when considering the NEAAs as an aggregated pool (Hobbie et al. 2017).

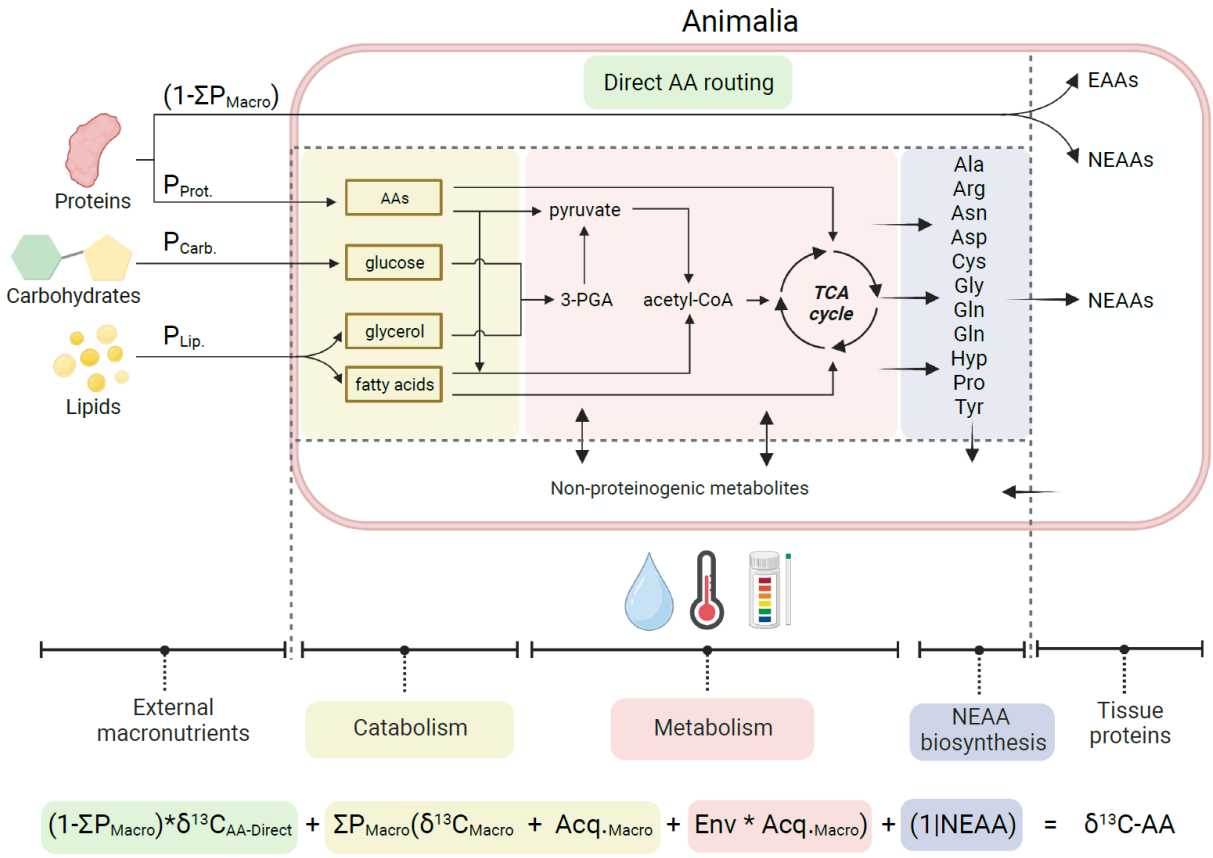

Figure 5. Schematic representation of the macronutrients (proteins, carbohydrates, lipids), metabolic processes, and environmental effects that contribute to the $\delta^{13}C$ values of amino acids (AA) in animals. The metabolic processes are divided into macronutrient catabolism, central metabolism including glycolysis and the tricarboxylic acid (TCA) cycle, and the biosynthesis of the non-essential AAs (NEAAs) that can be utilised for proteinogenic or non-proteinogenic purposes. All the essential AAs (EAAs) are assumed to be routed directly from proteinaceous dietary sources ($\Sigma P_{Macro} = 0$). A fraction of the dietary NEAAs may be routed directly to tissue proteins ($1 - \Sigma P_{Macro}$), which will have $\delta^{13}C$ values that reflect those of the dietary NEAAs. In terms of the sources and processes affecting d13C-NEAA values of tissue proteins, the molecular constituents of each macronutrient have their own initial isotopic composition, $\delta^{13}C_{Macro}$, and fractionation as they are converted to NEAA-precursors, $Acq._{Macro}$. As the catabolic networks are different for the three macronutrients (Fig. S1C), the effect of environment will likely induce different physiological responses in isotopic fractionations ($Env*Acq._{Macro}$). The contributions of different macronutrients to NEAA synthesis ($\Sigma P_{Macro} = P_{Prot.} + P_{Carb.} + P_{Lip.}$) may fluctuate with diet composition and covary with physiological changes such as the accumulation of adipose tissue, reproduction status or muscle catabolism. Tissue proteins may also be catabolised and re-enter the central metabolism. Taken together, the isotopic composition of tissue proteins will reflect the proportional mixture of directly routed dietary AAs plus those synthesised de novo following catabolism (for NEAAs), and the associated fractionations with each macronutrient (ca. Fig. 1). The

metabolic pathways are summarised based on Stryer et al. (2019). Abbreviations: 3-PGA, 3-Phosphoglyceric acid; Ala, alanine; Arg, arginine; Asn, asparagine; Asp, Asparagine; Cys, cysteine; Gly, glycine; Gln, glutamine; Glu, glutamic acid; Hyp, hydroxyglycine; Pro, proline; Ser, serine; Tyr, tyrosine. The illustration was created with BioRender.com.

5.2. Exploring full δ^{13}C amino acid datasets

The complexity and multitude of factors influencing NEAA sourcing, catabolism, and synthesis raise questions of the degree δ^{13}C-NEAA data can provide additional insights into past and current resource use. Nevertheless, consistency among empirical studies suggests that NEAAs could be valuable, as this implies that the various processes potentially imparting variation do not mask underlying dietary signals. A review on using δ^{13}C-AA values to trace the trophic fate of aquafeed macronutrients concluded that combined δ^{13}C-NEAA and δ^{13}C-EAA patterns could inform metabolic routing and utilisation of dietary lipids and carbohydrates when dietary parameters are well-defined (Larsen et al. 2022). Recent human epidemiological studies have shown that serum δ^{13}C-NEAA values reflect the intake of beverages sweetened with high-fructose corn syrup, a carbohydrate source with high δ^{13}C values (Choy et al. 2013, Yun et al. 2018, 2020, Johnson et al. 2021). Utilising NEAAs as nutritional markers in archaeological studies has also provided deeper insights into various dietary categories and subsistence strategies of past human populations. The δ^{13}C spacing between glycine and phenylalanine, first observed by Corr et al. (2005), can indicate whether a population primarily consumed C3 terrestrial or freshwater proteins. More recent ordination analyses of combined δ^{13}C-EAA and δ^{13}C-NEAA literature data show distinct clustering of populations with different subsistence strategies (Ma et al. 2021, Soncin et al. 2021, Brozou et al. 2022, Larsen et al. 2022b). These findings are encouraging, as they suggest that δ^{13}C-NEAA values in humans consistently reflect their subsistence strategies. In addition to considering δ^{13}C-NEAA values, both archaeological and ecological studies suggest that in certain contexts, baseline δ^{13}C-EAA values can help to constrain protein sources.

Currently, there are no default methodologies for utilising full δ^{13}C-AA datasets to predict the primary protein sources of consumers. To examine the importance of ordination techniques and data preprocessing methods in ensuring accurate predictions and assessments, we compiled archaeological δ^{13}C-AA values from human collagen and keratin across eight studies (see Appendix S4). These

populations, which span 6500 years and are situated in distinct geographical regions, were analysed using both PCA and LDA techniques to determine protein source categories: Freshwater (FP), marine (MP), terrestrial C3 (C3P), and terrestrial C4 (C4P). Additionally, we compared two types of data preprocessing: measured and EAA mean-centred δ^{13}C-AA data, and visualised the δ^{13}C-EAA mean values in the ordination plots. There is an important caveat to consider in our evaluation of δ^{13}C-AA data for past human populations: The protein sources of these populations cannot be independently verified using other lines of evidence. Our assessments depend solely on the contextual information provided by the archaeological studies, e.g. geographical locations where the samples were obtained, along with the baseline δ^{13}C-AA data. A comprehensive discussion of the results can be found in Appendix S4.

In summary, the ordination outcomes indicate that most populations primarily cluster near the anticipated protein sources, albeit with some discrepancies between data preprocessing and ordination approaches (Fig. 6). The predictions of the different combinations of ordination techniques and data preprocessing do not appear to be fundamentally different; however, LDA ordination results tend to align more closely with the expected protein sources of the human populations than PCA. In terms of the two data set representations (measured vs. mean-centred), 18 out of 64 unknown (predicted) individuals were categorised differently due to the slight structural differences. In the vast majority of these discrepancies, the use of measured data yields more accurate predictions of protein sources compared to mean-centred data. In terms of applying class probability assignments $p\theta(x)$ and likelihood $lx(\theta)$ functions to predict protein sources to the LDA output, we found that likelihood functions are comparatively less prone to false inferences. This is particularly true for samples that fall outside the mixing-space, in our case the ordination space defined by the classifier δ^{13}C-AA data with the four protein sources. We calculated Bhattacharyya coefficients to evaluate overlap between human populations and protein sources. Although overlaps help compare methodological approaches, they are less suited for assessing relative protein contributions, as populations falling between protein groups have low coefficient values. We show that regardless of preprocessing or ordination methods, a similar set of amino acids contribute to maximising intra- and inter-group variation. Phenylalanine and valine differentiate terrestrial and aquatic resources, while proline separates C3 protein groups (Honch et al. 2012, Larsen et al. 2013). The δ^{13}C patterns of glycine, alanine, and glutamate play an important role in distinguishing protein sources within terrestrial and aquatic groups. The relative δ^{13}C offsets among these NEAAs may partially reflect the balance of dietary fat to carbohydrate (Choy et al. 2013, Yun et al. 2018, 2020, Johnson et al. 2021, Larsen et al. 2022).

These findings provide a unique perspective on the consistency of δ^{13}C-AA patterns in humans, but may only apply to omnivores and warrant further investigation in different dietary contexts, such as obligate herbivores or carnivores. Reconstructing past human resources is challenging due to relatively limited information that can be obtained from geographical region, excavation artefacts, and skeletal remains examination. Despite these limitations, our ordination analysis supports the hypothesis that alanine, glutamate, glycine, and proline are suitable nutritional markers. The remarkable consistency in δ^{13}C-AA patterns across human tissue samples spanning 6,500 years holds potential for uncovering individual-level differences within populations. Analysing the full δ^{13}C-AA dataset may also provide insight into macronutrient balance, but further studies are needed to fully understand the metabolic controls of δ^{13}C-NEAA values.

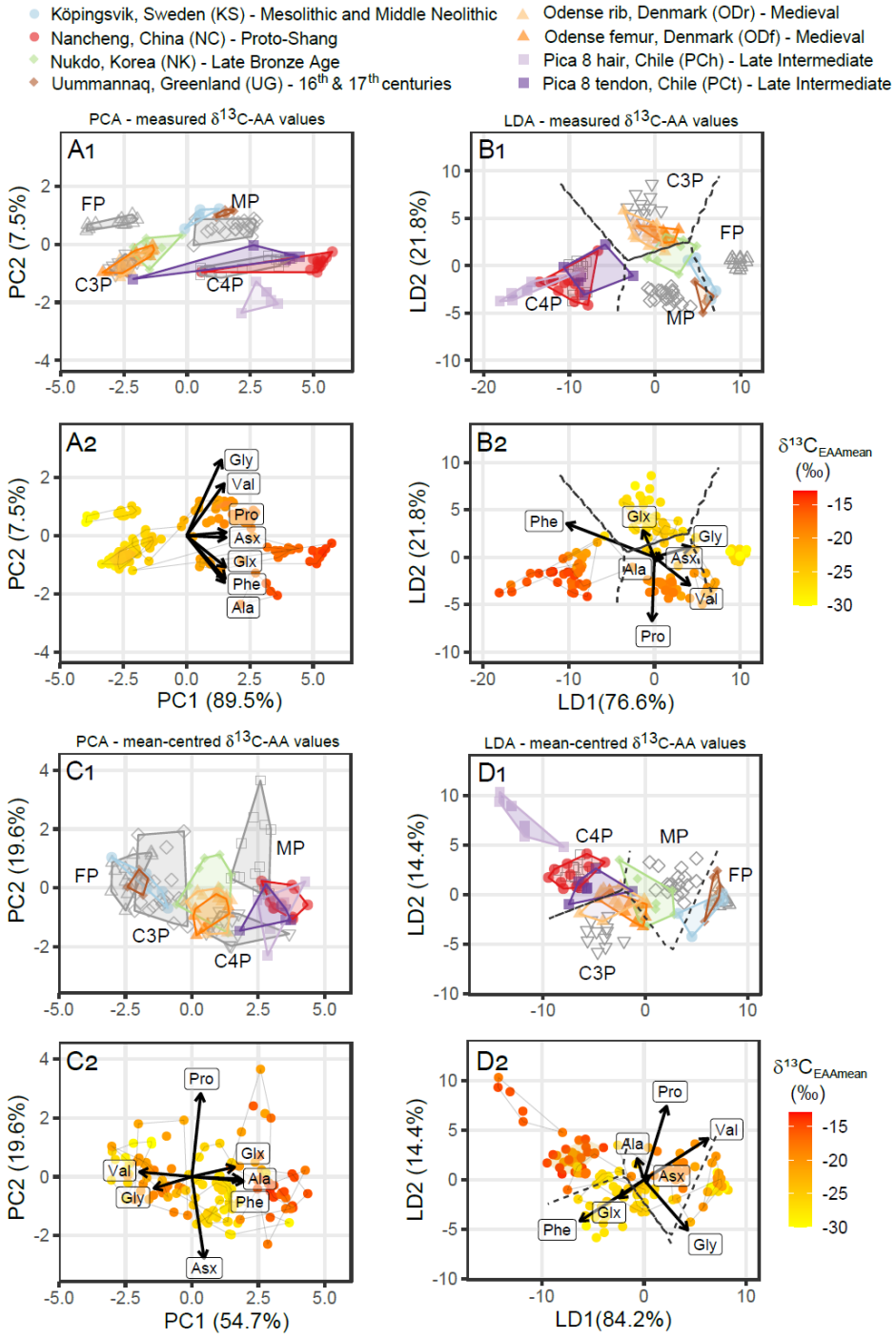

Figure 6. Ordination analysis with δ^{13}C values of alanine (Ala), aspartic acid/asparagine (Asx), glycine (Gly), glutamic acid/glutamine (Glx), phenylalanine (Phe), proline (Pro), and valine (Val) from archaeological human collagen and keratin samples. The left panel subplots depict the first two PCA components (subplots A and C) and the right panel subplots the first two LDA discriminants (subplots B and D). The ordination analyses in subplots A and B are based on measured δ^{13}C-AA data and subplots C and D on EAA (Phe and Val) mean-centred δ^{13}C-AA data. The broken lines

in the LDA plots indicate the decision boundaries for whether individuals predominantly obtained dietary proteins from freshwater (FP), marine (MP), terrestrial C3 (C3P), or terrestrial C4 (C4P) sources. To produce this categorisation, we selected a subset of individuals with clear archaeological and environmental contexts. These 'known' individuals, denoted with open blank symbols in subplots A_1, B_1, C_1 and D_1, originate from Belize, Brazil, Bulgaria, Greenland, Guatemala, Japan, Serbia, and Romania (data from Honch et al. 2012, Colonese et al. 2014). Populations with less certain diets are featured with distinctly coloured symbols and polygons (data from Choy et al. 2010, Raghavan et al. 2010, Mora et al. 2018, Webb et al. 2018, Ma et al. 2021, Brozou et al. 2022). Subplots A_2, B_2, C_2 and D_2 mirror A_1, B_1, C_1 and D_1, respectively, but the symbols are colour graded from yellow to red according to the δ^{13}C-EAA mean value of each sample. The Odense and Pica 8 populations are based on tissues from the same individuals that reflect short-term (rib and hair) or long-term (femur and tendon) dietary histories. Detailed information about each sample can be found in Appendix S4.

5.3. Baseline isotope values as complementary markers of basal resources

Our meta-analysis of human data demonstrates that, similar to bulk δ^{13}C values, baseline δ^{13}C-EAA data serve as robust source markers when the factors controlling them in basal resources are well constrained. However, it remains relatively rare for ecological studies to integrate both baseline δ^{13}C-EAA values and source diagnostic δ^{13}C-EAA patterns. A successful application of this integrative approach is Vane et al.'s (2018) study, which used δ^{13}C-EAA analysis to track ontogenetic resource utilisation and migration of acoupa weakfish (*Cynoscion acoupa*) by comparing otolith edges of juveniles and adults with resources in their environment. Since juveniles inhabit Brazilian mangrove estuaries before moving to the coastal shelf as adults, juvenile otoliths were expected to be influenced by baseline δ^{13}C-EAA values of freshwater phytoplankton, making them more ^{13}C depleted than adults. The study found that the first principal component, driven by the dynamic range in baseline δ^{13}C-EAA values, separated freshwater and marine resources, while the second principal component, driven by δ^{13}C-EAA patterns (intermolecular δ^{13}C relationships), distinguished among freshwater phytoplankton, detrital mangrove leaves, and mangrove root rhodophytes. Ordination analyses of measured δ^{13}C-EAA data (as opposed to mean-centred δ^{13}C-EAA data) have also been successfully applied to track basal resource contributions in coral reefs (McMahon et al. 2016) and salt marshes (Johnson et al. 2019).

As exemplified by our meta-analysis of human compilation data, researchers must have a thorough understanding of the environmental conditions in a habitat to determine if they result in distinct δ^{13}C-EAA baselines. Baseline δ^{13}C values in basal resources are influenced by inorganic carbon sources, physiological adaptation, response to environmental conditions, and carbon fractionation in biosynthetic

pathways (section 2). In polar regions, sea ice melt affects CO_2-carbonate chemistry and creates a distinction in baseline δ^{13}C-EAA values between ice algae and pelagic phytoplankton, which are not CO_2 limited (de la Vega et al. 2019). In lacustrine systems, changing boundary layer formation and primary production can make it challenging to confine baseline δ^{13}C values unless the system is closely monitored (Zimmer et al. 2020). In terrestrial habitats, refixation of respired CO_2 and shady conditions can result in more negative δ^{13}C values compared to canopy vegetation δ^{13}C values. The isotope dynamics between these two habitats are highly dependent on growth season, solar radiation, topography, and wind conditions affecting understory air turbulence (Tejada et al. 2020).

When models or observational data on the physiochemical environment are insufficient to constrain or create adequate differentiation in baseline δ^{13}C values of basal resources, we recommend caution in using baseline δ^{13}C-EAA information in ordination analysis. A study by Larsen et al. (2020) of four functional groups from the Baltic Sea, including pelagic piscivores, benthic predators, planktivores, and suspension feeders, found that in some systems, baseline δ^{13}C-EAA variability may obscure information about niche space. This is because consumer tissues are composed of a mixture of δ^{13}C-EAA values from various basal resources over time and in different habitats, making it challenging to use single δ^{13}C-EAA values as a proxy for changes in marine basal resource composition. To gain a better understanding of changes in basal resources, it is essential to characterise the ecosystem-specific δ^{13}C-EAA patterns in both basal resources and consumer tissues.

6. Considerations for using archival tissues

Changes in basal resource use can occur over ontogeny, both within and between populations, and over seasonal to millennial scales. Tracking these changes accurately depends on the rate of dietary AA incorporation in various animal tissues (relative to the rate of change) and their preservation. Selecting one or multiple specific tissues from an individual organism that vary in their incorporation rates can indicate the basal resource use during a couple of days to an entire lifetime of the individual. The ability to reconstruct past basal resource use by a species relies on the integrity and preservation of tissues and their δ^{13}C-AA values over long time scales. Natural and artificial preservation have the potential to extend the basal resource reconstructions over timescales of several thousands of years under certain conditions. In this section, we discuss the components of tissue sample selection that are important for enabling specific basal resource reconstructions over time and space.

6.1. Temporal resolutions with consumer tissues

The incorporation of AAs is not uniform across various tissues due to tissue turnover and growth during an organism's lifetime at different rates, and therefore different tissues may reflect different timeframes of dietary history. Blood and soft tissues such as liver and muscles can be turned over completely within days or months depending on the metabolic rate of the particular tissue, age class or animal (Boecklen et al. 2011, Thomas and Crowther 2015, Vander Zanden et al. 2015). Hard and semi-hard tissues such as bones and ligaments are remodelled throughout life, but at different turnover rates according to age, gender, and physiological and pathological conditions (Hadjidakis and Androulakis 2006). By analysing different bones from ribs to femurs, a reconstructed dietary history can span an entire decade or more (Tieszen 1983, Fahy et al. 2017, Matsubayashi and Tayasu 2019). This dietary timespan can be expanded to a complete lifetime by analysing other collagenous tissues that are metabolically inert and therefore not remodelled after formation such as human dentine (Brault et al. 2014). Such tissues will reflect dietary history of the period of their formation during an individual's ontogeny. Metabolically inert keratin excrescences such as hair, nails, and feathers in mammals and birds can give consecutive dietary information on seasonal scales as they grow continuously until replaced during moulting seasons. Other keratin tissues such as scales of fish and reptiles, and whale baleen grow in visible increments and can be used to reconstruct partial life histories. Entire dietary life histories can be reconstructed from metabolically inert calcium carbonate structures such as bivalve shells, coral skeletons, and fish otoliths. During a continuous layered calcification process from the early embryonic stage throughout the entire individual's lifetime, small amounts of protein are incorporated on a daily basis (Edeyer et al. 2000, Borelli et al. 2001, Falini et al. 2015). Opaque band formations within these carbonate structures indicate favourable growth periods with higher incorporation of protein concentrations (Watabe et al. 1982). These visible incremental bands can be formed on daily, monthly and (sub)annual basis and can be used for estimating the age of the organism (Payan et al. 1999, Borelli et al. 2001, Falini et al. 2015). Chitin structures, such as cephalopod beaks and gladii, and cartilage vertebrae of sharks grow throughout an individual's lifetime displaying incremental bands that can be sampled for life history variations in basal resource use (Cherel et al. 2009, 2019, Magozzi et al. 2021). Mechanical structures such as cephalopod beaks and whale baleen lose material due to wear and therefore their temporal information will be limited to a certain timespan before the collection (Aguilar and Borrell 2021).

The temporal resolution gained from the increments in biogenic carbonates, chitin structures, and keratin excrescences is dependent on the AA concentration, increment width, structure size, and minimum analytical volume. The AA concentrations in shells, fish otoliths and coral skeletons are often low, generally ranging between 0.5 and 2% but can be up to 10% protein content (Degens et al. 1969) and with exceptions in proteinaceous corals (Williams 2020). Moreover, the AA composition can significantly differ between species and tissue types,for example the EAA methionine concentrations are often very low in many tissues while the NEAA glycine in bones are high. Thus, minimum analytical sample volumes and the target AAs often determine the temporal resolution that can be sampled from biogenic carbonate samples with low protein contents as higher sample volumes requirements may have to be drawn from across multiple increments.

6.2 Natural and artificial preservation of tissues

As proteinogenic AAs can withstand high levels of heat, gamma radiation and temperature changes, their preservation in hard tissue samples largely depends on whether they are compromised by AA leaching, augmentation or bacterial reworking (Grupe 1995, Collins et al. 2002, Iglesias-Groth et al. 2011). Several degradation indicators such as D- and L-enantiomer ratios of AAs and relatively constant baseline δ^{13}C-AA and δ^{15}N-AA values and patterns show that high density carbonate matrices such as egg and bivalve shells remain inert for at least 10,000 years under favourable conditions (Tuross et al. 1988, Engel et al. 1994, Macko et al. 1994, Silfer et al. 1994, Johnson et al. 1998, O'Donnell et al. 2007, Misarti et al. 2017). Unbound protein fractions in high density matrices are more prone to leaching and can disappear within the first 6000 years after an organism death under hot and aqueous conditions (Bada et al. 1999, Ortiz et al. 2018). Exogenous AAs can accumulate on the outer surfaces of hard tissues and should be removed prior to analysis with mechanical drilling, short washing with diluted HCl or sonication in distilled water (Engel et al. 1994). Removing traces of diagenesis is more challenging in porous structures such as coral skeletons and bones where exogenous AAs can be deposited over a large internal surface area (Bada et al. 1999). Lower density matrices such as bones and elastic tissues do not persist on geological timescales except under extremely favourable conditions. For example, while collagen and elastin have been detected with synchrotron Fourier-transform infrared spectroscopy in fossils from the Jurassic period, it is at insufficient amounts for δ^{13}C-AA analysis (Lee et al. 2017, Boatman et al. 2019). Bone structures are also more sensitive to environmental fluctuations, i.e. humidity and temperature shifts that can accelerate AA degradation by creating micro-fissures and porous structures in

biomineralized tissues (Grupe 1995, Maurer et al. 2014). To assess protein preservation in bones on archaeological and historical timescales, measuring the nitrogen content and atomic ratios of carbon to nitrogen is often standard (Brock et al. 2012). For external hard tissues like feathers and fish scales, physical abrasion and leaching can diminish the amount of proteins available for analysis (Salvatteci et al. 2012).

Soft tissues that readily degrade are best preserved in dried or frozen state for extensive time periods. However, natural history museums and research institutions often preserve them in solvents such as ethanol or with embalming fluids containing methanol and formaldehydes. Storage with these chemical preservation techniques seems to have no significant short-term effects (<1 year) on δ^{13}C-AA or δ^{15}N-AA values (Strzepek et al. 2014, Hetherington et al. 2019, Durante et al. 2020, Swalethorp et al. 2020). Alterations to δ^{13}C-AA and δ^{15}N-AA values have been observed for samples preserved up to 27 years (Hannides et al. 2009, Hetherington et al. 2019, Durante et al. 2020, Swalethorp et al. 2020). Beyond this, it is unclear how solvents affect $\delta^{13}C_{AA}$ values in proteinaceous tissues, but storage over centennial timescales or heating causes tissue disintegration and loss of AAs to the surrounding solvent (Von Endt 2000, Marte et al. 2003). It is likely that the preservation chemicals affect tissue integrity by impacting the peptide and protein bonds. This could lead to unstructured AA leaching into the surrounding fluids in the long term and thus affecting the δ^{13}C-AA values of the tissue as a whole due to mass-based diffusion differences. To fully embrace δ^{13}C-AA analysis of chemically preserved tissues further investigations into the leaching of AAs are warranted.

7. Minimising analytical uncertainties in the measurements of δ^{13}C-AA values

Precise and consistently accurate measurements of δ^{13}C values in individual AAs are crucial to detect the fine distinctions in basal resource δ^{13}C-EAA fingerprints and consumer δ^{13}C-EAA patterns. The methodology for carbon isotope analysis in AAs is however longer and more complex (summarised in Fig. 7) than bulk stable isotope analysis, increasing the likelihood of errors in measured δ^{13}C-AA values. Prerequisites for bulk isotope analysis are limited to the weighing of dried tissue that is then completely combusted in the elemental analyser, although high concentrations of lipids or minerals may be chemically removed during tissue preparation. The amount of tissue material needed for bulk isotope analysis can be considerably less than for AA analysis (for carbonate analysis from ~25 µg to approximately 5 mg respectively), which can limit the resolution with which hard tissue increments can

be analysed. Typical protocols for AA analysis include acid hydrolysis of dried tissues, where strong acids (6M HCl) for 70 minutes to 21 hours at high temperatures of 110-150°C respectively, are used to break the peptide bonds and extract the individual AAs (Enggrob et al. 2019, Silverman et al. 2022). However, acids can lead to degradation of certain AAs, such as tryptophan and cysteine. Purification of tissues from non-AA compounds to prevent chromatographic co-elution can precede or follow the acid hydrolysis (Fig. 8). The measurement of carbon isotopes in AAs can be done on a gas chromatograph interfaced to a combustion reactor and isotope ratio mass spectrometer (GC-IRMS) or a set up with a liquid chromatograph (LC-IRMS). For GC-IRMS, naturally polar AAs need to be volatilized with derivatization protocols, whereas AAs can be directly analysed after acid hydrolysis and purification with a LC-IRMS. However, LC-IRMS has currently lower chromatographic AA separation abilities and needs approximately 20x more sample volume compared to GC-IRMS (Smith et al. 2009, Dunn et al. 2011). This limits its use, precluding small and/or low AA concentration samples such as otoliths or shells. To ensure stable isotopic measurements of AAs over long analytical periods, reference AA compounds should be added to the analysed AA sample or run alongside the analytes. Currently, diverse approaches to sample treatment, derivatization protocols, and instrumentation exist between laboratories with relatively unknown effects on δ^{13}C-AA measurements. We therefore highlight the most likely areas for error in sample preparation.

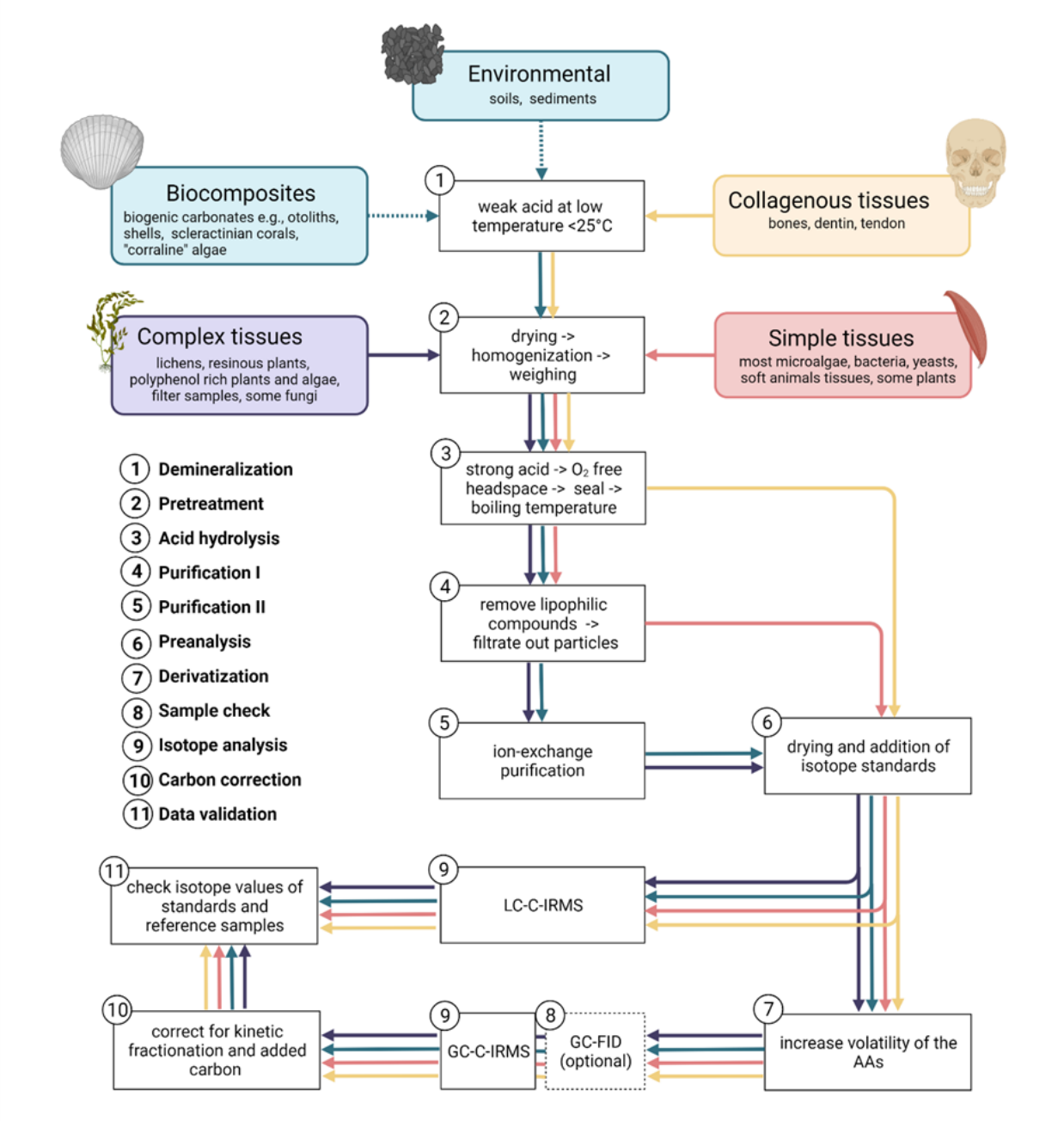

Figure 7. Proposed standardised analytical protocols for different sample types from sample preparation to post-analysis. Broken lines towards the mineralization step indicate that this treatment is only needed for certain sample types such as collagenous tissues or materials rich in biogenic minerals (step 1). Solvents should be evaporated instead of discarded to avoid potential AA loss with the exception of collagenous samples that are relatively insoluble. Remaining minerals will be removed with ion-exchange purification (step 5). With the derivatization method, methoxycarbonyl (MOC) esterification, the demineralization step of certain samples such as otoliths and shells can be bypassed due to the lack of water sensitive solvents. MOC derivatization is therefore also

directly applicable on blood samples without drying (Walsh et al 2012). All other tissue samples need to be dried (step 2) before acid hydrolysis (step 3). For samples with an excess of lipids or non-hydrolysable plant particles, a first purification with solvents can be applied (step 4) before isolating the AAs from all other compounds with ion-exchange columns (step 5). Solvent and bases eluting AA from the ion-exchange columns are evaporated and reference standards are added to the AA sample (step 6). After subsequently dissolving the AA sample in a slightly acidic solution, it can be analysed with liquid chromatography combustion isotope ratio mass spectrometry (LC-c-IRMS, step 9). Analysis on a gas chromatography combustion isotope ratio mass spectrometry (GC-c-IRMS) requires AA volatilisation by derivatization (step 7). As the GC-IRMS has a comparatively lower combustion capacity, a more accurate evaluation of the hydrolysable AA concentrations in the sample can be performed on a GC coupled to a flame ionisation detector (GC-FID, step 8). Derivatisation agents add distinct amounts of carbon according to the functional groups of individual AAs or also known as kinetic fractionation. Thus, the acquired $\delta^{13}C_{EAA}$ values have to be corrected with individually determined correction factors for each AA (step 10). Data validation for precision and accuracy of the measured δ^{13}C-EAA values can then be assessed with reference materials that have been analysed in parallel with the AA samples (step 11).

7.1. Purification of amino acid samples

The removal of non-AA compounds, such as lipids, minerals, calcium carbonate, and urea, is often one of the first steps to avoid error in stable isotope analysis. These compounds can co-elute with individual AA compounds in the chromatography or accumulate in the GC-IRMS liner that can lead to AA peak tailing and increased incidences of co-elution. As a chromatographic peak elutes with the lighter ^{12}C compounds first and then with the 'heavier' ^{13}C compounds, overlap or co-elution of AAs with either peak end or start of other compounds lead to inaccurate measurements of the individual δ^{13}C values of AAs (Meier-Augenstein 2002, Sessions 2006). Non-AA compounds can also react with derivatization chemicals and deplete them before reacting with the AAs, leading to lower AA concentrations eluting on the GC-IRMS. Some purification protocols use extensive treatments to remove non-AA compounds by soaking them in acidic solutions for extended periods followed by repeated rinses with purified water. Excess pretreatment fluids are then removed as supernatant or through filtering. As these aqueous pretreatments take place before acid hydrolysis, the tissue samples are still in their protein constellation, including small peptides and free (unbound) AAs. Due to the hydrophilic nature of some proteins (e.g. glycoproteins) and EAAs (e.g. lysine, tyrosine, histidine, threonine), this could potentially lead to their dissolvement and partial removal with the pretreatment fluids. This disposal of AA constituted compounds may lead to an alteration in the δ^{13}C-EAA values of the pre-treated tissue. These

pre-treatments are predominantly performed on consumer tissues to remove excess lipids or urea, while the dietary tissues are left untreated (see Appendix S5). With the potential loss of EAAs and subsequent alteration of the δ^{13}C-EAA values in the consumer tissue, this can result in an artificial offset between dietary and consumer tissue δ^{13}C-EAA values.

Comparing 17 controlled feeding studies that investigated the hypothesis of direct EAA routing from diet to tissue, where $\Delta^{13}C_{diet\text{-}tissue}$ values are expected to be ~0‰, some feeding studies observed $\Delta^{13}C_{diet\text{-}tissue}$ for individual EAAs can deviate by -12 to 13‰ without a consistent direction (Hare et al. 1991, Johnson et al. 1998, Howland et al. 2003, Jim et al. 2006, Newsome et al. 2011, 2014, 2020, Whiteman et al. 2018, Manlick and Newsome 2022, Fig. 8, Appendix S5). Other studies however observe values of approximately 0‰ for each individual EAA (McMahon et al. 2010, 2015b, Webb et al. 2017, Lui et al. 2018, Takizawa et al. 2020, Wang et al. 2019a, Huneau et al. 2019, Barreto-Curiel et al. 2019, Fig. 8, Appendix S5). Large offsets were found in studies that used extensive water rinses and light acidic treatments and mention removing these solutions from the consumer tissue samples (Fig. 8, Appendix S5). Other potential mechanisms for such differences may include analytical measurement deviations or experimental time periods that are shorter than the time needed for tissue δ^{13}C-EAA values to reach full equilibrium with the experimental diet. Also the analytical error enhanced by the correction for added carbon during derivatization, and the underrepresentation of the variation in dietary δ^{13}C-EAA values due to analysing too few diet samples can account for some of the offsets in all studies. However, as these are common considerations in controlled feeding studies, we do not believe that they are the main cause of the excessive offsets in δ^{13}C-EAA values between diet and consumer tissue.

Water rinses used for sample purification have been discouraged for bulk isotope analysis due to them resulting in large and inconsistent carbon isotopic variations (Serrano et al. 2008, Brodie et al. 2011, Schlacher and Connolly 2014, Pellegrini and Snoeck 2016). We therefore encourage investigating if the same issue arises with AA analysis. Until this has been resolved we recommend to apply purification protocols after acid hydrolysis with for example organic solvents only, and cation exchange or solid phase extraction columns (Fig. 7, McMahon et al. 2010, Takano et al. 2010, Ohkouchi et al. 2017). Organic solvents are usually used to separate high amounts of lipids in tissues or sample debris from the AAs. They include non-mixing solvents such as dichloromethane and n-hexane, where the latter is insoluble to AAs and removed. Cation exchange resins bind positively charged AAs to the negatively charged resins that are released when a strong base is run through. Solid phase extractions, however, are not efficient for demineralization as the minerals likely react with the solid phase and prevent AA elution (Vane pers.

obs.). Purification protocols with cation-exchange columns lead to negligible loss and carbon fractionation of AAs (Takano et al. 2010). The exception to applying acidic pretreatment are well preserved bone materials where whole bones are dissolved in light acids for a short period without powderizing to extract the collagen (Sealy et al. 2014). Removal of bone carbonate AA is necessary as it is more susceptible to diagenetic processes and has different turnover times than collagen (Stafford et al 1988, Lambert and Grupe 1993).

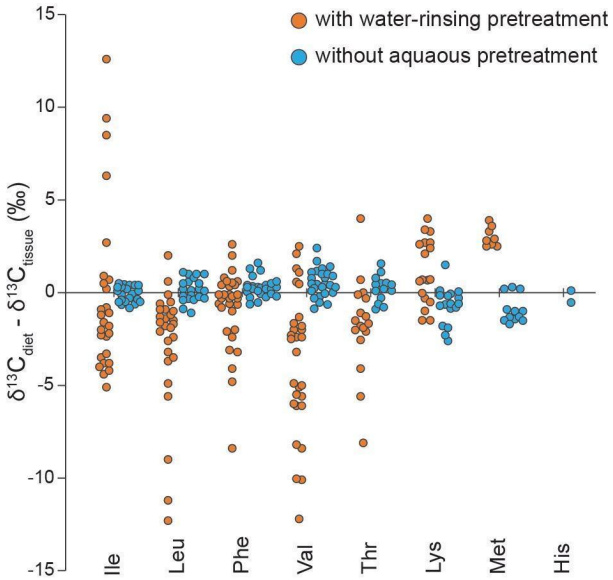

Figure 8. The differences in measured $\delta^{13}C$ values for individual EAAs, isoleucine (Ile), leucine (Leu), phenylalanine (Phe), valine (Val), threonine (Thr), lysine (Lys), methionine (Met), histidine (His), observed between diet and consumer tissue in 17 separate controlled feeding studies divided on the use of water-rinsing pretreatments of the tissue samples. Consumer tissues vary from muscle, intestinal, heart, and liver tissue, to bone collagen, blood plasma and eggshell, while diets were divided on for example C_3/C_4 origins, percentages of protein, carbohydrate and lipid, and prey organisms. See S5 for specific details on individual studies.

7.2. Error propagation, accuracy and precision during measurements of $\delta^{13}C$-AA values

Error propagation, large deviations in measured $\delta^{13}C$ values due to errors introduced into analytical processes, can arise from the derivatization protocols needed for analysis on a GC-IRMS and technical deviations in the instruments. Derivatization chemicals should be added in excess amounts to avoid rate-limited chemical reactions that could cause isotope effects. Since derivatization adds exogenous carbon to AAs, it is necessary to calculate the resulting offset in $\delta^{13}C$ values between the derivatized and

non-derivatized AAs. This can be done by leveraging mass-balance equations and predefined isotope correction factors, but it comes with the caveat that it can potentially introduce and propagate errors (Fig. 7, Docherty et al. 2001, Takizawa et al. 2020). These error propagations can be minimised with reagents that have $\delta^{13}C$ values closer to those of the analysed samples. The extent of the corrections and error is exacerbated by adding large carbon chains to individual AAs with derivatization methods such as *N*-pivaloyl/isopropyl esters (NP/iPr) and N-trifluoroacetyl isopropanol esters (TFAA) in comparison to methoxycarbonyl (MOC) esterification (Silfer et al. 1991, Corr et al. 2007, Walsh et al. 2014). Errors in measured $\delta^{13}C$-AA values can also be introduced when water-sensitive derivatization agents are used, such as acetyl chloride and acetic anhydride in *N*-acetylmethyl (NACME) and TFAA methods. This can lead to a reaction with the water retained by the hydrophilic $CaCl_2$ during the drying process of acid hydrolyzed $CaCO_3$, laboratory humidity or incomplete drying steps during the derivatization protocols. The formed compounds can appear in the chromatography and alter the $\delta^{13}C$ value measurements when co-eluting with AAs. Water-sensitive derivatization agents are absent in MOC protocols and thus there is no need for demineralization of samples and likely enables the analysis of small volume biogenic carbonate increment sampling (Vane et al. 2018). However, the slightly acidic starting solution in MOC affects the NEAA glutamic acid $\delta^{13}C$ values, and to a lesser extent aspartic acid, as the low pH and the catalysing pyridine will result in its cyclization into pyroglutamic acid (Walsh et al. 2014, Yarnes and Herszage 2017). There is an unknown effect of isotopic stability of TFAA derivatized samples that can only be kept for several days, while NACME and MOC derivatized AAs are known to be stable for several months. NACME is often a preferred derivatization protocol due to its high precision, long stability and enabling measurements of all hydrolysable NEAAs.

Ensuring consistency and comparability in $\delta^{13}C$-AA measurements across time and between analytical facilities is critical. Good chromatographic practices, including baseline separation between individual compounds, Gaussian peak shapes, and maintaining the linearity range of isotope analyses, promote accuracy and precision. Monitoring the analytical stability of instrumentation and the consistency of $\delta^{13}C$ values measurements of AAs across time and projects is crucial to avoid deviations in isotopic measurements (Meier-Augenstein and Schimmelmann 2019). This can be monitored by continuously running commercially available internal (added to the analysed sample) and external (run separately in between samples) reference compounds. Each set of references should ideally encompass $\delta^{13}C$ values at both the lower and upper extremes of the analysed sample spectrum. Reference compounds can be divided into those that require derivatization prior to GC analysis and those that do not. As for the

internal standards, pre-derivatization compounds such as aminocaproic acid (an isomer of lysine) or norleucine (an isomer of leucine) can either be added pre or post acid hydrolysis to monitor potential losses and isotope effects during these chemical steps. However, their practical use of internal references can be challenging as AA concentrations in samples are often unknown, making the estimation of internal reference material additions problematic, especially for samples with low AA concentrations. Post-derivatization compounds include *n*-alkanes, acetanilide, and caffeine. Users should check that these compounds do not co-elute with the derivatized sample AAs. When considering the sets of external reference compounds, it is critical to include a set of AAs with known isotope values with every batch of derivatized samples (Fig. 7, Roberts et al. 2018, Meier-Augenstein and Schimmelmann 2019). This accounts for isotope effects attributed to added carbon during derivatization and kinetic isotope effects during chemical reactions. The non-derivatized external references serve to calibrate the $\delta^{13}C$ value of the reference CO_2 monitoring gas and monitor long-term stability and instrument drift in $\delta^{13}C$ values. Typically, these external reference compounds consist of a set of short to long-chain n-alkanes with isotope values that have been validated and referenced across multiple analytical facilities (Schimmelmann et al. 2016).

To reduce the variability of carbon fractionation during the derivatization process, it is important to carry out complete reactions and thoroughly remove all derivatization solvents. The increased volatility of derivatized AAs means they can easily evaporate, particularly if overheating or prolonged drying occurs. This may result in partial or total evaporation of the derivatized AAs, with low-molecular weight derivatives being especially susceptible once they reach boiling point. As the composition of sample matrices often differs, even within a sample batch, meticulous attention should be given to achieving consistent dryness following each chemical treatment step as individual samples can have distinct drying times.

As discussed above, variations in analytical protocols, equipment, and sample matrices can lead to biases between datasets generated in disparate analytical facilities. To counteract these biases, it is essential to establish a widely available repository of biological reference materials. However, identifying appropriate biological reference materials for $\delta^{13}C$-AA analysis has proven challenging. Biological reference materials must be homogeneous, easily transportable, and ideally non-hazardous, i.e. they should not be biologically active. Similar to commercially available single compounds, there should be two sets of each biological reference material, ensuring they cover $\delta^{13}C$ values at both the lower and upper ends of the sample spectrum analysed. Possessing such reference materials would enable $\delta^{13}C$-AA data measured

across various studies and facilities to be compared accurately and with greater confidence. This would be further supported by increased standardisation of methodologies (Fig. 7), as the diverse protocols and chemicals currently utilised may introduce additional biases into isotopic values measured at different facilities.

8. From qualifying to quantifying basal resource contributions

Consumer δ^{13}C-EAA patterns are a composition, or linear combination, of the δ^{13}C-EAA patterns in the basal resources at the base of the food-web that are assimilated to synthesise their tissues (see section 4.1). This is known as a linear mixing system. Linear mixing systems and the analysis of compositional data have a long history spanning many branches of science where such data structures are common. Examples range from geology and the analysis of mineral composites (Weltje et al. 1997) to remote sensing where incoming spectra are mixtures of pure spectral components (Clevers and Zerita-Miller 2008). The statistical framework used to estimate the proportional contributions of known endmembers to compositional data is known as a linear (un)mixing model (Weltje et al. 1997, Phillips 2012, Parnell et al. 2013).

Over the past 20 years, there has been significant development of mixing models that specifically address many of the issues associated with biological systems. These include complex data structures, such as varying consumer traits and individual trophic specialisation that impart variation in basal resource use in individual consumers (Semmens et al. 2009, Stock et al. 2018); tracer concentration dependence (Phillips and Koch 2002); the multitude of potential basal resources within ecosystems, various combinations of which could result in the same δ^{13}C-EAA patterns (known as an under-determined mixing system, Parnell et al. 2010); and natural variations and measurement errors that add uncertainty to resource and consumer tracer values (Moore and Semmens 2008, Stock et al. 2018). In this section, we outline the use and application of mixing models pertaining to δ^{13}C-EAA data, highlighting key considerations, assumptions and limitations that bring both opportunities as well as caveats when applying mixing models. While several different implementations of mixing models are available (Wang et al. 2019b, Cheung and Szpak 2021, Heikkinen et al. 2022), we primarily focus on those

implemented in the MixSIAR package in *R* (Stock et al. 2018), due to its flexibility, relatively common use across ecological studies, and the familiarity of the authors with this software.

8.1. Consolidating basal resource information

The area bounded by basal resource δ^{13}C-EAA fingerprints (endmembers) demarcates the available mixing space: the area that defines all possible consumer tissue δ^{13}C-EAA patterns (mixtures, Phillips et al. 2014, Smith et al. 2013). The dimensionality of this mixing space is equal to the number of individual tracers. For δ^{13}C-EAA data, this is the number of EAAs, typically five or six. Hence, dimensionality reduction tools such as PCA are useful to visualise distinctions between different resources and alignment between basal resources and consumers. All potential basal resources that can contribute to consumer δ^{13}C-EAA values should be characterised (see section 3.2), otherwise information regarding the endmembers that constitute the mixture is incomplete. The proportional contributions of each basal resource are not independent of each other: they must, by definition, sum to one. Missing basal resources is therefore a general problem when resolving linear mixing systems (Weltje et al. 1997) and will result in inaccurate proportions regardless of the statistical approach. Consumer tissue δ^{13}C-EAA data falling outside of the mixing space can indicate missing resources. However, even if consumers fall within the basal resource mixing space, it is still possible that some basal resources used have not been characterised.

While missing endmembers are problematic, it is important to limit basal resources to only those that likely contribute to consumer tissues. While it may seem reasonable to include as many basal resources as possible, an underlying assumption of mixing models is that all defined endmembers contribute to the mixture to some degree, even if that contribution is only very small. Excluding unused basal resources limits model complexity, aiding model performance. Furthermore, it improves model accuracy by removing potentially isotopically feasible but biologically unrealistic resource combinations. Conversely, statistical artefacts arise when resolving mixing models with high numbers of basal resources regardless of the number of tracers used (solutions will tend towards 1/n for large n). Therefore, it is recommended to limit mixing models to seven or fewer resources (see Stock et al. 2018 for details). While data visualisation (e.g. PCAs) may help verify whether particular basal resources contribute to consumers, exclusion of basal resources should ideally be based on a priori knowledge of the study system.

Once the consumer-relevant basal resources have been determined, any modifications to tracer values between basal resources and the consumer tissues (and their variability) need to be defined. These are typically referred to as trophic discrimination factors (TDFs, which are tracer, source and even consumer specific). While TDFs present an additional consideration for other types of tracers (Schulting et al. 2022), they are considered negligible for δ^{13}C-EAA data. Due to the spatiotemporal consistency of δ^{13}C-EAA fingerprints, sampling does not need to occur during the time period in which AAs are incorporated into consumer tissues nor within the spatial extent of the consumers sampled (as is for the case for baseline δ^{13}C-EAA values or other tracers, Phillips et al. 2014). This is particularly pertinent to studies using historical data or retrospectively reconstructing time-series of basal resource use, easing the logistical infeasibility of complete resource characterisation. Consideration should also be given to other sources of uncertainty. Basal resource δ^{13}C-EAA data should include their natural variation along each AA. Logistical and analytical constraints may result in low sample replication of basal resources, and therefore isotopic variation being inadequately described. While the uncertainty due to low sample size can be incorporated into Bayesian mixing models, it will reduce precision in model solutions. Alternatively, basal resource $\delta^{13}C_{EAA}$ variation could be approximated using available literature sources that are well described. However, current differences in methodologies and analytical processes among studies without international reference materials impairs the use of basal resource δ^{13}C-EAA values collated from the literature. Interestingly, uncertainty in instrumental precision when measuring δ^{13}C-EAA values is rarely considered when quantifying basal resource use (Hopkins and Ferguson 2012; but see Vane et al. 2023). This may be because instrumental error has rarely been considered more generally within mixing models. The mixing model framework initially developed for bulk stable isotope analysis is based on data where instrumental error estimates are often very low and therefore can be considered negligible (typically 0.1-0.2‰ for bulk δ^{13}C and δ^{15}N). For δ^{13}C-EAA values, analytical uncertainty can vary between different AAs (~1‰), and therefore should be incorporated into mixing models to ensure model uncertainty estimates are not artificially deflated.

8.2. Modelling consumer behaviour

Once δ^{13}C-EAA values of basal resources have been established, focus should be given to the consumers. Specific hypotheses regarding their basal resource use will inform how mixing models will be structured.

Factors that may explain differences in basal resource use between individual consumers need to be accounted for. This could include characteristics such as species, biological sex, size/ontogenetic stage (e.g. juvenile, subadult, adult) or social status that may result in differences due to differing nutritional requirements or limiting access to specific dietary items. For example, smaller individuals may not be able to capture larger prey items or lower social status could restrict access to nutrient-dense foods, such as meat. Hierarchical spatial structuring of consumers should also be accounted for (e.g. distinct subpopulations within larger areas or spatially discrete sampling sites within a region). These can affect resource availability, and therefore the 'realised' basal resource use, even if preferences are the same among individuals (Semmens et al. 2009). This similarly applies to consumers that were sampled at different time periods (e.g., seasons, years). Bias in consumer sampling or failing to account for these potential drivers can lead to false inferences as estimates will not reflect the realised basal resource use of the true population(s).

A key strength of Bayesian mixing models is the ability to incorporate prior information on basal resource use. External estimates of resource use, for example from mass-balanced food web models, can be directly incorporated to inform model solutions (Stock et al. 2018). However, such approaches should be used with caution, especially if prior information is itself biassed (e.g. stomach and scat data towards poorly-digestible prey), as they can overly restrict mixing model solutions (Swan et al. 2020). Theoretically, known nutritional limitations, such as macronutrient requirements, could be included for cases where consumers are omnivorous with considerable diversity in diet quality. While incorporating informative priors can be fruitful, it is important to recognise that such prior information often relates to questions of diet (i.e. the proportions of various prey assimilated by a consumer) and may therefore not be applicable when regarding hypotheses of basal resource use using δ^{13}C-EAA data.

Error structures, although important, are often overlooked in mixing models. For groups of consumers, residual errors in MixSIAR are modelled as a multiplicative term (called a residual stretch error, rather than additive Gaussian noise) that stretches or compresses the variance attributed to model processes (point source sampling, and source and TDF variance) to fit to the consumer data (Stock et al. 2016, 2018). This is conducted separately for each isotopic tracer. The ecological justification is that consumers sample sources many times as they assimilate dietary biomolecules into their tissues through feeding

events, and therefore should dampen the natural isotopic variation observed in sources. This contrasts the underlying mathematics that sample source tracer values from their distributions only once when estimating model solutions. Residual stretch errors are therefore expected to take values between 0 and 1 in order to compress variation due to feeding behaviours. Values approaching zero can be interpreted as an increase in the number of feeding events reflected in the consumer tissue, synonymous with a slower tissue turnover rate. However, values in excess of one indicate that further processes are causing variation other than those captured by the mixing model structure. In this framework, consideration needs to be given to the prevailing drivers of within-group isotopic variation in consumers (which mixing models assume to have identical diets) and how they obtain their proteins. For more passive trophic behaviours such as sessile filter-feeding or grazing, the stretch error approach appears to work well (Stock et al. 2016). However, active and selective feeding modes in motile consumers may violate the assumption of stochastic source sampling across individuals, and will result in inflated residual stretch error estimates. In such instances it may be more appropriate to model unique diets to each individual by incorporating individuals as a random effect in the model structure. The drawback of this approach is that it will result in all residual intra-group variation in δ^{13}C-EAA values, after accounting for modelled factors, being solely attributed to differences in individual resource use. In reality, most systems likely comprise some degree of individual variation in resource use as well as other undefined sources of isotopic variation. While the suitability of different error structures can be explored in terms of the goodness of fit of the mixing model (Cheung and Szpak 2021), emphasis should be given to the biological interpretations and their trade-offs within the studied system.

8.3. Mixing model output: Interpretation and considerations

Implemented mixing models provide a suite of solutions for the given model structure and set of basal resources. Contemporary mixing model software packages implement a Monte-Carlo Markov Chain (MCMC) Bayesian framework providing model solutions as a set of posterior draws (Parnell et al. 2013). Average proportional contributions, the effects of the various modelled factors (e.g. size, biological sex), and desired confidence intervals can then be calculated from the posteriors. If further indices or metrics are required, such as the degree of dietary overlap between individuals, then these should be calculated within each posterior draw of mixing model solutions, providing a posterior estimate of the metric itself. It is necessary however to first check whether basic model assumptions are met, the model has properly

converged, and the optimal model structure has been determined (see Phillips et al. 2014 for details on these general aspects of mixing models).

One key aspect of a mixing model's ability to accurately estimate basal resource use by the consumer is the distinction between basal resources. If two basal resources cannot be distinguished, i.e. do not have unique δ^{13}C-EAA fingerprints, then this will result in a strong negative correlation between the proportional contributions of those two sources across model solutions and potential bimodality in their proportional distributions (Phillips et al., 2014). In such cases it is prudent to, post-analysis, combine the proportional contributions of the two indistinguishable basal resources into a single group. While this reduces the basal resource resolution, often it will drastically reduce the uncertainty in proportional resource contributions. Basal resources that highly overlap in PCA space, i.e. have very similar δ^{13}C-EAA patterns (Fig. 4), will be indistinguishable from a mixing model perspective. This is often tested for statistically by comparing the mean δ^{13}C-EAA values of sources for each AA separately: basal resources whose δ^{13}C-EAA values do not statistically differ across all EAAs are considered indistinguishable. However, such statistical tests depend on large sample sizes to be robust measures of equality of means (Stock et al. 2018), which is typically not the case for δ^{13}C-EAA data. Furthermore, while mean δ^{13}C values may be similar for some EAAs, this does not reflect the multivariate space within which the mixing models operate and differences between variances and covariances of basal resources are not examined. If required, statistical scrutiny should be conducted using a multivariate approach, such as estimating pairwise Bhattacharyya coefficients (see Fig. 4) that quantify the alignment or 'closeness' of multidimensional distributions. If two or more sources are isotopically similar, it is still recommended that their proportional contributions be combined post analysis rather than merging them prior to implementing the mixing model (Stock et al. 2018). During individual statistical comparisons of source tracers, it may be identified that all sources may exhibit similar means across one or more EAAs. It may seem logical to remove statistically similar tracers to reduce model complexity and aid model convergence. However, in doing so users could unintentionally be removing AA tracers that help mixing models to resolve by reducing information on differences in basal resource variances or covariances. Increasing numbers of tracers in mixing models can only maintain or reduce overall model uncertainty (assuming the tracers are robust), therefore it is recommended that all available measured tracers are included in mixing models. This has been demonstrated for δ^{13}C-EAA data with mice fed varying specialised and mixed experimental diets, with mixing models including the full suite of AAs giving solutions closest to the various known diets with reduced uncertainties compared to those using a

restricted set of AAs and other statistical approaches used to quantify basal resource use (Manlick et al. 2022).

Consideration should be given to the trade-off of attributing intra-group variability in consumer tissue δ^{13}C-EAA values to consumer-resource sampling processes (with residual stretch errors) or differences in individual basal resource use using random effects (see section 8.2). If implemented, interrogation of stretch errors can identify whether one or more basal resources have been insufficiently characterised or if there are other issues with model components, e.g. analytical uncertainty. Stretch errors slightly greater than one are not necessarily suggestive of poor quality of results. There are many complex biological and ecological processes and interactions that impart variability: it is simply not feasible to measure and capture them all within statistical models. However, stretch error values that are much greater than one are a potential indication of one or more substantive processes that are lacking from the mixing model. If stretch errors are inflated for many to all of the EAA tracers, then this likely indicates missing but significant driver(s) of basal resource use from the model structure. Likely factors that may be missing, such as age-based variations in resource use, should be identified and incorporated into the mixing model structure if feasible. Conversely, if only one or a few EAA tracers have inflated stretch errors, then it is unlikely that this could be attributed to unexplained differences in basal resource use (which would typically affect all tracers in the mixing model). Instead, more EAA tracer-specific sources of variation need to be identified. This could include a missing basal resource that significantly differs in δ^{13}C values for the identified EAAs (Vane et al. 2023). Poorly constrained EAA specific TDFs/variances due to, for example, varying analytical precisions across EAAs that are not included in the model may also result in EAA-specific stretching. Finally, it could be an indication of a potentially unknown EAA routing mechanism in the consumer. While such situations may be problematic when addressing specific hypotheses, they can be useful in pinpointing further avenues of research by highlighting inadequacies in current knowledge or assumptions.

The ability of a mixing model to partition basal resource use with precision ultimately depends on the mixing space, the positions of basal resources and consumers within it, and their uncertainties. Robustly quantifying basal resource use can therefore be highly ecosystem-specific. A large mixing area relative to the variation observed within basal resource δ^{13}C-EAA patterns is ideal in reducing uncertainty in estimates. If consumers are specialised in utilising only a few, isotopically similar basal resources, then their δ^{13}C-EAA pattern mixing area will also be restricted. This can be exacerbated if other sources of uncertainty, such as measurement errors for individual EAAs, are large. Small signal to noise ratios in

δ^{13}C-EAA data are reflected in large uncertainties in mixing model proportional estimates. Large confidence/credible intervals in model estimates in these cases reflect the true uncertainty associated with disentangling basal resource use given the EAA tracers and system structure. In such instances, the use of δ^{13}C-EAA baseline values instead of δ^{13}C-EAA patterns, may prove fruitful where strong environmental gradients separate δ^{13}C-EAA baseline values in basal resources, enlarging the mixing area (Vane et al. 2023). However, this requires basal resources to be sampled within the same spatiotemporal window as the consumers (see section 5.1).

8.4. Conceptualising the quantification of basal resource EAA use

Carbon stable isotope analysis of EAAs presents opportunities and additional complexities for isotope-based mixing model approaches compared to those focused on bulk stable isotope data. The relatively direct routing of EAAs into consumer tissues results in the δ^{13}C-EAA values of basal resources remaining little altered as they pass through food webs. δ^{13}C-EAA values are therefore ideally suited to address hypotheses such as the flow of basal resource biomass through food webs. This contrasts with the theoretical underpinning upon which ecological mixing models were developed, which was to address questions of consumer diets, i.e., the identity of ingested biomass (prey items) that is assimilated into consumer tissues. While these conceptual differences appear nuanced, they need to be considered during study design, sample collection and data analysis to avoid erroneous inferences. Fundamentally, which (and how) sources are collected and analysed will depend on whether the research objectives focus around questions of basal resource use or diet (Parnell et al. 2014).

The application of basal resource training datasets is becoming commonplace in δ^{13}C-EAA studies (section 4.1), and more expansive (e.g. Arsenault et al. 2022b). Due to the ecosystem-specific and potentially study-specific nature of δ^{13}C-EAA fingerprints (section 3.1), and the lack of interlaboratory reference materials (section 4.1 and 7.2), using such training datasets results in inflated variation and potential bias (mean offsets) in quantified basal resource δ^{13}C-EAA fingerprints. Therefore using training datasets when estimating consumer-basal resource use is questionable. This is highlighted in Fig. 9 where we show in LDA space how the global compilation of basal resource δ^{13}C-EAA patterns inflates variation compared to more suitable in-study sampling designs for two disparate ecosystems. Mean δ^{13}C-EAA pattern bias can also be observed for several basal resource groups (notably fungi, plants, marine microalgae and red macroalgae). Mixing models are sensitive to input data, including

endmember values (Bond and Diamond 2011). Therefore, applying mixing models with broad training datasets would increase uncertainty in mixing model solutions and could lead to false inferences as implausible basal resource combinations adequately resolve consumer δ^{13}C-EAA patterns (Manlick and Newsome 2022). However, logistical constraints often limit basal resource sampling and analysis. In such instances, the application of compilation data requires a balance between inadequate but system-specific sampling versus selectively compiled out-of-study basal resources that will incorporate variability and biases from processes beyond the ecosystem of interest.

Quantifying proportional basal resource use by metazoans through mixing models in a rigorous manner is by no means trivial. As described throughout this section there are many underlying conditions and assumptions for robust proportional estimations. Consequently, other semi-quantitative techniques have recently been implemented to resolve mixing systems, notably LDA-based classification approaches (Radice et al. 2019, Fox et al. 2019, Skinner et al. 2021, Arsenault et al. 2022). Arguments advocating for this approach include a "less rigid framework" regarding uncharacterised resources and multivariate mixing space geometry (Fox et al. 2019, Manlick and Newsome 2022). Such arguments misconstrue that the "rigid" assumptions are inherent to the Bayesian mixing model methodology rather than being fundamental to mixing systems themselves. For example, individual δ^{13}C-EAA values of consumers falling outside of the basal resource mixing space after accounting for modifications implies an inadequately described mixing system (section 8.1). This general problem can often be masked by LDA dimensionality reduction, but is likely more noticeable when implementing Bayesian mixing models. Recent simulations on lake ecosystem data highlight that significant bias can occur between known basal resource contributions and those estimated using the LDA approach (Saboret et al. 2023). Moreover, we argue that the perceived limitations of mixing models should be considered a strength in that they require adequate prior understanding of the system (Makarewicz and Sealy 2015) for robust proportional estimates. It is frequently highlighted that mixing models are only as good as the data that goes into them (Phillips et al. 2014), yet they can also only be as good as our understanding of system processes. If we cannot describe these using mathematical abstraction, then attempting to quantify them becomes folly.

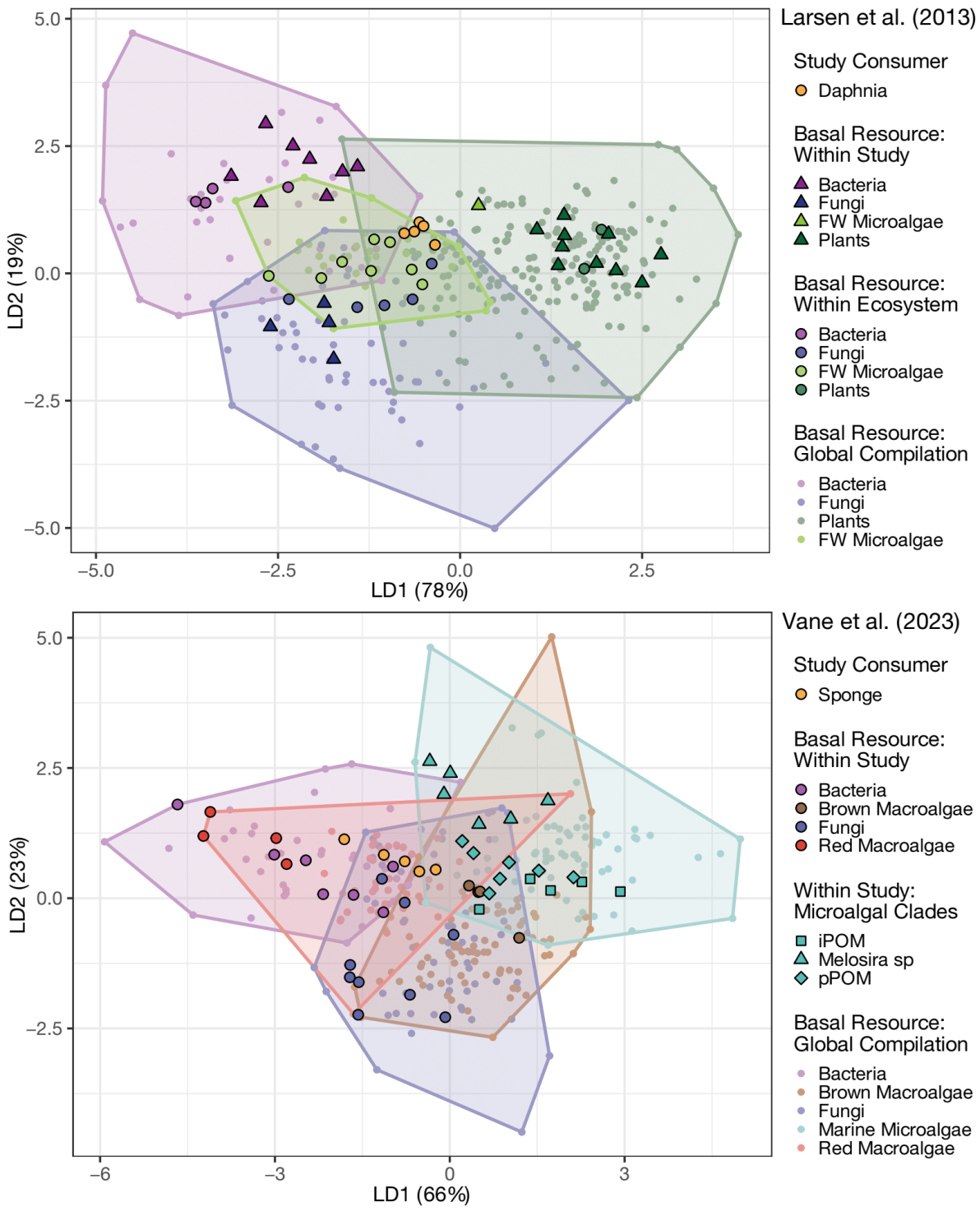

Figure 9. LDA plots highlighting the increased variation and potential offsets introduced to the characterisation of basal resource δ^{13}C-EAA patterns when using global compilation datasets (individual data points plus their convex

hulls, Fig. 4) compared to within study sampling designs relevant to the studied metazoan. Data from two study systems have been used A) the water flea *Daphnia* sp. in Arctic freshwater lakes of Alaska (Larsen et al. 2013) and B) an Arctic sponge at the sea ice marginal zone in the northern Barents Sea (Vane et al. 2023). CAM plants and extremophile bacteria were excluded a priori as they do not contribute to study ecosystems (section 3.1). Larsen et al. (2013) sampled basal organisms directly from within the study ecosystem (within study, denoted by triangles) and from other similar but spatially separated ecosystems, including phytoplankton cultures (within ecosystem, denoted by circles). The within ecosystem freshwater (FW) microalgae sampling from Larsen et al. (2013) consisted of a single replica of seston filtrate composite, which falls outside of the compilation data and likely consists of a mixture of microalgae and other allochthonous SPOM sources. Vane et al. sampled three distinct clades of marine microalgae: ice algae particulate organic matter filtrates (iPOM); sub-ice algae strands of *Melosira* sp.; and pelagic particulate organic matter filtrates (pPOM), denoted by square, triangle, and diamond symbols respectively.

9. Perspectives on δ^{13}C-AA applications in food web ecology

Carbon stable isotope analysis of AAs represents a considerable leap forward in the analytical tools available for retrospective basal resource tracing in the biological and paleontological sciences. This compound-specific approach offers increased dimensionality facilitating the disentanglement of intertwined trophic, metabolic and environmental processes that often obscure interpretations in traditional bulk stable isotope approaches (Yun et al. 2022). Although such detailed analyses may necessitate more extended sample processing time and incur increased costs, they yield richly layered datasets capable of addressing more intricate or nuanced hypotheses. With respect to carbon stable isotope analyses of AAs specifically, the consistent relative offsets between different EAAs produced by basal organisms over diverse environments enable direct comparisons between organisms sampled from different locations and at different points in time. This continuity, coupled with the longevity of AAs in well-preserved consumer tissues, allows for extensions far back into the paleontological record. These characteristics set EAAs apart from bulk stable isotopes whose values fluctuate with the spatially and temporally varying environmental background. Yet, these environmental effects are still captured within the measured δ^{13}C-EAA values (termed baseline δ^{13}C-EAA values in basal organisms), allowing inferences about the in situ environment to be made retrospectively. As EAAs are major, trophically-unaltered structural components of biomass, δ^{13}C-EAA values are a consistent tracer of their biosynthetic origins. Furthermore, δ^{13}C-NEAA values in metazoans, which reflect a combination of direct routing from dietary NEAAS and de novo synthesis from catabolised macronutrients, offer valuable insight into dietary

macronutrient content and therefore diet quality in consumers. Given the diverse roles of AAs as metabolites, or precursors in the synthesis of metabolites and other non-proteinaceous structural components, the stable isotope compositions of the suite of AAs may also help to infer metabolic processes that underpin cellular and tissue functioning. As such, δ^{13}C-AA data can unlock valuable insights into the trophic interactions, nutrient flows, and physiological responses to environments that structure food webs. Moreover, δ^{13}C-AA data can illucidate spatiotemporal dynamics of basal resource use by consumers in response to natural or anthropogenic induced changes in the ecosystem. Harnessing the trove of information embedded in δ^{13}C-AA data relies on a solid mechanistic comprehension of the complex processes that contribute to individual AA carbon isotope values. While progress has started to be made in recent years (e.g. Larsen et al. 2015, Manlick et al. 2022, Elliot Smith et al. 2022, Stahl et al. 2023), this has been outpaced by the broad and expanding applications of carbon stable isotope analyses of AAs in the current literature. As underscored throughout this review, existing knowledge gaps may impede the wider use of δ^{13}C-AA data or result in the dependence on unacknowledged and occasionally unfounded assumptions.

One of the major knowledge gaps is the relatively unknown level of specificity reflected in δ^{13}C-EAA patterns of basal resources. While some studies suggest a high degree of taxonomic resolution (Scott et al. 2006, Larsen et al. 2020, Vane et al. 2023, Stahl et al. 2023), lack of data impede comprehensive analyses of δ^{13}C-EAA pattern specificity across different basal organisms. Interestingly, different EAAs appear to be diagnostic at different ranks of taxonomic resolution (section 3.1). Misalignment between the ecological or functional discriminations desired and those observed within δ^{13}C-EAA data, even with high specificity, need to be acknowledged. For instance, discerning between fresh vs detrital material of basal organisms with δ^{13}C-EAA data can be challenging (Vane et al. 2023), as the δ^{13}C-EAA patterns remain consistent when the basal organism tissue undergoes leaf necrosis, fragmentation and detrital transport (Larsen et al 2013, Elliott Smith et al. 2022). Similarly different phenotypic growth forms may occur between and within cultured organisms and those sampled in the environment (Vane et al. 2023). Facultative EAA prototrophy may further complicate distinctions between basal organisms (section 3.2), especially if multiple groups directly route molecules from the same external pools, resulting in their δ^{13}C-EAA patterns to converge and therefore limit the potential for δ^{13}C-EAA fingerprints to occur. However, given the intense competition and resulting functional niche separation among saprotrophic communities, considerable δ^{13}C-EAA pattern convergence seems unlikely (Dang et al. 2022).

The current logistical constraints associated with obtaining δ^{13}C-AA data have likely contributed to the trend of incorporating external training data into study designs. This usage varies from selecting specific basal organism groups for graphical comparisons (e.g. Stahl et al. 2023) to extensive compilations used within mixing models (e.g. Arsenault et al. 2022b). Given the potential for high specificity in broad basal resource groups (e.g. plant vs. fungal derived AAs) within and across ecosystems, incorporating extensive training data sets from a multitude of studies, biomes and sampled species into mixing models can be problematic, as depicted in Fig. 9. Moreover, even when training data are used solely for comparisons, differences in analytical protocols and equipment can introduce biases between datasets generated in different research labs (section 7).

The issue of interlab comparisons is not unique to the carbon stable isotope analyses of AAs. For many years, there has been ongoing development and evaluation of suitable external reference materials for calibrations in stable isotope analyses in general (e.g. Stichler 1995, Gröning 2004, de Laeter 2005). These efforts aim to establish globally recognised standards that promote precision and accuracy across different laboratories. Assuming suitable internal standards for intra-laboratory precision are also met, finding suitable external reference materials for δ^{13}C-AA analysis still poses unique challenges. One of the key challenges lies in identifying internationally acceptable materials that chemically align with sample material for derivatization methods and analyte-dependent fractionations. Having such reference materials would allow for δ^{13}C-AA data measured across studies and labs to be compared accurately and with confidence. This would be further facilitated by greater standardisation of methodologies (Fig. 7), as the varying protocols and chemicals currently in use may be adding additional biases in data measured at different research facilities (e.g. Fig. 8). Interlab comparison studies of different methodological approaches could at least pinpoint the specific processes within protocols that cause measurement biases, and improve understanding of the specific fractionations associated with specific workflows. One immediate benefit of accurate interlab comparisons would be the ability to collate δ^{13}C-AA values measured into a single databank that could be used as a reference library for future studies that could be used to look-up δ^{13}C-AA data already quantified for different taxa. While there are wider calls for a centralised repository for isotope data (Pauli et al. 2017), this constitutes a separate functional role to that of a δ^{13}C-AA value reference library.

Expediting data sharing and transfer through a database of δ^{13}C-AA values could help to navigate current limitations that impede wider application of δ^{13}C-AA patterns. With standardised training data readily available, researchers could compile and tailor training data sets to specific ecosystems or consumers in

an open and transparent manner. A reference library would also provide an opportunity to explore the issue of specificity within δ^{13}C-AA patterns of broad basal organism groups by extending preliminary analyses like those conducted here on vascular plants (see Appendix S3) to other phylogenetic clades and incorporating a wider number of species. Such knowledge would guide future decisions about whether species-specific samples are required for retrospective basal resource use studies due to high specificity, or whether data from more distantly related species may serve as suitable analogues for the δ^{13}C-AA patterns of basal organisms of interest.

The power of δ^{13}C-AA data extends beyond simply reconstructing basal resource use in consumers. Given that individual AAs are synthesised through distinct metabolic pathways, and additionally serve as key metabolites, viewing δ^{13}C-AA data through the lens of physiological processes can provide metabolic insights and generate new hypotheses. This includes the hypothesis proposed in section 3.1 that the synthesis of ^{13}C deplete lignin results in relatively enriched δ^{13}C values of phenylalanine in vascular plants. Furthermore, δ^{13}C-AA analyses could shed light on quantifying the degree of direct AA incorporation in facultative prototrophs. By culturing of basal organisms on AA-free media, we can establish the δ^{13}C-AA pattern of purely de novo synthesised AAs. Comparing these cultured δ^{13}C patterns with those sampled in the environment, along with heterotrophic sources, could reveal the degree to which heterotrophic AAs are directly assimilated into the proteins of facultative AA prototrophs in situ. This approach could provide insights into the biochemical functioning of bacterial and fungal saprotrophic communities and disentangle the role of heterotrophy in mixotrophic algae. For instance, are ingested AAs directly assimilated into tissue structures or used as a source of nitrogen for other metabolic processes under nutrient limitation where the remaining carbon skeleton is subsequently respired? These questions underscore the potential depth of understanding that δ^{13}C-AA data can provide.

The application of δ^{13}C-EAA fingerprints holds immense potential for addressing pressing ecological questions on carbon transfer from basal resources to consumer proteins in food webs. However, the application comes with pitfalls. There is a need for having a basic understanding of the underlying isotopic mechanisms, an a priori knowledge on the ecologies of specific basal organisms and studied consumers, and the adherence to best practices for robust proportional calculations with mixing models. Many of these limitations are not unique to the stable isotope analyses of amino acids, having already been recognised in traditional bulk stable isotope applications. The advantage of δ^{13}C-EAA fingerprints is the increased data complexity and the nuanced insight it provides. When correctly applied, δ^{13}C-EAA

fingerprinting affords the opportunity to explore carbon flux questions on spatiotemporal scales without having to characterise changes in baseline δ^{13}C-EAA values, offering unparalleled specificity and inclusivity in basal resource characterisation and tracing. This is an immense benefit for understanding how basal resource use by metazoans has shifted due to anthropogenic climate change and pollution. Questions such as whether consumers have adapted to the anthropogenic changes in their environment by changing specific basal resource use have scarcely been explored. Similarly, changes in basal resource use during the life history of consumers, over seasons, years or populations are not well understood, in part due to the required extensive basal resource sampling. Understanding the basal resource use by metazoan species in conjunction with changes in basal resource abundance, composition, nutritional quality, and the environment can give insight into the resilience of differing food webs across the world.

Acknowledgements

This study was co-funded by the Natural Environment Research Council (NERC) under the grant number NE/R012520/1 and the German Federal Ministry of Education and Research (BMBF) with project number 03F0800A in the joint funding scheme Changing Arctic Oceans. MRDC was supported by an Irish Research Council Laureate Award IRCLA/2017/186 to Andrew L. Jackson, Trinity College Dublin, and the Academy of Finland project grant 351860, FreshRestore, BiodivERsA, awarded to Antti P. Eloranta. TL was supported by BMBF with project number 03V01459 in the joint funding scheme Changing Arctic Oceans with contributions from the Max Planck Society. We also thank our colleagues Clive Trueman, Mikko Kiljunen, Antti P. Eloranta, Sebastian Rokitta, Hauke Flores, and Erik Hobbie for their valuable feedback on the first version of this manuscript.

Data availability statement: Metadata pertaining to the basal resource, human population and tissue-diet offset compilations are available on the Figshare repository (doi:10.6084/m9.figshare.22852355).

Author contributions: All authors contributed equally to this manuscript.

Conflict of interest statement: The authors declare no conflicts of interest.

References

Abelson, P. H. 1954. “Amino acids in fossils.” *Science* 119: 576.

Aguilar, A., and A. Borrell. 2021. “Growth of baleen along the baleen rack is constant in balaenopterid whales.” *Polar Biology* 44: 1223–1225. https://doi.org/10.1007/s00300-021-02877-6.

Algora Gallardo, C., P. Baldrian, and R. López-Mondéjar. 2021. “Litter-inhabiting fungi show high level of specialization towards biopolymers composing plant and fungal biomass.” *Biology and Fertility of Soils* 57:77-88. https://doi.org/10.1007/s00374-020-01507-3.

Aniszewski, T. 2007. “Alkaloids-Secrets of Life: Alkaloid Chemistry, Biological Significance, Applications and Ecological Role.” Elsevier.

Akman Gündüz, E., and A. E. Douglas. 2009. Symbiotic bacteria enable insects to use a nutritionally inadequate diet. *Proceedings of the Royal Society B: Biological Sciences* 276(1658): 987-991. https://doi.org/10.1098/rspb.2008.1476.

Arsenault, E. R., J. H. Liew, and J. R. Hopkins. 2022a. “Substrate composition influences amino acid carbon isotope profiles of fungi: Implications for tracing fungal contributions to food webs.” *Environmental Microbiology* 24(4): 2089-2097. https://doi.org/10.1111/1462-2920.15961.

Arsenault, E. R., J. H. Thorp, M. J. Polito, M. Minder, W. K. Dodds, F. Tromboni, A. Maasri, M. Pyron, B. Mendsaikhan, A. Otgonganbat, S. Altangerel, S. Chandra, R. Shields, C. Artz, and H. Bennadji. 2022b. “Intercontinental analysis of temperate steppe stream food webs reveals consistent autochthonous support of fishes.” *Ecology Letters* 25(12): 2624-2636. https://doi.org/10.1111/ele.14113.

Arthur, K. E., S. Kelez, T. Larsen, C. A. Choy, and B. N. Popp. 2014. “Tracing the biosynthetic source of essential amino acids in marine turtles using $\delta^{13}C$ fingerprints.” *Ecology* 95(5): 1285–1293. https://doi.org/10.1890/13-0263.1.

Ayayee, P. A., S. C. Jones, and Z. L. Sabree. 2015. “Can ^{13}C stable isotope analysis uncover essential amino acid provisioning by termite-associated gut microbes?” *PeerJ* 3: e1218. https://doi.org/10.7717/peerj.1218.

Ayayee, P. A., G. Kinney, C. Yarnes, T. Larsen, G. F. Custer, L. T. A. Van Diepen, and A. Muñoz-Garcia. 2020. “Role of the gut microbiome in mediating standard metabolic rate after dietary shifts in the viviparous cockroach, *Diploptera punctata*.” *Journal of Experimental Biology* 223(11): jeb.218271. https://doi.org/10.1242/jeb.218271.

Ayayee, P. A., T. Larsen, C. Rosa, G. W. Felton, J. G. Ferry, and K. Hoover. 2016a. “Essential amino acid supplementation by gut microbes of a wood-feeding cerambycid.” *Environmental Entomology* 45(1): 66–73. https://doi.org/10.1093/ee/nvv153.

Ayayee, P. A., Larsen T., and Z. Sabree. 2016b. “Symbiotic essential amino acids provisioning in the American cockroach, *Periplaneta americana* (Linnaeus) under various dietary conditions.” *PeerJ* 4: e2046. https://doi.org/10.7717/peerj.2046.

Bada, J. L., X. S. Wang, and H. Hamilton. 1999. “Preservation of key biomolecules in the fossil record: Current knowledge and future challenges.” *Philosophical Transactions of the Royal Society B: Biological Sciences* 354(1379): 77–87. https://doi.org/10.1098/rstb.1999.0361.

Barreto-Curiel, F., U. Focken, L. R. D’Abramo, J. Mata-Sotres, and M. T. Viana. 2019. “Assessment of amino acid requirements for *Totoaba macdonaldi* at different levels of protein using stable isotopes and a non-digestible protein source as a filler.” *Aquaculture* 503: 550–561.

https://doi.org/10.1016/j.aquaculture.2019.01.038.

Barreto-Curiel, F., U. Focken, L. R. D'Abramo, and M. T. Viana. 2017. "Metabolism of *Seriola lalandi* during starvation as revealed by fatty acid analysis and compound-specific analysis of stable isotopes within amino acids." *PLoS ONE* 12(1): e0170124. https://doi.org/10.1371/journal.pone.0170124.

Batista García, R., M. Sánchez, P. Talia, S. Jackson, N. O' Leary, A. Dobson, and J. Folch-Mallol. 2016. "From lignocellulosic metagenomes to lignocellulolytic genes: trends, challenges and future prospects: From lignocellulosic metagenomes to lignocellulolytic genes." *Biofuels, Bioproducts and Biorefining* 10(6): 864-882. https://doi.org/10.1002/bbb.1709.

Battezzati, A., D. Brillon, and D. Matthews. 1995. "Oxidation of glutamic acid by the splanchnic bed in humans." *American Journal of Physiology-Endocrinology and Metabolism* 269(2): E269-E276. https://doi.org/10.1152/ajpendo.1995.269.2.E269.

Battezzati, A., M. Haisch, D. J. Brillon, and D. E. Matthews. 1999. "Splanchnic utilization of enteral alanine in humans." *Metabolism* 48(7): 915-921. https://doi.org/10.1016/S0026-0495(99)90229-9.

Belghit, I., M. Varunjikar, M-C. Lecrenier, A. Steinhilber, A. Niedzwiecka, Y. V. Wang, M. Dieu, D. Azzollini, K. Lie et al. 2021. "Future feed control – Tracing banned bovine material in insect meal." *Food Control* 128: 108183. https://doi.org/10.1016/j.foodcont.2021.108183.

Benner, R., M. L. Fogel, E. K. Sprague, and R. E. Hodson. 1987. "Depletion of ^{13}C in lignin and its implications for stable carbon isotope studies." *Nature* 329: 708-710. https://doi.org/10.1038/329708a0.

Besser, A. C., E. A. Elliott Smith, and S. D. Newsome. 2022. "Assessing the potential of amino acid $\delta^{13}C$ and $\delta^{15}N$ analysis in terrestrial and freshwater ecosystems." *Journal of Ecology* 110(4): 935-950. https://doi.org/10.1111/1365-2745.13853.

Bhattacharyya, A. 1946. "On a measure of divergence between two multinomial populations." *Sankhyā: the Indian journal of statistics* 7(4):401-406. https://www.jstor.org/stable/25047882.

Blanchard, J. L., S. Jennings, R. Holmes, J. Harle, G. Merino, J. I. Allen, J. Holt, N. K. Dulvy, and M. Barange. 2012. "Potential consequences of climate change for primary production and fish production in large marine ecosystems." *Philosophical Transactions of the Royal Society B: Biological Sciences* 367(1605): 2979–2989. https://doi.org/10.1098/rstb.2012.0231.

Biolo, G., P. Tessari, S. Inchiostro, D. Bruttomesso, C. Fongher, L. Sabadin, M. G. Fratton, A. Valerio, and A. Tiengo. 1992. "Leucine and phenylalanine kinetics during mixed meal ingestion: a multiple tracer approach." *American Journal of Physiology-Endocrinology and Metabolism* 262(4): E455-E463. https://doi.org/10.1152/ajpendo.1992.262.4.E455.

Biro, J. C. 2006. "Amino acid size, charge, hydropathy indices and matrices for protein structure analysis." *Theoretical Biology and Medical Modelling* 3: 15. https://doi.org/10.1186/1742-4682-3-15.

Boatman, E. M., M. B. Goodwin, H. N. Holman, W. Zheng, R. Gronsky, and M. H. Schweitzer. 2019. "Mechanisms of soft tissue and protein preservation in Tyrannosaurus rex." *Scientific Reports* 9: 15678. https://doi.org/10.1038/s41598-019-51680-1.

Boecklen, W. J., C. T. Yarnes, B. A. Cook, and A. C. James. 2011. "On the use of stable isotopes in trophic ecology." *Annual Review of Ecology, Evolution, and Systematics* 42(1): 411–440. https://doi.org/10.1146/annurev-ecolsys-102209-144726.

Bolin, J. F., K. U. Tennakoon, M. B. A. Majid, and D. D. Cameron. 2017. "Isotopic evidence of partial mycoheterotrophy in *Burmannia coelestis* (Burmanniaceae)." *Plant Species Biology* 32(1): 74-80. https://doi.org/10.1890/09-2409.1.

Bolnick, D. I., R. Svanbäck, J. A. Fordyce, L. H. Yang, J. M. Davis, C. D. Hulsey, and M. L. Forister. 2003. "The Ecology of Individuals: Incidence and Implications of Individual Specialization." *The American Naturalist* 161(1): 1–28. https://doi.org/10.1086/343878.

Bond, A. L., and A. W. Diamond. 2011. "Recent Bayesian stable-isotope mixing models are highly sensitive to variation in discrimination factors." *Ecological Application*. 21(4): 1017-1023.

https://doi.org/10.1890/09-2409.

Borelli, G., N. Mayer-Gostan, H. De Pontual, G. Boeuf, and P. Payan. 2001. "Biochemical relationships between endolymph and otolith matrix in the trout (*Oncorhynchus mykiss*) and turbot (*Psetta maxima*)." *Calcified Tissue International* 69(6): 356–364. https://doi.org/10.1007/s00223-001-2016-8.

Brault, E. K., P. L. Koch, E. Gier, R. I. Ruiz-Cooley, J. Zupcic, K. N. Gilbert, and M. D. McCarthy. 2014. "Effects of decalcification on bulk and compound-specific nitrogen and carbon isotope analyses of dentin." *Rapid Communications in Mass Spectrometry* 28(24): 2744–2752. https://doi.org/10.1002/rcm.7073.

Britton, K., B. E. Crowley, C. P. Bataille,J. H. Miller, and M. J. Woller. 2022. " Editorial: A golden age for strontium isotope research? Current advances in paleoecological and archaeological research." *Frontiers in Ecology and Evolution* 9: 820295. https://doi.org/10.3389/fevo.2021.820295.

Brock, F., R. Wood, T. F. G. Higham, P. Ditchfield, A. Bayliss, and C. B. Ramsey. 2012. "Reliability of nitrogen content (%N) and carbon:nitrogen atomic ratios (C:N) as indicators of collagen preservation suitable for radiocarbon dating." *Radiocarbon* 54(3-4): 879–886. https://doi.org/10.1017/S0033822200047524.

Brodie, C. R., M. J. Leng, J. S. L. Casford, C. P. Kendrick, J. M. Lloyd, Z. Yongqiang, and M. I. Bird. 2011. "Evidence for bias in C and N concentrations and $\delta^{13}C$ composition of terrestrial and aquatic organic materials due to pre-analysis acid preparation methods." *Chemical Geology* 282(3-4): 67–83. https://doi.org/10.1016/j.chemgeo.2011.01.007.

Brozou, A., B. T. Fuller, V. Grimes, G. Van Biesen, Y. Ma, J. L. Boldsen, and M. A. Mannino. 2022. "Aquatic resource consumption at the Odense leprosarium: Advancing the limits of palaeodiet reconstruction with amino acid $\delta^{13}C$ measurements." *Journal of Archaeological Science* 141: 105578. https://doi.org/10.1016/j.jas.2022.105578.

Burian, A., J. M. Nielsen, T. Hansen, R. Bermudez, and M. Winder. 2020. "The potential of fatty acid isotopes to trace trophic transfer in aquatic food-webs." *Philosophical Transactions of the Royal Society B: Biological Sciences* 375(1804): 20190652. https://doi.org/10.1098/rstb.2019.0652.

Burrin, D. G., and B. Stoll. 2009. "Metabolic fate and function of dietary glutamate in the gut." *The American Journal of Clinical Nutrition* 90(3): 850S-856S. https://doi.org/10.3945/ajcn.2009.27462Y.

Carter, J. F., and B. Fry. 2013. "Ensuring the reliability of stable isotope ratio data - Beyond the principle of identical treatment." *Analytical and Bioanalytical Chemistry* 405(9): 2799–2814. https://doi.org/10.1007/s00216-012-6551-0.

Caut, S., Angulo E, Courchamp F. 2009. "Variation in discrimination factors ($\Delta^{15}N$ and $\Delta^{13}C$): the effect of diet isotopic values and applications for diet reconstruction." *Journal of Applied Ecology* 46: 443-453. https://doi.org/10.1111/j.1365-2664.2009.01620.x.

Casey, M. M., and D. M. Post. 2011. "The problem of isotopic baseline: Reconstructing the diet and trophic position of fossil animals." *Earth-Science Reviews* 106: 131–148. https://doi.org/10.1016/j.earscirev.2011.02.001.

Casey, J. M.,C. P. Meyer, F. Morat, S. J. Brandl, S. Planes, V. Parravicini. 2019. "Reconstructing hyperdiverse food webs: Gut content metabarcoding as a tool to disentangle trophic interactions on coral reefs." *Methods in Ecology and Evolution* 10(8): 1157-1170. https://doi.org/10.1111/2041-210X.13206.

Chen, Y., B. Zhou, J. Li, H. Tang, J. Tang, and Z. Yang. 2018. "Formation and change of chloroplast-located plant metabolites in response to light conditions." *International Journal of Molecular Sciences* 19(3): 654. https://doi.org/10.3390/ijms19030654.

Cherel, Y., P. Bustamante, and P. Richard. 2019. "Amino acid $\delta^{13}C$ and $\delta^{15}N$ from sclerotized beaks: a new tool to investigate the foraging ecology of cephalopods, including giant and colossal squids." *Marine Ecology Progress Series* 624: 89–102. https://doi.org/10.3354/meps13002.

Cherel, Y., C. Fontaine, G. D. Jackson, C. H. Jackson, and P. Richard. 2009. “Tissue, ontogenic and sex-related differences in $\delta^{13}C$ and $\delta^{15}N$ values of the oceanic squid *Todarodes filippovae* (Cephalopoda: Ommastrephidae).” *Marine Biology* 156(4): 699–708. https://doi.org/10.1007/s00227-008-1121-x.

Cheung, C. and P. Szpak. 2021. “Interpreting past human diets using stable isotope mixing models.” *Journal of Archaeological Method and Theory* 28(4): 1106-1142. https://doi.org/10.1007/s10816-021-09514-w.

Chidawanyika, F., P. Mudavanhu, and C. Nyamukondiwa. 2019. “Global climate change as a driver of bottom-up and top-down factors in agricultural landscapes and the fate of host-parasitoid interactions.” *Frontiers in Ecology and Evolution* 7: 80. https://doi.org/10.3389/fevo.2019.00080.

Choy, K., C. I. Smith, B. T. Fuller, and M. P. Richards. 2010. “Investigation of amino acid $\delta^{13}C$ signatures in bone collagen to reconstruct human palaeodiets using liquid chromatography-isotope ratio mass spectrometry.” *Geochimica et Cosmochimica Acta* 74: 6093-6111. https://doi.org/10.1016/j.gca.2010.07.025.

Choy, K., S. H. Nash, A. R. Kristal, S. Hopkins, B. B. Boyer, and D. M. O’Brien. 2013. “The carbon isotope ratio of alanine in red blood cells is a new candidate biomarker of sugar-sweetened beverage intake.” *Journal of Nutrition* 143: 878–884. https://doi.org/10.3945/jn.112.172999.

Clevers, J. G. P. W., and R. Zurita-Milla. 2008. “Multisensor and multiresolution image fusion using the linear mixing model.” In *Image Fusion: Algorithms and Applications* 67-84. https://doi.org/10.1016/B978-0-12-372529-5.00004-4.

Collins, M. J., C. M. Nielsen-Marsh, J. Hiller, C. I. Smith, J. P. Roberts, R. V. Prigodich, T. J. Wess, J. Csapò, A. R. Millard, and G. Turner-Walker. 2002. “The survival of organic matter in bone: A review.” *Archaeometry* 44(3): 383–394. https://doi.org/10.1111/1475-4754.t01-1-00071.

Colonese, A. C., M. Collins, A. Lucquin, M. Eustace, Y. Hancock, R. de Almeida Rocha Ponzoni, A. Mora, C. Smith et al. 2014. Long-term resilience of late Holocene coastal subsistence system in southeastern South America. *Plos ONE* 9(4): e93854. https://doi.org/10.1371/journal.pone.0093854.

Corr, L. T., R. Berstan, and R. P. Evershed. 2007. “Optimisation of derivatisation procedures for the determination of $\delta^{13}C$ values of amino acids by gas chromatography/combustion/isotope ratio mass spectrometry.” *Rapid Communications in Mass Spectrometry* 21: 3759–3771. https://doi.org/10.1002/rcm.3252.

Corr, L. T., J. C. Sealy, M. C. Horton, and R. P. Evershed. 2005. “A novel marine dietary indicator utilising compound-specific bone collagen amino acid $\delta^{13}C$ values of ancient humans.” *Journal of Archaeological Science* 32: 321–330. https://doi.org/10.1016/j.jas.2004.10.002.

D’Souza, G., S. Waschina, S. Pande, K. Bohl, C. Kaleta, and C. Kost. 2014. “Less is more: Selective advantages can explain the prevalent loss of biosynthetic genes in bacteria.” *Evolution* 68(9): 2559–2570. https://doi.org/10.1111/evo.12468.

Dabrowski, K., B. F. Terjesen, Y. Zhang, J. M. Phang, and K. J. Lee. 2005. “A concept of dietary dipeptides: a step to resolve the problem of amino acid availability in the early life of vertebrates.” *Journal of Experimental Biology* 208(15): 2885-2894. https://doi.org/10.1242/jeb.01689.

Dall, S. R. X., A. M. Bell, D. I. Bolnick, and F. L. W. Ratnieks. 2012. “An evolutionary ecology of individual differences.” *Ecology Letters* 15(10): 1189–1198. https://doi.org/10.1111/j.1461-0248.2012.01846.x.

Dai, Z. L., X. L. Li, P. B. Xi, J. Zhang, G. Wu, and W. Y. Zhu. 2012. “Metabolism of select amino acids in bacteria from the pig small intestine.” *Amino Acids* 42: 1597-1608. https://doi.org/10.1007/s00726-011-0846-x.

Dang, C., J. G. Walkup, B. A. Hungate, R. B. Franklin, E. Schwartz, and E. M. Morrissey. 2022. “Phylogenetic organization in the assimilation of chemically distinct substrates by soil bacteria.” *Environmental Microbiology* 24(1): 357-369. https://doi.org/10.1111/1462-2920.15843.

de la Vega, C., R. M. Jeffreys, R. Tuerena, R. Ganeshram, and C. Mahaffey. 2019. “Temporal and spatial trends in marine carbon isotopes in the Arctic Ocean and implications for food web studies.” *Global Change Biology* 25(12): 4116-4130. https://doi.org/10.1111/gcb.14832.

Degens, E. T., W. G. Deuser, and R. L. Haedrich. 1969. “Molecular structure and composition of fish otoliths.” *Marine Biology* 2: 105–113. https://doi.org/10.1007/BF00347005.

Deniro, M. J., and S. Epstein. 1977. “Mechanism of carbon isotope fractionation associated with lipid-synthesis.” *Science* 197: 261-263. https://doi.org/10.1126/science.327543.

D'Mello, J. F. 2017. “The handbook of microbial metabolism of amino acids.” CAB International.

Docherty, G., V. Jones, and R. P. Evershed. 2001. “Practical and theoretical considerations in the gas chromatography/combustion/isotope ratio mass spectrometry $\delta^{13}C$ analysis of small polyfunctional compounds.” *Rapid Communications in Mass Spectrometry* 15(9): 730–738. https://doi.org/10.1002/rcm.270.

Docmac, F., M. Araya, I. A. Hinojosa, C. Dorador, and C. Harrod. 2017. “Habitat coupling writ large: pelagic-derived materials fuel benthivorous macroalgal reef fishes in an upwelling zone.” *Ecology* 98(9): 2267-2272. https://doi.org/10.1002/ecy.1936.

Dunn, P. J. H., N. V. Honch, and R. P. Evershed. 2011. “Comparison of liquid chromatography-isotope ratio mass spectrometry (LC/IRMS) and gas chromatography-combustion-isotope ratio mass spectrometry (GC/C/IRMS) for the determination of collagen amino acid $\delta^{13}C$ values for palaeodietary and palaeoecological reconstruction.” *Rapid Communications in Mass Spectrometry* 25: 2995–3011. https://doi.org/10.1002/rcm.5174.

Durante, L. M., A. J. M. Sabadel, R. D. Frew, T. Ingram, and S. R. Wing. 2020. “Effects of fixatives on stable isotopes of fish muscle tissue: implications for trophic studies on preserved specimens.” *Ecological Applications* 30(4): e02080. https://doi.org/10.1002/eap.2080.

Edeyer, A., H. De Pontual, P. Payan, H. Troadec, A. Sévère, and N. Mayer-Gostan. 2000. “Daily variations of the saccular endolymph and plasma compositions in the turbot *Psetta maxima*: Relationship with the diurnal rhythm in otolith formation.” *Marine Ecology Progress Series* 192: 287–294. https://doi.org/10.3354/meps192287.

Eisert, R. 2011. “Hypercarnivory and the brain: Protein requirements of cats reconsidered.” *Journal of Comparative Physiology B: Biochemical, Systemic, and Environmental Physiology* 181: 1–17. https://doi.org/10.1007/s00360-010-0528-0.

Eker-Develi, E., A. E. Kideys, and S. Tugrul. 2006. “Role of Saharan dust on phytoplankton dynamics in the northeastern Mediterranean.” *Marine Ecology Progress Series* 314: 61–75. https://doi.org/10.3354/meps314061.

Elliott Smith, E. A., M. D. Fox, M. L. Fogel, and S. D. Newsome. 2022. “Amino acid $\delta^{13}C$ fingerprints of nearshore marine autotrophs are consistent across broad spatiotemporal scales: An intercontinental isotopic dataset and likely biochemical drivers.” *Functional Ecology* 36(5): 1191-1203. https://doi.org/10.1111/1365-2435.14017.

Elliott Smith, E. A., C. Harrod, and S. D. Newsome. 2018. “The importance of kelp to an intertidal ecosystem varies by trophic level: insights from amino acid $\delta^{13}C$ analysis.” *Ecosphere* 9(11): e02516. https://doi.org/10.1002/ecs2.2516.

Von Endt, D. W. 2000. “Staying in shape: the stability of structural proteins in natural history museum storage fluids.” *Polymer Preprints* 41(2): 1794–1795.

Engel, M. H., G. A. Goodfriendt, Y. Qian, and S. A. Mackot. 1994. “Indigeneity of organic matter in fossils: A test using stable isotope analysis of amino acid enantiomers in Quaternary mollusk shells.” *Geology* 91(22): 10475–10478. https://doi.org/10.1073/pnas.91.22.10475.

Enggrob, K. L., T. Larsen, M. Larsen, L. Elsgaard, and J. Rasmussen. 2019. “The influence of hydrolysis and derivatization on the determination of amino acid content and isotopic ratios in dual-labeled (^{13}C, ^{15}N) white clover.” *Rapid Communications in Mass Spectrometry* 33: 21–30.

https://doi.org/10.1002/rcm.8300.

Erkosar, B., G. Storelli, A. Defaye, and F. Leulier. 2013. “Host-intestinal microbiota mutualism: “learning on the fly.”.” *Cell Host and Microbe* 13: 8–14. https://doi.org/10.1016/j.chom.2012.12.004.

Espiñeira, J. M., E. Novo Uzal, L. V. Gómez Ros, J. S. Carrión, F. Merino, A. Ros Barceló, and F. Pomar. 2011. “Distribution of lignin monomers and the evolution of lignification among lower plants.” *Plant Biology* 13: 59–68. https://doi.org/10.1111/j.1438-8677.2010.00345.x.

Fagan, R. P., and N. F. Fairweather. 2014. “Biogenesis and functions of bacterial S-layers.” *Nature Reviews Microbiology* 12(3): 211–222. https://doi.org/10.1038/nrmicro3213.

Fahy, G., C. Deter, R. Pitfield, J. Miszkiewicz, and P. Mahoney. 2017. “Bone deep: Variation in stable isotope ratios and histomorphometric measurements of bone remodelling within adult humans.” *Journal of Archaeological Science* 87: 10–16. https://doi.org/10.1016/j.jas.2017.09.009.

Falini, G., S. Fermani, and S. Goffredo. 2015. C”oral biomineralization: A focus on intra-skeletal organic matrix and calcification.” *Seminars in Cell & Developmental Biology* 46: 17–26. https://doi.org/10.1016/j.semcdb.2015.09.005.

Faure, E., F. Not, A.-S. Benoiston, K. Labadie, L. Bittner, and S.-D. Ayata. 2019. “Mixotrophic protists display contrasted biogeographies in the global ocean.” *The ISME Journal* 13: 1072–1083. https://doi.org/10.1038/s41396-018-0340-5.

Feehily, C., and K. A. Karatzas. 2013. “Role of glutamate metabolism in bacterial responses towards acid and other stresses.” *Journal of Applied Microbiology* 114(1): 11-24. https://doi.org/10.1111/j.1365-2672.2012.05434.x.

Ferrier-Pagès, C., S. Martinez, R. Grover, J. Cybulski, E. Shemesh, and D. Tchernov. 2021. “Tracing the trophic plasticity of the coral-dinoflagellate symbiosis using amino acid compound-specific stable isotope analysis.” *Microorganisms* 9(1): 182. https://doi.org/10.3390/microorganisms9010182.

Fine, M., and Y. Loya. 2002. “Endolithic algae: an alternative source of photoassimilates during coral bleaching.” *Proceedings of the Royal Society of London. Series B: Biological Sciences* 269(1497): 1205-1210. https://doi.org/10.1098/rspb.2002.1983.

Firmin, A., M. A. Selosse, C. Dunand, and A. Elger. 2022. “Mixotrophy in aquatic plants, an overlooked ability.” *Trends in Plant Science* 27(2): 147-157. https://doi.org/10.1016/j.tplants.2021.08.011.

Fox, M. D., E. A. E. Smith, J. E. Smith, and S. D. Newsome. 2019. “Trophic plasticity in a common reef - building coral: Insights from $\delta^{13}C$ analysis of essential amino acids”. *Functional Ecology* 33(11): 2203–2214. https://doi.org/10.1111/1365-2435.13441.

Frayn, K. N., and R. Evans. 2019. “Human Metabolism: A Regulatory Perspective”. Wiley-Blackwell. ISBN: 978-1-119-33143-8.

Fry, B. 2006. “Stable isotope ecology”. New York: Springer. ISBN: 978-0-387-33745-6

Fuller, M. F., and P. J. Reeds. 1998. “Nitrogen cycling in the gut.” *Annual Review of Nutrition* 18: 385-411. https://doi.org/10.1146/annurev.nutr.18.1.385.

Geigl, E. M., U. Baumer, and J. Koller. 2004. “New approaches to study the preservation of biopolymers in fossil bones”. *Environmental Chemistry Letters* 2: 45-48. https://doi.org/10.1007/s10311-004-0059-6.

Geraldes V., and E. Pinto. 2021. “Mycosporine-Like Amino Acids (MAAs): Biology, Chemistry and Identification Features”. *Pharmaceuticals* 14(1): 63. https://doi.org/10.3390/ph14010063.

Giesemann, P., and G. Gebauer. 2022. “Distinguishing carbon gains from photosynthesis and heterotrophy in C_3-hemiparasite–C_3-host pairs”. *Annals of Botany* 129(6): 647-656. https://doi.org/10.1093/aob/mcab153.

Glasl, B., S. Robbins, P. R. Frade, E. Marangon, P. W. Laffy D. G. Bourne, and N. S. Webster 2020. “Comparative genome-centric analysis reveals seasonal variation in the function of coral reef microbiomes.” *The ISME journal* 14(6): 1435-1450. https://doi.org/10.1038/s41396-020-0622-6.

Gröning, M. 2004. “International stable isotope reference materials.” In: *Handbook of stable isotope*

analytical techniques. 874-906. Elsevier. ISBN 0444511148

Grupe, G. 1995. “Preservation of collagen in bone from dry, sandy soil.” *Journal of Archaeological Science* 22(2): 193–199. https://doi.org/10.1006/jasc.1995.0021.

Guiry, E. 2019. “Complexities of stable carbon and nitrogen isotope biogeochemistry in ancient freshwater ecosystems: Implications for the study of past subsistence and environmental change.” *Frontiers in Ecology and Evolution* 7: 313. https://doi.org/10.3389/fevo.2019.00313.

Gupta, R., and N. Gupta. 2021. “Fundamentals of Bacterial Physiology and Metabolism.” Springer Nature Singapore.

Güven, K. C., A. Percot, and E. Sezik. 2010. “Alkaloids in marine algae.” *Marine Drugs* 8(2): 269-284. https://doi.org/10.3390/md8020269.

Hadjidakis, D. J., and I. I. Androulakis. 2006. “Bone remodeling.” *Annals of the New York Academy of Sciences* 1092: 385–396. https://doi.org/10.1196/annals.1365.035

Hannides, C. C. S., B. N. Popp, M. R. Landry, and B. S. Graham. 2009. “Quantification of zooplankton trophic position in the North Pacific Subtropical Gyre using stable nitrogen isotopes.” *Limnology and Oceanography* 54: 50–61. https://doi.org/10.4319/lo.2009.54.1.0050.

Hare, P. E., M. L. Fogel, T. W. Stafford, A. D. Mitchell, and T. C. Hoering. 1991. “The isotopic composition of carbon and nitrogen in individual amino acids isolated from modern and fossil proteins.” *Journal of Archaeological Science* 79(5): 512–515. https://doi.org/10.1001/archderm.1959.01560170010002.

Hayes, J. M. 2001. “Fractionation of the isotopes of carbon and hydrogen in biosynthetic processes.” Pages in Stable Isotope Geochemistry, edited by J. W. Valley and D. R. Cole, 225–277. Mineralogical Society of America, Washington.

Heikkinen, R., H. Hämäläinen, M. Kiljunen, S. Kärkkäinen, J. Schilder, R. I. and Jones. 2022. “A Bayesian stable isotope mixing model for coping with multiple isotopes, multiple trophic steps and small sample sizes.” *Methods in Ecology and Evolution* 13(11): 2586-2602. https://doi.org/10.1111/2041-210X.13989.

Heizer, E. M., D. W. Raiford, M. L. Raymer, T. E. Doom, R. V. Miller, D. E. Krane. 2006. “Amino Acid Cost and Codon-Usage Biases in 6 Prokaryotic Genomes: A Whole-Genome Analysis.” *Molecular Biology and Evolution* 23(9): 1670-1680. https://doi.org/10.1093/molbev/msl029.

Hesse, T., M. Nachev, S. Khaliq, M. A. Jochmann, F. Franke, J. P. Scharsack, J. Kurtz, B. Sures, and T. C. Schmidt. 2022. “Insights into amino acid fractionation and incorporation by compound-specific carbon isotope analysis of three-spined sticklebacks.” *Scientific Reports* 12: 11690. https://doi.org/10.1038/s41598-022-15704-7.

Hetherington, E. D., C. M. Kurle, M. D. Ohman, and B. N. Popp. 2019. “Effects of chemical preservation on bulk and amino acid isotope ratios of zooplankton, fish, and squid tissues.” *Rapid Communications in Mass Spectrometry* 33(10): 935-945. https://doi.org/10.1002/rcm.8408.

Hobbie, E. A., R. A. Werner. 2004. “Intramolecular, Compound-Specific, and Bulk Carbon Isotope Patterns in C_3 and C_4 Plants: A Review and Synthesis.” *The New Phytologist* 161: 371-385. https://doi.org/10.1111/j.1469-8137.2004.00970.x.

Hoegh-Guldberg, O., and J. F. Bruno. 2010. “The impact of climate change on the world’s marine ecosystems.” *Science* 328: 1523–1528. https://doi.org/10.1126/science.1189930.

Hoerr, R. A., D. E. Matthews, B. M. Bier, and V. R. Young. 1991. “Leucine kinetics from [2H3]-and [13C] leucine infused simultaneously by gut and vein.” *American Journal of Physiology-Endocrinology and Metabolism* 260: E111-E117. https://doi.org/10.1152/ajpendo.1991.260.1.E111.

Honch, N. V., J. S. O. McCullagh, and R. E. M. Hedges. 2012. “Variation of bone collagen amino acid $\delta^{13}C$ values in archaeological humans and fauna with different dietary regimes: Developing frameworks of dietary discrimination.” *American Journal of Physical Anthropology* 148(4): 495–511. https://doi.org/10.1002/ajpa.22065.

Hondorp, D. W., D. L. Breitburg, and L. A. Davias. 2010. “Eutrophication and fisheries: separating the effects of nitrogen loads and hypoxia on the pelagic-to-demersal ratio and other measures of landings composition.” *Marine and Coastal Fisheries* 2: 339–361. https://doi.org/10.1577/C09-020.1.

Hopkins, J. B. III, and J. M. Ferguson. 2012. “Estimating the diets of animals using stable isotopes and a comprehensive Bayesian mixing model.” *PloS ONE* 7(1): e28478. https://doi.org/10.1371/journal.pone.0028478.

Hosie, A. H., P. S. Poole. 2001. “Bacterial ABC transporters of amino acids.” *Research in microbiology* 152(3-4): 259-270. https://doi.org/10.1016/S0923-2508(01)01197-4.

Hou, Y., Y. Yin, and G. Wu. 2015. “Dietary essentiality of “nutritionally non-essential amino acids” for animals and humans.” *Experimental Biology and Medicine* 240(8): 997–1007. https://doi.org/10.1177/1535370215587913.

Howland, M. R., L. T. Corr, S. M. M. Young, V. Jones, S. Jim, N. J. Van Der Merwe, A. D. Mitchell, and R. P. Evershed. 2003. “Expression of the dietary isotope signal in the compound-specific $\delta^{13}C$ values of pig bone lipids and amino acids.” *International Journal of Osteoarchaeology* 13(1-2): 54–65. https://doi.org/10.1002/oa.658.

Huneau, J. F., O. L. Mantha, D. Hermier, V. Mathé, G. Galmiche, F. Mariotti, and H. Fouillet. 2019. “Natural isotope abundances of carbon and nitrogen in tissue proteins and amino acids as biomarkers of the decreased carbohydrate oxidation and increased amino acid oxidation induced by caloric restriction under a maintained protein intake in obese rats.” *Nutrients* 11(5): 1–16. https://doi.org/10.3390/nu11051087.

Iglesias-Groth, S., F. Cataldo, O. Ursini, and A. Manchado. 2011. “Amino acids in comets and meteorites: Stability under gamma radiation and preservation of the enantiomeric excess.” *Monthly Notices of the Royal Astronomical Society* 410(3): 1447–1453. https://doi.org/10.1111/j.1365-2966.2010.17526.x.

Jarman, C. L., T. Larsen, T. Hunt, C. Lipo, R. Solsvik, N. Wallsgrove, C. Ka’apu-Lyons, H. G. Close, and B. N. Popp. 2017. “Diet of the prehistoric population of Rapa Nui (Easter Island, Chile) shows environmental adaptation and resilience.” *American Journal of Physical Anthropology* 164(2): 343–361. https://doi.org/10.1002/ajpa.23273.

Jastrzębowska K, and I. Gabriel. 2015. “Inhibitors of amino acids biosynthesis as antifungal agents.” *Amino Acids* 47(2): 227-249. https://doi.org/10.1007/s00726-014-1873-1.

Jim, S., V. Jones, S. H. Ambrose, and R. P. Evershed. 2006. “Quantifying dietary macronutrient sources of carbon for bone collagen biosynthesis using natural abundance stable carbon isotope analysis.” *British Journal of Nutrition* 95(6): 1055. https://doi.org/10.1079/BJN20051685.

Jimenez-Diaz, L., A. Caballero, and A. Segura. 2017. “Pathways for the degradation of fatty acids in bacteria.” In: Aerobic Utilization of Hydrocarbons, Oils and Lipids. Handbook of Hydrocarbon and Lipid Microbiology. Springer. https://doi.org/10.1007/978-3-319-39782-5_42-1.

Johnson, B. J., M. L. Fogel, and G. H. Miller. 1998. “Stable isotopes in modern ostrich eggshell: A calibration for paleoenvironmental applications in semi-arid regions of southern Africa.” *Geochimica et Cosmochimica Acta* 62(14): 2451–2461. https://doi.org/10.1016/S0016-7037(98)00175-6.

Johnson, J. J., J. A. Olin, and M. J. Polito. 2019. “A multi-biomarker approach supports the use of compound-specific stable isotope analysis of amino acids to quantify basal carbon source use in a salt marsh consumer.” *Rapid Communications in Mass Spectrometry* 33(23): 1781–1791. https://doi.org/10.1002/rcm.8538.

Johnson, J. J., P. A. Shaw, E. J. Oh, M. J. Wooller, S. Merriman, H. Y. Yun, T. Larsen, J. Krakoff, S. B. Votruba, and D. M. O’Brien. 2021. “The carbon isotope ratios of nonessential amino acids identify sugar-sweetened beverage (SSB) consumers in a 12-wk inpatient feeding study of 32 men with

varying SSB and meat exposures." *The American journal of clinical nutrition* 113(5): 1256–1264. https://doi.org/10.1093/ajcn/nqaa374.

Jones, R. I. 2000. "Mixotrophy in planktonic protists: an overview." *Freshwater biology* 45(2): 219-226. https://doi.org/10.1046/j.1365-2427.2000.00672.x.

Jourdan, M., N. E. Deutz, L. Cynober, and C. Aussel. 2011. "Features, causes and consequences of splanchnic sequestration of amino acid in old rats." *Plos One* 6(11): e27002. https://doi.org/10.1371/journal.pone.0027002.

Kędra, M., C. Moritz, E. S. Choy, C. David, R. Degen, S. Duerksen, I. Ellingsen, B. Górska, J. M. Grebmeier, D. Kirievskaya, D. van Oevelen, K. Piwosz, A. Samuelsen, and J. M. Węsławski. 2015. "Status and trends in the structure of Arctic benthic food webs." *Polar Research* 339: 23775. https://doi.org/10.3402/polar.v34.23775.

KEGG PATHWAY. In: Dubitzky, W., Wolkenhauer, O., Cho, KH., Yokota, H. (eds). 2013. "Encyclopaedia of Systems Biology." Springer, New York.

Kellermann M. Y., G. Wegener, M. Elvert, M. Y. Yoshinaga, Y-S. Lin, T. Holler, X. P. Mollar, K. Knittel, and K-U. Hinrichs. 2012. "Autotrophy as a predominant mode of carbon fixation in anaerobic methane-oxidizing microbial communities." *Proceedings of the National Academy of Sciences* 109: 19321-19326. https://doi.org/10.1073/pnas.1208795109.

Kielland, K. 1994 "Amino acid absorption by Arctic plants: implications for plant nutrition and nitrogen cycling." *Ecology* 75(8): 2373-2383 https://doi.org/10.2307/1940891.

Klap, V. A., M. A. Hemminga, and J. J. Boon. 2000. "Retention of lignin in seagrasses: Angiosperms that returned to the sea." *Marine Ecology Progress Series* 194: 1–11. https://doi.org/10.3354/meps194001.

Kopp, C., I. Domart-Coulon, S. Escrig, B. M. Humbel, M. Hignette, and A. Meibom. 2015. "Subcellular investigation of photosynthesis-driven carbon assimilation in the symbiotic reef coral *Pocillopora damicornis*." *MBio* 6(1): e02299-14. https://doi.org/10.1128/mBio.02299-14.

Kortsch, S., R. Primicerio, M. Fossheim, A. V Dolgov, and M. Aschan. 2015. "Climate change alters the structure of arctic marine food webs due to poleward shifts of boreal generalists." *Proceedings of the Royal Society B: Biological Sciences* 282: 20151546. https://doi.org/10.1098/rspb.2015.1546.

Kwong, W. K., J. Del Campo, V. Mathur, M. J. Vermeij, and P. J. Keeling. 2019. "A widespread coral-infecting apicomplexan with chlorophyll biosynthesis genes." Nature 568(7750): 103-107. https://doi.org/10.1038/s41586-019-1072-z.

de la Vega, C., C. Mahaffey, R. M. Jeffreys, R. Tuerena, and R. Ganeshram. 2019. "Temporal and spatial trends in marine carbon isotopes in the Arctic Ocean and implications for food web studies." *Global Change Biology* 25(12): 4116-4130. https://doi.org/10.1111/gcb.14832.

Labeeuw L., P. T. Martone, Y. Boucher, R. J. Case. 2015. "Ancient origin of the biosynthesis of lignin precursors." *Biology Direct* 10:23. https://doi.org/10.1186/s13062-015-0052-y.

de Laeter, J. R. 2005. "The role of isotopic reference materials for the analysis of "non-traditional" stable isotopes." *Geostandards and Geoanalytical Research* 29(1): 53-61. https://doi.org/10.1111/j.1751-908X.2005.tb00655.x.

Lambert, J. B., and G. Grupe. 1993. "Prehistoric human bone - Archaeology at the molecular level." Berlin: Springer-Verlag Berlin.

Larsen, T., L. T. Bach, R. Salvatteci, Y. V. Wang, N. Andersen, M. Ventura, and M. D. McCarthy. 2015. "Assessing the potential of amino acid ^{13}C patterns as a carbon source tracer in marine sediments: Effects of algal growth conditions and sedimentary diagenesis." *Biogeosciences* 12(16): 4979–4992. https://doi.org/10.5194/bg-12-4979-2015.

Larsen, T., T. Hansen, and J. Dierking. 2020. "Characterizing niche differentiation among marine consumers with amino acid $\delta^{13}C$ fingerprinting." *Ecology and Evolution* 10(14): 7768-7782. https://doi.org/10.1002/ece3.6502.

Larsen, T., M. M. Pollierer, M. Holmstrup, A. D'Annibale, K. Maraldo, N. Andersen, and J. Eriksen. 2016a. "Substantial nutritional contribution of bacterial amino acids to earthworms and enchytraeids: A case study from organic grasslands." *Soil Biology and Biochemistry* 99: 21–27. https://doi.org/10.1016/j.soilbio.2016.03.018.

Larsen, T., D. L. Taylor, M. B. Leigh, and D. M. O'Brien. 2009. "Stable isotope fingerprinting: a novel method for identifying plant, fungal, or bacterial origins of amino acids." *Ecology* 90(12): 3526–3535. https://doi.org/10.1890/08-1695.1.

Larsen, T., M. Ventura, N. Andersen, D. M. O'Brien, U. Piatkowski, and M. D. McCarthy. 2013. "Tracing carbon sources through aquatic and terrestrial food webs using amino acid stable isotope fingerprinting." *PLoS ONE* 8(9): e73441. https://doi.org/10.1371/journal.pone.0073441.

Larsen, T., M. Ventura, K. Maraldo, X. Triadó-Margarit, E. O. Casamayor, Y. V. Wang, N. Andersen, and D. M. O'Brien. 2016b. "The dominant detritus-feeding invertebrate in Arctic peat soils derives its essential amino acids from gut symbionts." *The Journal of animal ecology* 85(5): 1275–1285. https://doi.org/10.1111/1365-2656.12563.

Larsen T., Y. Yokoyama, R. Fernandes. 2018. "Radiocarbon ecology: Insights and perspectives from aquatic and terrestrial studies." *Methods in Ecology and Evolution* 9(1): 181-190. https://doi.org/10.1111/2041-210X.12851.

Larsen, T., Y. V. Wang, and A. H. L. Wan. 2022a. "Tracing the trophic fate of aquafeed macronutrients with carbon isotope ratios of amino acids." *Frontiers in Marine Science* 9: 1–14. https://doi.org/10.3389/fmars.2022.813961.

Larsen T., R. Fernandes, Y. V. Wang, and P. Roberts. 2022b. "Reconstructing Hominin Diets with Stable Isotope Analysis of Amino Acids: New Perspectives and Future Directions." *Bioscience* 72(7): 618-637. https://doi.org/10.1093/biosci/biac028.

Larsen, T., M. J. Wooller, M. L. Fogel, and D. M. O'Brien. 2012. "Can amino acid carbon isotope ratios distinguish primary producers in a mangrove ecosystem?" *Rapid Communications in Mass Spectrometry* 26(13): 1541–1548. https://doi.org/10.1002/rcm.6259.

Lee, Y., C. Chiang, P. Huang, C. Chung, T. D. Huang, C. Wang, C. Chen, R. Chang, C. Liao, and R. R. Reisz. 2017. "Evidence of preserved collagen in an Early Jurassic sauropodomorph dinosaur revealed by synchrotron FTIR microspectroscopy." *Nature Communications* 8: 14220. https://doi.org/10.1038/ncomms14220.

Lepiniec, L., I. Debeaujon, J. M. Routaboul, A. Baudry, L. Pourcel, N. Nesi, and M. Caboche. 2006. "Genetics and biochemistry of seed flavonoids." *Annual Review of Plant Biology* 57(1): 405–430. https://doi.org/10.1146/annurev.arplant.57.032905.105252.

Llewellyn C. A., C. Greig, A. Silkina, B. Kultschar, M.D. Hitchings, and G. Farnham. 2020. "Mycosporine-like amino acid and aromatic amino acid transcriptome response to UV and far-red light in the cyanobacterium *Chlorogloeopsis fritschii* PCC 6912." *Scientific Reports* 10: 20638. https://doi.org/10.1038/s41598-020-77402-6.

Liew, J. H., K. W. J. Chua, E. R. Arsenault, J. H. Thorp, A. Suvarnaraksha, A. Amirrudin, and D. C. J. Yeo. 2019. "Quantifying terrestrial carbon in freshwater food webs using amino acid isotope analysis: Case study with an endemic cavefish." *Methods in Ecology and Evolution* 10(9): 1594–1605. https://doi.org/10.1111/2041-210X.13230.

Liu, H. Z., L. Luo, and D. L. Cai. 2018. "Stable carbon isotopic analysis of amino acids in a simplified food chain consisting of the green alga *Chlorella* spp., the calanoid copepod *Calanus sinicus*, and the japanese anchovy (*Engraulis japonicus*)." *Canadian Journal of Zoology* 96: 23–30. https://doi.org/10.1139/cjz-2016-0170.

Lynch, A. H., N. J. Kruger, R. E. M. Hedges, and J. S. O. McCullagh. 2016. "Variability in the carbon isotope composition of individual amino acids in plant proteins from different sources: 1 Leaves." *Phytochemistry* 125: 27–34. https://doi.org/10.1016/j.phytochem.2016.01.011.

Lynch, A. H., J. S. O. McCullagh, and R. E. M. Hedges. 2011. “Liquid chromatography/isotope ratio mass spectrometry measurement of $\delta^{13}C$ of amino acids in plant proteins.” *Rapid Communications in Mass Spectrometry* 25(20): 2981–2988. https://doi.org/10.1002/rcm.5142.

Lytle, C. R., and E. M. Perdue. 1981. “Free proteinaceous, and humic-bound amino acids in river water containing high concentrations of aquatic humus.” *Environmental Science & Technology* 15(2): 224-228. https://doi.org/10.1021/es00084a009.

Ma, Y., V. Grimes, G. Van Biesen, L. Shi, K. Chen, M. A. Mannino, and B. T. Fuller. 2021. “Aminoisoscapes and palaeodiet reconstruction: New perspectives on millet-based diets in China using amino acid $\delta^{13}C$ values.” *Journal of Archaeological Science* 125: 105289. https://doi.org/10.1016/j.jas.2020.105289.

Macartney, K. J., M. Slattery, and M. P. Lesser. 2020. “Trophic ecology of Caribbean sponges in the mesophotic zone.” *Limnology and Oceanography* 66(4): 1113-1124. https://doi.org/10.1002/lno.11668.

Macko, S. A., M. H. Engel, and Y. Qian. 1994. “Early diagenesis and organic matter preservation - a molecular stable carbon isotope perspective.” *Chemical Geology* 114: 365–379. https://doi.org/10.1016/0009-2541(94)90064-7.

Magozzi, S., S. R. Thorrold, L. Houghton, V. A. Bendall, S. Hetherington, G. Mucientes, L. J. Natanson, N. Queiroz, M. N. Santos, and C. N. Trueman. 2021. “Compound-Specific Stable Isotope Analysis of Amino Acids in Pelagic Shark Vertebrae Reveals Baseline, Trophic, and Physiological Effects on Bulk Protein Isotope Records.” *Frontiers in Marine Science* 8: 1–17. https://doi.org/10.3389/fmars.2021.673016.

Magozzi, S., A. Yool, H. B. Vander Zanden, M. B. Wunder, and C. N. Trueman. 2017. “Using ocean models to predict spatial and temporal variation in marine carbon isotopes.” *Ecosphere* 8(5): e01763. https://doi.org/10.1002/ecs2.1763.

Manlick, P. J., J. A. Cook, and S. D. Newsome. 2022. “The coupling of green and brown food webs regulates trophic position in a montane mammal guild.” *Ecology* 104(2): 1–13. https://doi.org/10.1002/ecy.3949.

Manlick, P. J., and S. D. Newsome. 2022. “Stable isotope fingerprinting traces essential amino acid assimilation and multichannel feeding in a vertebrate consumer.” *Methods in Ecology and Evolution* 13(8): 1819–1830. https://doi.org/10.1111/2041-210X.13903.

Makarewicz, C. A., and J. Sealy. 2015. “Dietary reconstruction, mobility, and the analysis of ancient skeletal tissues: Expanding the prospects of stable isotope research in archaeology.” *Journal of Archaeological Science* 56: 146-158. https://doi.org/10.1016/j.jas.2015.02.035.

Marte, F., C. Solazzo, D. von Endt, D. Erhardt, and C. Tumosa. 2003. The stability of natural history specimens in fluid-preserved collections. In: 6th International Congress, Cultural Heritage: Context and Conservation in Havana, Cuba.

Martinez, A. M., and A. C. Kak. 2001. “PCA versus LDA.” *IEEE transactions on pattern analysis and machine intelligence* 23(2): 228-233. https://doi.org/10.1109/34.908974.

Martinez, S., J. Bellworthy, C. Ferrier-Pagès, and T. Mass. 2021. “Selection of mesophotic habitats by *Oculina patagonica* in the Eastern Mediterranean Sea following global warming.” *Scientific Reports* 11: 1–15. https://doi.org/10.1038/s41598-021-97447-5.

Martinez, S., M. Lalzar, E. Shemesh, S. Einbinder, B. Goodman Tchernov, and D. Tchernov. 2020. “Effect of Different Derivatization Protocols on the Calculation of Trophic Position Using Amino Acids Compound-Specific Stable Isotopes.” *Frontiers in Marine Science* 7: 1–7. https://doi.org/10.3389/fmars.2020.561568.

Martin-Perez M, and Villén J. 2015. “Feasibility of protein turnover studies in prototroph *Saccharomyces cerevisiae* strains.” *Analytical Chemistry* 87(7): 4008-4014. https://doi.org/10.1021/acs.analchem.5b00264.

Martone, P. T., J. M. Estevez, F. Lu, K. Ruel, M. W. Denny, C. Somerville, and J. Ralph. 2009. “Discovery of Lignin in Seaweed Reveals Convergent Evolution of Cell-Wall Architecture.” *Current Biology* 19(2): 169–175. https://doi.org/10.1016/j.cub.2008.12.031.

Matantseva O. V., and S. O. Skarlato. 2013. “Mixotrophy in microorganisms: Ecological and cytophysiological aspects.” *Journal of Evolutionary Biochemistry and Physiology* 49: 377-388. https://doi.org/10.1134/S0022093013040014.

Matsubayashi, J., and I. Tayasu. 2019. “Collagen turnover and isotopic records in cortical bone.” *Journal of Archaeological Science* 106: 37–44. https://doi.org/10.1016/j.jas.2019.03.010.

Matthews D., M. Marano, and R. Campbell. 1993. “Splanchnic bed utilization of leucine and phenylalanine in humans.” *American Journal of Physiology-Endocrinology and Metabolism* 264(1): E109-E118. https://doi.org/10.1152/ajpendo.1993.264.1.E109.

Maurer, A. F., A. Person, T. Tütken, S. Amblard-Pison, and L. Ségalen. 2014. “Bone diagenesis in arid environments: An intra-skeletal approach.” *Palaeogeography, Palaeoclimatology, Palaeoecology* 416: 17–29. https://doi.org/10.1016/j.palaeo.2014.08.020.

McCarthy M. W., and T. J. Walsh. 2018. “Amino Acid Metabolism and Transport Mechanisms as Potential Antifungal Targets.” *International Journal of Molecular Science* 19(3): 909. https://doi.org/10.3390/ijms19030909.

McCormack, J., P. Szpak, N. Bourgon, M. Richards, C. Hyland, P. Méjean, J. Hublin, and K. Jaouen. 2021. “Zinc isotopes from archaeological bones provide reliable trophic level information for marine mammals.” *Communications Biology* 4: 683. https://doi.org/10.1038/s42003-021-02212-z.

McMahon, K. W., M. L. Fogel, T. S. Elsdon, and S. R. Thorrold. 2010. “Carbon isotope fractionation of amino acids in fish muscle reflects biosynthesis and isotopic routing from dietary protein.” *Journal of Animal Ecology* 79(5): 1132–1141. https://doi.org/10.1111/j.1365-2656.2010.01722.x.

McMahon, K. W., M. D. McCarthy, O. A. Sherwood, T. Larsen, and T. P. Guilderson. 2015a. “Millennial-scale plankton regime shifts in the subtropical North Pacific Ocean.” *Science* 350(6267): 1530–1533. https://doi.org/10.1126/science.aaa9942.

McMahon, K. W., M. J. Polito, S. Abel, M. D. Mccarthy, and S. R. Thorrold. 2015b. “Carbon and nitrogen isotope fractionation of amino acids in an avian marine predator, the gentoo penguin (*Pygoscelis papua*).” *Ecology and Evolution* 5(6): 1278-1290. https://doi.org/10.1002/ece3.1437.

McMahon, K. W., S. R. Thorrold, L. A. Houghton, and M. L. Berumen. 2016. “Tracing carbon flow through coral reef food webs using a compound-specific stable isotope approach.” *Oecologia* 180(3): 809-821. https://doi.org/10.1007/s00442-015-3475-3.

McMahon, K. W., B. Williams, T. P. Guilderson, D. S. Glynn, and M. D. McCarthy. 2018. “Calibrating amino acid $\delta^{13}C$ and $\delta^{15}N$ offsets between polyp and protein skeleton to develop proteinaceous deep-sea corals as paleoceanographic archives.” *Geochimica et Cosmochimica Acta* 220: 261–275. https://doi.org/10.1016/j.gca.2017.09.048.

McMahon, K. W. and S. D. Newsome. 2019. “Amino acid isotope analysis: a new frontier in studies of animal migration and foraging ecology.” In *Tracking animal migration with stable isotopes*. Academic Press.

McMeans, B. C., K. S. McCann, M. Humphries, N. Rooney, and A. T. Fisk. 2015. “Food Web Structure in Temporally-Forced Ecosystems.” *Trends in Ecology & Evolution* 30: 662–672. https://doi.org/10.1016/j.tree.2015.09.001.

Melzer E., and H. L. Schmidt. 1987. “Carbon Isotope Effects on the Pyruvate-Dehydrogenase Reaction and Their Importance for Relative ^{13}C Depletion in Lipids.” *Journal of Biological Chemistry* 262(17): 8159-8164. https://doi.org/10.1016/S0021-9258(18)47543-6.

Meier-Augenstein, W. 1999. “Applied gas chromatography coupled to isotope ratio mass spectrometry.” *Journal of Chromatography A* 842(1-2): 351–371. https://doi.org/10.1016/S0021-9673(98)01057-7.

Meier-Augenstein, W. 2002. “Stable isotope analysis of fatty acids by gas chromatography-isotope ratio

mass spectrometry." *Analytica Chimica Acta* 465(1-2): 63–79. https://doi.org/10.1016/S0021-9673(98)01057-7.

Meier-Augenstein, W. 2018. "Stable isotope forensics: methods and forensic applications of stable isotope analysis." John Wiley & Sons, Ltd.

Meier-Augenstein, W., and A. Schimmelmann. 2019. "A guide for proper utilisation of stable isotope reference materials." *Isotopes in Environmental and Health Studies* 55(2): 113–128. https://doi.org/10.1080/10256016.2018.1538137.

Misarti, N., E. Gier, B. Finney, K. Barnes, and M. McCarthy. 2017. "Compound-specific amino acid $\delta^{15}N$ values in archaeological shell: Assessing diagenetic integrity and potential for isotopic baseline reconstruction." *Rapid Communications in Mass Spectrometry* 31(2): 1881–1891. https://doi.org/10.1002/rcm.7963.

Moloney, C. L., M. A. St John, K. L. Denman, D. M. Karl, F. W. Köster, S. Sundby, and R. P. Wilson. 2011. "Weaving marine food webs from end to end under global change." *Journal of Marine Systems* 84(1-2): 106–116. https://doi.org/10.1016/j.jmarsys.2010.06.012.

Moore, J. W., and B. X. Semmens. 2008. "Incorporating uncertainty and prior information into stable isotope mixing models." *Ecology Letters* 11(5): 470–480. https://doi.org/10.1111/j.1461-0248.2008.01163.x.

Mora, A., A. Pacheco, C. Roberts, and C. Smith. 2018. "Pica 8: Refining dietary reconstruction through amino acid $\delta^{13}C$ analysis of tendon collagen and hair keratin." *Journal of Archaeological Science* 93: 94–109. https://doi.org/10.1016/j.quaint.2016.10.018.

Morrissey, E. M., J. Kane, B. M. Tripathi, M. S. I. Rion, B. A. Hungate, R. Franklin, C. Walter, B. Sulman, and E. Brzostek. 2023. "Carbon acquisition ecological strategies to connect soil microbial biodiversity and carbon cycling." *Soil Biology and Biochemistry* 177: 108893. https://doi.org/10.1016/j.soilbio.2022.108893.

Nakazawa, T. 2015. "Ontogenetic niche shifts matter in community ecology: a review and future perspectives. Population Ecology 57(2): 347–354." https://doi.org/10.1007/s10144-014-0448-z.

Nayfach S., S. Roux, R. Seshadri, D. Udwary, N. Varghese, F. Schulz, D. Wu, D. Paez-Espino et al. 2021. "A genomic catalog of Earth's microbiomes." *Nature Biotechnology* 39: 499-509. https://doi.org/10.1038/s41587-020-0718-6.

Neis, E. P. J. G., C. H. C. Dejong, and S. S. Rensen. 2015. "The role of microbial amino acid metabolism in host metabolism." *Nutrients* 7(4): 2930–2946. https://doi.org/10.3390/nu7042930.

Newsome, S. D., K. L. Feeser, C. J. Bradley, C. Wolf, C. Takacs-Vesbach, and M. L. Fogel. 2020. Isotopic and genetic methods reveal the role of the gut microbiome in mammalian host essential amino acid metabolism. *Proceedings of the Royal Society B* 287(1922): 20192995. https://doi.org/10.1098/rspb.2019.2995.

Newsome, S. D., M. L. Fogel, L. Kelly, and C. M. Del Rio. 2011. "Contributions of direct incorporation from diet and microbial amino acids to protein synthesis in Nile tilapia." *Functional Ecology* 25(5): 1051–1062. https://doi.org/10.1111/j.1365-2435.2011.01866.x.

Newsome, S. D., N. Wolf, J. Peters, and M. L. Fogel. 2014. "Amino acid $\delta^{13}C$ analysis shows flexibility in the routing of dietary protein and lipids to the tissue of an omnivore." *Integrative and comparative biology* 54(5): 890–902. https://doi.org/10.1093/icb/icu106.

Nicholson, G. M., and K. D. Clements. 2023. "Micro-photoautotroph predation as a driver for trophic niche specialization in 12 syntopic Indo-Pacific parrotfish species." *Biological Journal of the Linnean Society*:1–24. https://doi.org/10.1093/biolinnean/blad005.

Nielsen, J. M., E. L. Clare, B. Hayden, M. T. Brett, and P. Kratina. 2017. "Diet tracing in ecology: Method comparison and selection." *Methods in Ecology and Evolution* 9(2): 278–291. https://doi.org/10.1111/2041-210X.12869.

Nifong J. C., C. A. Layman, and B. R. Silliman. 2015. "Size, sex and individual-level behaviour drive

intrapopulation variation in cross-ecosystem foraging of a top-predator." *Journal of Animal Ecology* 84(1): 35-48. https://doi.org/10.1111/1365-2656.12306.

O'Donnell, T. H., S. A. Macko, and J. F. Wehmiller. 2007. "Stable carbon isotope composition of amino acids in modern and fossil *Mercenaria*." *Organic Geochemistry* 38(3): 485–498. https://doi.org/10.1016/j.orggeochem.2006.06.010-

O'Leary, M. H. 1988. "Carbon Isotopes in Photosynthesis." *BioScience* 38(5): 328–336. https://doi.org/10.2307/1310735.

Ohkouchi, N., Y. Chikaraishi, H. G. Close, B. Fry, T. Larsen, D. J. Madigan, M. D. McCarthy, K. W. McMahon, T. Nagata, Y. I. Naito, N. O. Ogawa, B. N. Popp, S. Steffan, Y. Takano, I. Tayasu, A. S. J. Wyatt, Y. T. Yamaguchi, and Y. Yokoyama. 2017. "Advances in the application of amino acid nitrogen isotopic analysis in ecological and biogeochemical studies." *Organic Geochemistry* 113: 150–174. https://doi.org/10.1016/j.orggeochem.2017.07.009.

Ortiz, J. E., Y. Sánchez-Palencia, I. Gutiérrez-Zugasti, T. Torres, and M. González-Morales. 2018. "Protein diagenesis in archaeological gastropod shells and the suitability of this material for amino acid racemisation dating: *Phorcus lineatus* (da Costa, 1778)." *Quaternary Geochronology* 46: 16–27. https://doi.org/10.1016/j.quageo.2018.02.002.

Parks D. H. , M. Chuvochina, P. A. Chaumeil, C. Rinke, A. J. Mussig, and P. Hugenholtz. 2020. "A complete domain-to-species taxonomy for Bacteria and Archaea." *Nature Biotechnology* 38: 1079-1086. https://doi.org/10.1038/s41587-020-0501-8.

Parnell, A. C., R. Inger, S. Bearhop, and A. L. Jackson. 2010. Source partitioning using stable isotopes coping with too much variation. *PLoS ONE* 5(3): e9672. https://doi.org/10.1016/10.1371/journal.pone.0009672.

Parnell, A. C., D. L. Phillips, S. Bearhop, B. X. Semmens, E. J. Ward, J. W. Moore, A. L. Jackson, J. Grey, D. J. Kelly, and R. Inger. 2013. Bayesian stable isotope mixing models." *Environmetrics* 24(6): 387-399. https://doi.org/10.1016/10.1002/env.2221.

Pauli, J. N., S. D. Newsome, J. A. Cook, C. Harrod, S. A. Steffan, C. J. Baker, ... & B. Hayden. 2017. "Why we need a centralized repository for isotopic data." *Proceedings of the National Academy of Sciences*, 114(12), 2997-3001. https://doi.org/10.1073/pnas.170174211

Pauly, D., and V. Christensen. 1995. "Primary production required to sustain global fisheries." *Nature* 374(6519): 255-257. https://doi.org/10.1016/10.1038/374255a0.

Payan, P., A. Edeyer, H. de Pontual, G. Borelli, G. Boeuf, and N. Mayer-Gostan. 1999. "Chemical composition of saccular endolymph and otolith in fish inner ear: lack of spatial uniformity." *The American journal of physiology* 277(1): R123-R131. https://doi.org/10.1152/ajpregu.1999.277.1.R123.

Pellegrini, M., and C. Snoeck. 2016. "Comparing bioapatite carbonate pre-treatments for isotopic measurements: Part 2 - Impact on carbon and oxygen isotope compositions." *Chemical Geology* 420: 88–96. https://doi.org/10.1016/10.1016/j.chemgeo.2015.10.038.

Pempkowiak, J. 2020. "Limitation of lignin derivatives as biomarkers of land derived organic matter in the coastal marine sediments." *Oceanologia* 62(3): 374–386. https://doi.org/10.1016/j.oceano.2020.04.004.

Pernice, M., J. B. Raina, N. Rädecker, A. Cárdenas, C. Pogoreutz, and C. R. Voolstra. 2020. "Down to the bone: the role of overlooked endolithic microbiomes in reef coral health." *The ISME Journal* 14: 325–334. https://doi.org/10.1038/s41396-019-0548-z.

Peterson, B. J., and B. Fry. 1987. "Stable isotopes in ecosystem studies." *Annual Review of Ecology and Systematics* 18(1): 293–320. https://doi.org/10.1146/annurev.es.18.110187.001453.

Phillips, D. L. 2012. "Converting isotope values to diet composition: the use of mixing models." *Journal of Mammalogy* 93(2): 342–352. https://doi.org/10.1644/11-MAMM-S-158.1.

Phillips, D. L., R. Inger, S. Bearhop, A. L. Jackson, J. W. Moore, A. C. Parnell, B. X. Semmens, and E. J. Ward.

2014. “Best practices for use of stable isotope mixing models in food-web studies.” *Canadian Journal of Zoology* 92(10): 823–835. https://doi.org/10.1139/cjz-2014-0127.

Phillips, D. L., and P. L. Koch. 2002. “Incorporating concentration dependence in stable isotope mixing models: a reply to Robbins, Hilderbrand and Farley (2002).” *Oecologia* 130: 114–125. https://doi.org/10.1007/s00442-002-0977-6.

Phillips, N. D., E. A. Elliott Smith, S. D. Newsome, J. D. R. Houghton, C. D. Carson, J. Alfaro-Shigueto, J. C. Mangel, L. E. Eagling, L. Kubicek, and C. Harrod. 2020. “Bulk tissue and amino acid stable isotope analyses reveal global ontogenetic patterns in ocean sunfish trophic ecology and habitat use.” *Marine Ecology Progress Series* 633: 127–140. https://doi.org/10.3354/meps13166.

Pita, L., L. Rix, B. M. Slaby, A. Franke, and U. Hentschel. 2018. “The sponge holobiont in a changing ocean: from microbes to ecosystems.” *Microbiome* 6: 46. https://doi.org/10.1186/s40168-018-0428-1.

Pollierer, M. M., and S. Scheu. 2021. “Stable isotopes of amino acids indicate that soil decomposer microarthropods predominantly feed on saprotrophic fungi.” *Ecosphere* 12(3): e03425. https://doi.org/10.1002/ecs2.3425.

Pollierer, M. M., S. Scheu, and A. V. Tiunov. 2020. “Isotope analyses of amino acids in fungi and fungal feeding Diptera larvae allow differentiating ectomycorrhizal and saprotrophic fungi-based food chains.” *Functional Ecology* 34(11): 2375–2388. https://doi.org/10.1111/1365-2435.13654.

Portune, K. J., M. Beaumont, A. Davila, D. Tom, F. Blachier, and Y. Sanz. 2016. “Gut microbiota role in dietary protein metabolism and health-related outcomes: The two sides of the coin.” *Trends in Food Science & Technology* 57: 213–232. https://doi.org/10.1016/j.tifs.2016.08.011.

Price, M. N., G. M. Zane, J. V. Kuehl, R. A. Melnyk, J. D. Wall, A. M. Deutschbauer, and A. P. Arkin. 2018. “Filling gaps in bacterial amino acid biosynthesis pathways with high-throughput genetics.” *PLoS Genetics* 14: e1007147. https://doi.org/10.1371/journal.pgen.1007147.

Prigent, S., G. Collet, S. M. Dittami, L. Delage, F. E. De Corny, O. Dameron, D. Eveillard, S. Thiele, J. Cambefort, C. Boyen, A. Siegel, and T. Tonon. 2014. “The genome-scale metabolic network of *Ectocarpus siliculosus* (EctoGEM): A resource to study brown algal physiology and beyond.” *Plant Journal* 80(2): 367–381. https://doi.org/10.1111/tpj.12627.

Radice, V. Z., M. T. Brett, B. Fry, M. D. Fox, O. Hoegh-Guldberg, and S. G. Dove. 2019. “Evaluating coral trophic strategies using fatty acid composition and indices.” *PloS ONE* 14(9): e0222327. https://doi.org/10.1371/journal.pone.0222327.

Raghavan, M., J. S. O. McCullagh, N. Lynnerup, and R. E. M. Hedges. 2010. “Amino acid $\delta^{13}C$ analysis of hair proteins and bone collagen using liquid chromatography/isotope ratio mass spectrometry: paleodietary implications from intra-individual comparisons.” *Rapid Communications in Mass Spectrometry* 24(5): 541–548. https://doi.org/10.1002/rcm.4398.

Raubenheimer, D., S. J. Simpson, and A. H. Tait. 2012. “Match and mismatch: Conservation physiology, nutritional ecology and the timescales of biological adaptation.” *Philosophical Transactions of the Royal Society B: Biological Sciences* 367(1596): 1628–1646. https://doi.org/10.1098/rstb.2012.0007.

Reed, K. 2021. “Food systems in archaeology. Examining production and consumption in the past.” *Archaeological Dialogues* 28(1): 51-75. https://doi.org/10.1017/S1380203821000088.

Reeds, P. J., D. G. Burrin, F. Jahoor, L. Wykes, J. Henry, and E. M. Frazer. 1996. “Enteral glutamate is almost completely metabolized in first pass by the gastrointestinal tract of infant pigs.” *American Journal of Physiology-Endocrinology and Metabolism* 270(3): E413-E418. https://doi.org/10.1152/ajpendo.1996.270.3.E413.

Richards, T. A., J. B. Dacks, S. A. Campbell, J. L. Blanchard, P. G. Foster, R. McLeod, and C. W. Roberts. 2006. “Evolutionary origins of the eukaryotic shikimate pathway: Gene fusions, horizontal gene transfer, and endosymbiotic replacements.” *Eukaryotic Cell* 5(9): 1517–1531.

https://doi.org/10.1128/EC.00106-06.

Riedijk., M. A., D. A. de Gast-Bakker, J. L. Wattimena, and J. B. van Goudoever. 2007. “Splanchnic oxidation is the major metabolic fate of dietary glutamate in enterally fed preterm infants.” *Pediatric research* 62(4): 468-473. https://doi.org/10.1203/PDR.0b013e31813cbeba.

Rivkin, R. B., and M. Putt. 1987. “Heterotrophy and photoheterotrophy by Antarctic microalgae: light-dependent incorporation of amino acids and glucose.” *Journal of Phycology* 23(3): 442-452. https://doi.org/10.1111/j.1529-8817.1987.tb02530.x.

Roberts, P., R. Fernandes, O. E. Craig, T. Larsen, A. Lucquin, J. Swift, and J. Zech. 2018. “Calling all archaeologists: guidelines for terminology, methodology, data handling, and reporting when undertaking and reviewing stable isotope applications in archaeology.” *Rapid Communications in Mass Spectrometry* 32(5): 361–372. https://doi.org/10.1002/rcm.8044.

Rowe, A. G., K. Iken, A. L. Blanchard, D. M. O’Brien, R. Døving Osvik, M. Uradnikova, and M. J. Wooller. 2019. “Sources of primary production to Arctic bivalves identified using amino acid stable carbon isotope fingerprinting.” *Isotopes in Environmental and Health Studies* 55(4): 366–384. https://doi.org/10.1080/10256016.2019.1620742.

Ruess, L., and D. C. Müller-Navarra. 2019. “Essential biomolecules in food webs.” *Frontiers in Ecology and Evolution* 7: 1–18. https://doi.org/10.3389/fevo.2019.00269.

Ruiz-Dueñas F. J., J. M Barrasa, M. Sánchez-García, S. Camarero, S. Miyauchi, A. Serrano, D. Linde, R. Babiker, E. Drula et al. 2021. “Genomic Analysis Enlightens Agaricales Lifestyle Evolution and Increasing Peroxidase Diversity.” *Molecular Biology and Evolution* 38(4): 1428-1446. https://doi.org/10.1093/molbev/msaa301.

Saboret, G., D. Stalder, B. Matthews, J. Brodersen, and C. J. Schubert. 2023. “Autochthonous production sustains food webs in large perialpine lakes, independent of trophic status: Evidence from amino acid stable isotopes.” *Freshwater Biology*, 68: 870-887. https://doi.org/10.1111/fwb.14071.

Salvatteci, R., D. B. Field, T. Baumgartner, V. Ferreira, and D. Gutierrez. 2012. “Evaluating fish scale preservation in sediment records from the oxygen minimum zone off Peru.” *Paleobiology* 38: 52–78. https://doi.org/10.1017/s0094837300000403.

Sanders, R. W. 1991. “Mixotrophic protists in marine and freshwater ecosystems.” *The Journal of protozoology* 38(1): 76-81. https://doi.org/10.1111/j.1550-7408.1991.tb04805.x.

Schaart M. W., H. Schierbeek, S. R. van der Schoor, B. Stoll, D. G. Burrin, P. J. Reeds, J. B. van Goudoever. 2005. “Threonine utilization is high in the intestine of piglets.” *The Journal of Nutrition* 135(4): 765-770. https://doi.org/10.1093/jn/135.4.765.

Schlacher, T. A., and R. M. Connolly. 2014. “Effects of acid treatment on carbon and nitrogen stable isotope ratios in ecological samples: A review and synthesis.” *Methods in Ecology and Evolution* 5(6): 541–550. https://doi.org/10.1111/2041-210X.12183.

Schlichter, D., B. Zscharnack, and H. Krisch. 1995. “Transfer of photoassimilates from endolithic algae to coral tissue.” *Naturwissenschaften* 82(12): 561-564. https://doi.org/10.1007/BF01140246.

Schmidt, S. A., J. A. Raven, and C. Paungfoo-Lonhienne. 2013. “The mixotrophic nature of photosynthetic plants.” *Functional Plant Biology* 40: 425–438. https://doi.org/10.1071/FP13061.

Schulting, R. J., R. MacDonald, and M.P. Richards. 2022. “FRUITS of the sea? A cautionary tale regarding Bayesian modelling of palaeodiets using stable isotope data.” *Quaternary International* 650: 52-61. https://doi.org/10.1016/j.quaint.2022.02.012.

Scott, J. H., D. M. O’Brien, D. Emerson, H. Sun, G. D. McDonald, A. Salgado, and M. L. Fogel. 2006. “An examination of the carbon isotope effects associated with amino acid biosynthesis.” *Astrobiology* 6(6): 867–880. https://doi.org/10.1089/ast.2006.6.867.

Sealy, J., M. Johnson, M. Richards, and O. Nehlich. 2014. “Comparison of two methods of extracting bone collagen for stable carbon and nitrogen isotope analysis: Comparing whole bone demineralization with gelatinization and ultrafiltration.” *Journal of Archaeological Science* 47: 64–69.

https://doi.org/10.1016/j.jas.2014.04.011.

Selosse M. A., M. Roy. 2009. “Green plants that feed on fungi: facts and questions about mixotrophy.” *Trends in Plant Science* 14(2): 64-70. https://doi.org/10.1016/j.tplants.2008.11.004.

Selosse, M. A., M. F. Bocayuva, M. C. M. Kasuya, and P. E. Courty. 2016. “Mixotrophy in mycorrhizal plants: extracting carbon from mycorrhizal networks.” In: *Molecular mycorrhizal symbiosis.* John Wiley & Sons, Inc. https://doi.org/10.1002/9781118951446.ch25.

Selosse, M. A., M. Charpin, and F. Not. 2017. “Mixotrophy everywhere on land and in water: the grand écart hypothesis.” *Ecology Letters* 20(2): 246-263. https://doi.org/10.111/ele.12714.

Semmens, B. X., E. J. Ward, J. W. Moore, and C. T. Darimont. 2009. “Quantifying inter-and intra-population niche variability using hierarchical bayesian stable isotope mixing models.” *PLoS ONE* 4(7): e6187. https://doi.org/10.1371/journal.pone.0006187.

Serrano, O., L. Serrano, M. A. Mateo, I. Colombini, L. Chelazzi, E. Gagnarli, and M. Fallaci. 2008. “Acid washing effect on elemental and isotopic composition of whole beach arthropods: Implications for food web studies using stable isotopes.” *Acta Oecologica* 34: 89–96. https://doi.org/10.1016/j.actao.2008.04.002.

Sessions, A. L. 2006. “Isotope-ratio detection for gas chromatography.” *Journal of Separation Science* 29(12): 1946–1961. https://doi.org/10.1002/jssc.200600002.

Sharp, K. H., Z. A. Pratte, A. H. Kerwin, R. D. Rotjan, and F. J. Stewart. 2017. “Season, but not symbiont state, drives microbiome structure in the temperate coral *Astrangia poculata*.” *Microbiome* 5(1): 120. 10.1186/s40168-017-0329-8.

Shih, J. L., K. E. Selph, C. B. Wall, N. J. Wallsgrove, M. P. Lesser, and B. N. Popp. 2020. “Trophic ecology of the tropical Pacific sponge *Mycale grandis* inferred from amino acid compound-specific isotopic analyses.” *Microbial Ecology* 79(2): 495–510. https://doi.org/10.1007/s00248-019-01410-x.

Silfer, J. A., M. H. Engel, S. A. Macko, and E. J. Jumeau. 1991.” Stable carbon isotope analysis of amino acid enantiomers by conventional isotope ratio mass spectrometry and combined gas chromatography/isotope ratio mass spectrometry.” *Analytical Chemistry* 63(4): 370–374. https://doi.org/10.1021/ac00004a014.

Silfer, J. A., Y. Qian, S. A. Macko, and M. H. Engel. 1994. “Stable carbon isotope compositions of individual amino acid enantiomers in mollusc shell by GC/C/IRMS.” *Organic Geochemistry* 21(6-7): 603-609. https://doi.org/10.1016/0146-6380(94)90006-X.

Silhavy, T. J., D. Kahne, and S. Walker. 2010. “The Bacterial Cell Envelope.“ *Cold Spring Harbour Perspectives in Biology* 2: a000414. https://doi.org/10.1101/cshperspect.a000414.

Silverman, S. N., A. A. Phillips, G. M. Weiss, E. B. Wilkes, J. M. Eiler, and A. L. Sessions. 2022. “Practical considerations for amino acid isotope analysis.” *Organic Geochemistry* 164: 104345. https://doi.org/10.1016/j.orggeochem.2021.104345.

Skinner, C., A. C. Mill, M. D. Fox, S. P. Newman, Y. Zhu, A. Kuhl, and N. V. C. Polunin. 2021. “Offshore pelagic subsidies dominate carbon inputs to coral reef predators.” *Science Advances* 7(8): eabf3792. https://doi.org/10.1126/sciadv.abf3792.

Skinner, C., M. R. D. Cobain, Y. Zhu, A. S. J. Wyatt, and N. V. C. Polunin. 2022. “Progress and direction in the use of stable isotopes to understand complex coral reef ecosystems: A review.” *Oceanography and Marine Biology: An Annual Review* 60: 373-432. https://doi.org/10.1201/9781003288602-8.

Smith, C. I., B. T. Fuller, K. Choy, and M. P. Richards. 2009. “A three-phase liquid chromatographic method for $\delta^{13}C$ analysis of amino acids from biological protein hydrolysates using liquid chromatography-isotope ratio mass spectrometry.” *Analytical Biochemistry* 390(2): 165–172. https://doi.org/10.1016/j.ab.2009.04.014.

Smith, J. A., D. Mazumder, I. M. Suthers, and M. D. Taylor. 2013. “To fit or not to fit: evaluating stable isotope mixing models using simulated mixing polygons.” *Methods in Ecology and Evolution* 4(7): 612-618. https://doi.org/10.1111/2041-210X.12048.

Soncin S, H. M. Talbot, R. Fernandes, A. Harris, M. von Tersch, H. K. Robson, J. K. Bakker, K. K. Richter, M. Alexander et al. 2021. “High-resolution dietary reconstruction of victims of the 79 CE Vesuvius eruption at Herculaneum by compound-specific isotope analysis.” *Science Advances* 7: eabg5791. https://doi.org/10.1126/sciadv.abg5791.

Soto, D. X., L. I. Wassenaar, and K. A. Hobson. “Stable hydrogen and oxygen isotopes in aquatic food webs are tracers of diet and provenance.” *Functional Ecology* 27(2): 535-543. https://doi.org/10.1111/1365-2435.12054.

Søreide, J. E., H. Hop, M. L. Carroll, S. Falk-Petersen, and E. N. Hegseth. 2006. “Seasonal food web structures and sympagic–pelagic coupling in the European Arctic revealed by stable isotopes and a two-source food web model.” *Progress in Oceanography* 71(1): 59-87. https://doi.org/10.1016/j.pocean.2006.06.001.

Stahl, A. R., T. A. Rynearson, and K. W. Mcmahon. 2023. Amino acid carbon isotope fingerprints are unique among eukaryotic microalgal taxonomic groups:1–15. https://doi.org/10.1002/lno.12350

Stafford. T. W., K. Brendel, D.R. Cuhamel. 1988 “Radiocarbon, ^{13}C and ^{15}N analysis of fossil bone: removal of humates with XAD-2 resin.” *Geochimica et Cosmochimica Acta* 52(9): 2257-2267. https://doi.org/10.1016/0016-7037(88)90128-7.

Stichler, W. 1995. “Interlaboratory comparison of new materials for carbon and oxygen isotope ratio measurements.” in *Reference and intercomparison materials for stable isotopes of light elements*, IAEA-TECDOC-825, 67-74.

Stock, B.C., and B. X. Semmens. 2016. “Unifying error structures in commonly used biotracer mixing models.” *Ecology* 97(10): 2562-2569. https://doi.org/10.1002/ecy.1517.

Stock, B. C., A. L. Jackson, E. J. Ward, A. C. Parnell, D. L. Phillips, and B. X. Semmens. 2018. “Analyzing mixing systems using a new generation of Bayesian tracer mixing models.” *PeerJ* 6(6): e5096. https://doi.org/10.7717/peerj.5096.

Stoecker, D. K., M. D. Johnson, C. de Vargas, and F. Not. 2009. “Acquired phototrophy in aquatic protists.” *Aquatic Microbial Ecology* 57(3): 279-310. https://doi.org/10.3354/ame01340.

Stoecker, D. K., P. J. Hansen, D. A. Caron, and A. Mitra. 2017. “Mixotrophy in the marine plankton.” *Annual Review of Marine Science* 9: 311-335. https://doi.org/10.1146/annurev-marine-010816-060617.

Stoll, B., and B. G. Burrin. 2006. “Measuring splanchnic amino acid metabolism in vivo using stable isotopic tracers”. *Journal of Animal Science* 84(suppl_13): E60-E72. https://doi.org/10.2527/2006.8413_supplE60x.

Strnad, P., V. Usachov, C. Debes, F. Gräter, D. A. Parry, M. B. Omary. 2011. “Unique amino acid signatures that are evolutionarily conserved distinguish simple-type, epidermal and hair keratins.” *Journal of Cell Science* 124(24): 4221-4232. https://doi.org/10.1242/jcs.089516.

Stryer, L., J. Berg, J. Tymoczko, and G. Gatto G. 2019. “Biochemistry.” Macmillan Learning.

Strzepek, K. M., R. E. Thresher, A. T. Revill, C. I. Smith, A. F. Komugabe, and S. F. Fallon. 2014. “Preservation effects on the isotopic and elemental composition of skeletal structures in the deep-sea bamboo coral *Lepidisis* spp. (Isididae).” *Deep-Sea Research Part II: Topical Studies in Oceanography* 99: 199–206. https://doi.org/10.1016/j.dsr2.2013.07.010.

Stubbs, J. L., A. T. Revill, R. D. Pillans, and M. A. Vanderklift. 2022. “Stable isotope composition of multiple tissues and individual amino acids reveals dietary variation among life stages in green turtles (*Chelonia mydas*) at Ningaloo Reef.” *Marine Biology* 169(6): 72. https://doi.org/10.1007/s00227-022-04055-6.

Svanbäck, R., M. Quevedo, J. Olsson, and P. Eklöv. 2015. “Individuals in food webs: the relationships between trophic position, omnivory and among-individual diet variation.” *Oecologia* 178: 103–114. https://doi.org/10.1007/s00442-014-3203-4.

Swalethorp, R., L. Aluwihare, A. R. Thompson, M. D. Ohman, and M. R. Landry. 2020. “Errors associated

with compound-specific $\delta^{15}N$ analysis of amino acids in preserved fish samples purified by high-pressure liquid chromatography." *Limnology and Oceanography: Methods* 18(6): 259–270. https://doi.org/10.1002/lom3.10359.

Swan, G. J. F., S. Bearhop, S. M. Redpath, M. J. Silk, C. E. D. Goodwin, R. Inger, and R. A. McDonald. 2020. "Evaluating Bayesian stable isotope mixing models of wild animal diet and the effects of trophic discrimination factors and informative priors." *Methods in Ecology and Evolution* 11: 139–149. https://doi.org/10.1111/2041-210X.13311.

Takano, Y., Y. Chikaraishi, H. Imachi, Y. Miyairi, N. O. Ogawa, M. Kaneko, Y. Yokoyama, M. Krüger, and N. Ohkouchi. 2018. "Insight into anaerobic methanotrophy from $^{13}C/^{12}C$- amino acids and $^{14}C/^{12}C$-ANME cells in seafloor microbial ecology." *Scientific Reports* 8: 14070. https://doi.org/10.1038/s41598-018-31004-5.

Takano, Y., Y. Kashiyama, N. O. Ogawa, Y. Chikaraishi, and N. Ohkouchi. 2010. "Isolation and desalting with cation-exchange chromatography for compound-specific nitrogen isotope analysis of amino acids: application to biogeochemical samples." *Rapid Communications in Mass Spectrometry* 24(16): 2317–2323. https://doi.org/10.1002/rcm.4651.

Takizawa, Y., P. S. Dharampal, S. A. Steffan, Y. Takano, N. Ohkouchi, and Y. Chikaraishi. 2017. Intra-trophic isotopic discrimination of $^{15}N/^{14}N$ for amino acids in autotrophs: Implications for nitrogen dynamics in ecological studies. *Ecology and Evolution* 7(9): 2916–2924. https://doi.org/10.1002/ece3.2866.

Takizawa, Y., Y. Takano, B. Choi, P. S. Dharampal, S. A. Steffan, N. O. Ogawa, N. Ohkouchi, and Y. Chikaraishi. 2020. "A new insight into isotopic fractionation associated with decarboxylation in organisms: implications for amino acid isotope approaches in biogeoscience." *Progress in Earth and Planetary Science* 7: 50. https://doi.org/10.1186/s40645-020-00364-w.

Tamelander, T., C. Kivimäe, R. G. J. Bellerby, P. E. Renaud, and S. Kristiansen. 2009. "Base-line variations in stable isotope values in an Arctic marine ecosystem: effects of carbon and nitrogen uptake by phytoplankton." *Hydrobiologia* 630: 63–73. https://doi.org/10.1007/s10750-009-9780-2.

Tejada, J. V., J. J. Flynn, P-O. Antoine, V. Pacheco, R. Salas-Gismondi, T. E. Cerling. 2020. "Comparative isotope ecology of western Amazonian rainforest mammals." *Proceedings of the National Academy of Sciences* 117(42): 26263-26272. https://doi.org/10.1073/pnas.2007440117.

Tejada, J. V., J. J. Flynn, R. MacPhee, T. C. O'Connell, T. E. Cerling, L. Bermudez, C. Capuñay, N. Wallsgrove, and B. N. Popp. 2021. "Isotope data from amino acids indicate Darwin's ground sloth was not an herbivore." *Scientific Reports* 11: 1844. https://doi.org/10.1038/s41598-021-97996-9.

Thomas, S. M., and T. W. Crowther. 2015. "Predicting rates of isotopic turnover across the animal kingdom: A synthesis of existing data." *Journal of Animal Ecology* 84(3): 861–870. https://doi.org/10.1111/1365-2656.12326.

Tieszen, L. L. 1983. "Fractionation and turnover of stable isotopes in animal tissues." *Oecologia* 57(1-2): 32–37. https://doi.org/10.1007/BF00379558.

Tomé, C. P., E. A. Elliott Smith, S. K. Lyons, S. D. Newsome, and F. A. Smith. 2020. "Changes in the diet and body size of a small herbivorous mammal (hispid cotton rat, *Sigmodon hispidus*) following the late Pleistocene megafauna extinction." *Ecography* 43(4): 604–619. https://doi.org/10.1111/ecog.04596.

Tremblay, P., R. Grover, J. F. Maguer, L. Legendre, and C. Ferrier-Pagès. 2012. "Autotrophic carbon budget in coral tissue: a new ^{13}C-based model of photosynthate translocation." *Journal of Experimental Biology* 215(8): 1384-1393. https://doi.org/10.1242/jeb.065201.

Tuchman, N. C., M. A. Schollett, S. T. Rier, and P. Geddes. 2006. "Differential heterotrophic utilization of organic compounds by diatoms and bacteria under light and dark conditions." *Hydrobiologia* 561: 167-177. https://doi.org/10.1007/s10750-005-1612-4.

Tuross, N., M. L. Fogel, and P. E. Hare. 1988. "Variability in the preservation of the isotopic composition of collagen from fossil bone." *Geochimica et Cosmochimica Acta* 52(4): 929–935.

https://doi.org/10.1016/0016-7037(88)90364-X.

Ungar, P. S., F. E. Grine, and M. F. Teaford. 2006. “Diet in Early Homo: A Review of the Evidence and a New Model of Adaptive Versatility.” *Annual Review of Anthropology* 35: 209-228. https://doi.org/10.1146/annurev.anthro.35.081705.123153.

Vane, K., M. R. D. Cobain, C. N. Trueman, T. R. Vonnahme, S. Rokitta, N. V. C. Polunin, and H. Flores. 2023. “Tracing basal resource use across sea-ice, pelagic, and benthic habitats in the early Arctic spring food web with essential amino acid carbon isotopes.” *Limnology and Oceanography* 68(4): 862-877. https://doi.org/10.1002/lno.12315.

Vane, K., T. Larsen, B. M. Scholz-Böttcher, B. Kopke, and W. Ekau. 2018. “Ontogenetic resource utilization and migration reconstruction with $\delta^{13}C$ values of essential amino acids in the *Cynoscion acoupa* otolith.” *Ecology and Evolution* 8(19): 9859-9869. https://doi.org/10.1002/ece3.4471.

Van Goudoever, J., B. Stoll, J. Henry, D. Burrin, P. Reeds. 2000. “Adaptive regulation of intestinal lysine metabolism.” *Proceedings of the National Academy of Sciences* 97(2): 11620-11625. https://doi.org/10.1073/pnas.200371497

Velasco, A. M., J. I. Leguina, and A. Lazcano. 2002. “Molecular evolution of the lysine biosynthetic pathways.” *Journal of Molecular Evolution* 55(4): 445–459. https://doi.org/10.1007/s00239-002-2340-2.

Verity, P. G., V. Smetacek, and T. J. Smayda. 2002. “Status, trends and the future of the marine pelagic ecosystem.” *Environmental Conservation* 29(2): 207–237. https://doi.org/10.1017/S0376892902000139.

Vining, B. R., A. Hillman, and D. A. Contreras. 2022. “El Niño Southern Oscillation and enhanced arid land vegetation productivity in NW South America.” *Journal of Arid Environments* 198: 104695. https://doi.org/10.1016/j.jaridenv.2021.104695.

Vokhshoori, N. L., B. J. Tipple, L. Teague, A. Bailess, and M. D. McCarthy. 2022. “Calibrating bulk and amino acid $\delta^{13}C$ and $\delta^{15}N$ isotope ratios between bivalve soft tissue and shell for paleoecological reconstructions.” *Palaeogeography, Palaeoclimatology, Palaeoecology* 595: 110979. https://doi.org/10.1016/j.palaeo.2022.110979.

Waibel, A., H. Peter, and R. Sommaruga. 2019. Importance of mixotrophic flagellates during the ice-free season in lakes located along an elevational gradient.” *Aquatic sciences* 81: 45. https://doi.org/10.1007/s00027-019-0643-2.

Wall, C. B., N. J. Wallsgrove, R. D. Gates, and B. N. Popp. 2021. “Amino acid $\delta^{13}C$ and $\delta^{15}N$ analyses reveal distinct species-specific patterns of trophic plasticity in a marine symbiosis.” *Limnology and Oceanography* 66(5): 2033–2050. https://doi.org/10.1002/lno.11742.

Walsh, R. G., S. He, and C. T. Yarnes. 2014. “Compound-specific $\delta^{13}C$ and $\delta^{15}N$ analysis of amino acids: A rapid, chloroformate-based method for ecological studies.” *Rapid Communications in Mass Spectrometry* 28: 96–108. https://doi.org/10.1002/rcm.6761.

Wang, Y. V, A. H. L. Wan, Å. Krogdahl, M. Johnson, and T. Larsen. 2019a. “^{13}C values of glycolytic amino acids as indicators of carbohydrate utilization in carnivorous fish.” *PeerJ* 7: e7701. https://doi.org/10.7717/peerj.7701.

Wang, J., N. Lu, and B. Fu. 2019b. “Inter-comparison of stable isotope mixing models for determining plant water source partitioning.” *Science of the Total Environment* 666: 685-693. https://doi.org/10.1016/j.scitotenv.2019.02.262.

Ward, B. A. 2019. “Mixotroph ecology: More than the sum of its parts.” *Proceedings of the National Academy of Sciences* 116(13): 5846-5848. https://doi.org/10.1073/pnas.190210611.

Watabe, N., K. Tanaka, J. Yamada, and J. M. Dean. 1982. “Scanning electron microscope observations of the organic matrix in the otolith of the teleost fish *Fundulus heteroclitus* (Linnaeus) and *Tilapia nilotica* (Linnaeus).” *Journal of Experimental Marine Biology and Ecology* 58: 127–134. 10.1016/0022-0981(82)90100-9.

Webb, E. C., N. V Honch, P. J. H. Dunn, A. Linderholm, G. Eriksson, K. Lidén, and R. P. Evershed. 2018. "Compound-specific amino acid isotopic proxies for distinguishing between terrestrial and aquatic resource consumption." *Archaeological and Anthropological Science* 10: 1–18. 10.1007/s12520-015-0309-5.

Webb, E. C., J. Lewis, A. Shain, E. Kastrisianaki-Guyton, N. V. Honch, A. Stewart, B. Miller, J. Tarlton, and R. P. Evershed. 2017. "The influence of varying proportions of terrestrial and marine dietary protein on the stable carbon-isotope compositions of pig tissues from a controlled feeding experiment." *STAR: Science & Technology of Archaeological Research* 3: 36–52. https://doi.org/10.1080/20548923.2016.1275477.

Weber D., H. Kexel, H. L. Schmidt. 1997. "^{13}C-Pattern of Natural Glycerol: Origin and Practical Importance." *Journal of Agricultural and Food Chemistry* 45(6): 2042-2046. https://doi.org/10.1021/jf970005o.

Weltje, G. J. 1997. "End-member modeling of compositional data: Numerical-statistical algorithms for solving the explicit mixing problem." *Mathematical Geology* 29(4): 503-549. https://doi.org/10.1007/BF02775085.

Whiteman, J. P., S. L. Kim, K. W. Mcmahon, P. L. Koch, and S. D. Newsome. 2018. "Amino acid isotope discrimination factors for a carnivore: physiological insights from leopard sharks and their diet." *Oecologia* 188(4): 977–989. https://doi.org/10.1007/s00442-018-4276-2.

Williams, B. 2020. "Proteinaceous corals as proxy archives of paleo-environmental change." *Earth-Science Reviews* 209: 103326. https://doi.org/10.1016/j.earscirev.2020.103326.

Wu G., F. Bazer, S. Datta, G. Johnson, P. Li, M. Satterfield, T. Spencer. 2008. "Proline metabolism in the conceptus: implications for fetal growth and development." Amino acids 35(4): 691-702. https://doi.org/10.1007/s00726-008-0052-7.

Wu, G. 2009. Amino acids: Metabolism, functions, and nutrition. Amino Acids 37:1–17. https://doi.org/10.1007/s00726-009-0269-0.

Wu, G., F. W. Bazer, Z. Dai, D. Li, J. Wang, and Z. Wu. 2014. Amino acid nutrition in animals: Protein synthesis and beyond. *Annual Review of Animal Biosciences* 2: 387–417. https://doi.org/10.1146/annurev-animal-022513-114113.

Yarnes, C. T., and J. Herszage. 2017. "The relative influence of derivatization and normalization procedures on the compound-specific stable isotope analysis of nitrogen in amino acids." *Rapid Communications in Mass Spectrometry* 31(8): 693–704. https://doi.org/10.1002/rcm.7832.

Yamaguchi Y. T., Y. Chikaraishi, Y. Takano, N. O. Ogawa, H. Imachi, Y. Yokoyama, and N. Ohkouchi. 2017. "Fractionation of nitrogen isotopes during amino acid metabolism in heterotrophic and chemolithoautotrophic microbes across Eukarya, Bacteria, and Archaea: Effects of nitrogen sources and metabolic pathways." *Organic Geochemistry* 111: 101-112. https://doi.org/10.1016/j.orggeochem.2017.04.004.

Yamanaka, T., S. Shimamura, H. Nagashio, S. Yamagami, Y. Onishi, A. Hyodo, M. Mampuku, and C. Mizota. 2015. "A compilation of the stable isotopic compositions of carbon, nitrogen, and sulfur in soft body parts of animals collected from deep-sea hydrothermal vent and methane seep fields: Variations in energy source and importance of subsurface microbial processes in the sediment-hosted systems." in *Subseafloor Biosphere Linked to Hydrothermal Systems: TAIGA Concept*. J. Ishibashi, K. Okino and M. Sunamura. Tokyo, Springer Japan: 105-129.

Yu, Y., R. Yang, D. Matthews, Z. M. Wen, J. Burke, D. Bier, and V. Young. 1985. "Quantitative aspects of glycine and alanine nitrogen metabolism in postabsorptive young men: effects of level of nitrogen and dispensable amino acid intake." *The Journal of Nutrition* 115(3): 399-410. https://doi.org/10.1093/jn/115.3.399.

Yun, H. Y., J. W. Lampe, L. F. Tinker, M. L. Neuhouser, S. A. A. Beresford, K. R. Niles, Y. Mossavar-Rahmani Yasmin, L. G. Snetselaar, L. Van Horn, R. L. Prentice, D. M. O'Brien. 2018. "Serum Nitrogen and

Carbon Stable Isotope Ratios Meet Biomarker Criteria for Fish and Animal Protein Intake in a Controlled Feeding Study of a Women's Health Initiative Cohort." *The Journal of Nutrition* 148: 1931-1937. https://doi.org/10.1093/jn/nxy168.

Yun, H. Y., T. Larsen, B. Choi, E. Won, and K. Shin. 2022. "Amino acid nitrogen and carbon isotope data: Potential and implications for ecological studies." *Ecology and Evolution* 12(6): 1–22. https://doi.org/10.1002/ece3.8929.

Yun, H. Y., L. F. Tinker, M. L. Neuhouser, D. A. Schoeller, Y. Mossavar-Rahmani, L. G. Snetselaar, L. V. van Horn, C. B. Eaton, R. L. Prentice, J. W. Lampe, and D. M. O'Brien. 2020. "The carbon isotope ratios of serum amino acids in combination with participant characteristics can be used to estimate added sugar intake in a controlled feeding study of US postmenopausal women." *Journal of Nutrition* 150(10): 2764–2771. https://doi.org/10.1093/jn/nxaa195.

Vander Zanden, M. J., M. K. Clayton, E. K. Moody, C. T. Solomon, and B. C. Weidel. 2015. Stable Isotope Turnover and Half-Life in Animal Tissues: A Literature Synthesis. *PLoS ONE* 10(1): e0116182. 10.1371/journal.pone.0116182.

Zhao Z-k, Wang J-k, Chen S-x, Zhong Y-m. 1993. Amino acid composition of dinosaur eggshells nearby the K/T boundary in Nanxiong Basin, Guangdong Province, China. *Palaeogeography, Palaeoclimatology, Palaeoecology* 104(1-2): 213-218. https://doi.org/10.1016/0031-0182(93)90132-3.

Zimmer K. D., R. C. Grow, A. R. Tipp, B. R. Herwig, D. F. Staples, J. B. Cotner, and P. C. Jacobson. 2020. "Stable isotope patterns in lake food webs reflect productivity gradients." *Ecosphere* 11(9): e03244. https://doi.org/10.1002/ecs2.3244.

Appendix S1

The power and pitfalls of amino acid carbon stable isotopes for tracing the use and fate of basal resources in food webs

Vane K., Cobain M.R.D., Larsen T.

Three detailed figures of metabolic networks in plant, heterotrophic bacteria, and animal cells

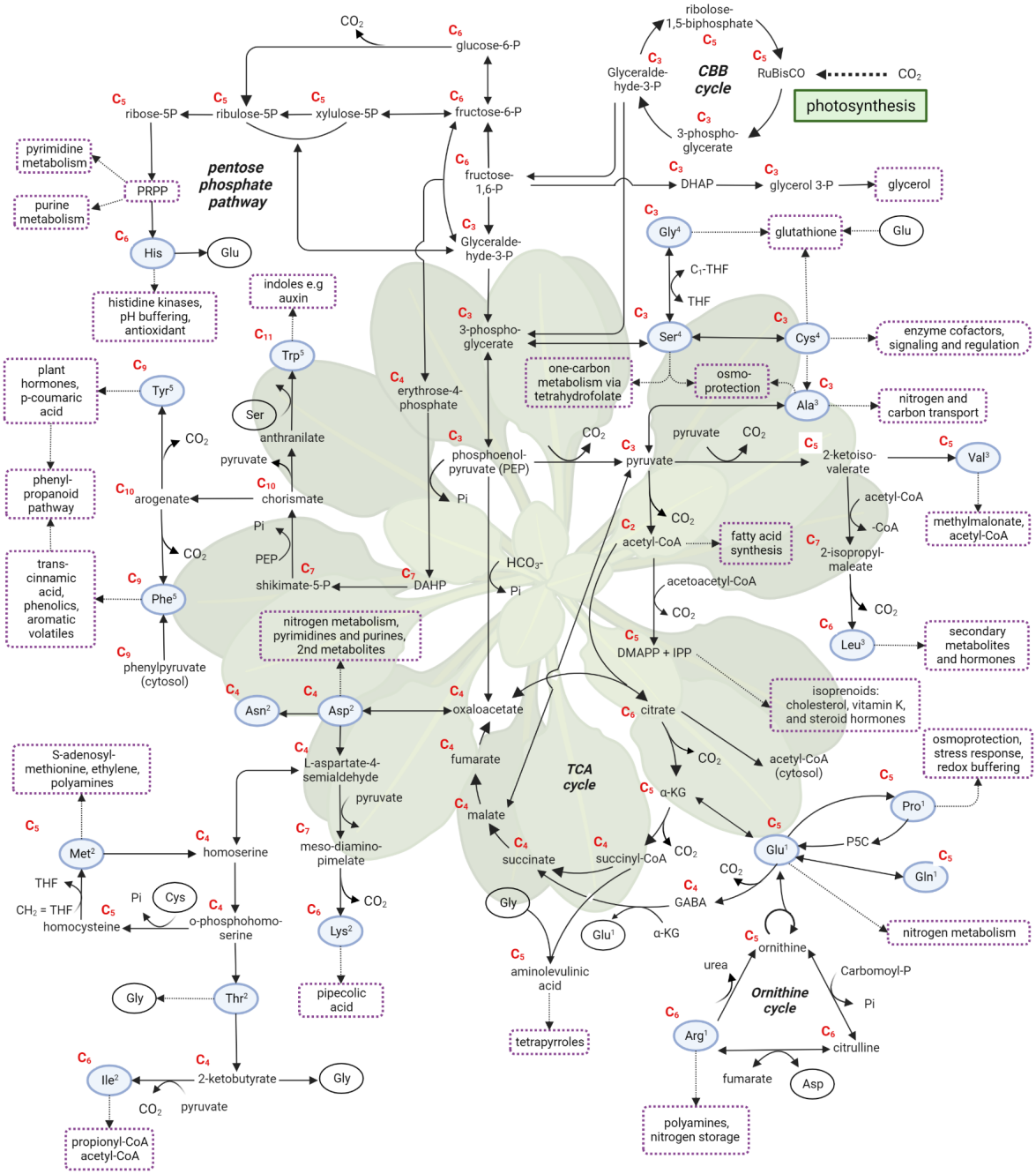

Figure S1A. Amino acid biosynthesis pathways in plants. Simplified schematic overview of the anabolic and catabolic amino acid (AA) pathways in plants, using *Arabidopsis thaliana* as a model species. Based on chemical similarities and precursors, the AAs can be categorized into five groups: 1) the glutamate family, originating from alpha-ketoglutarate (α-KG); 2) the aspartate family, originating from oxaloacetate; 3) the pyruvate group; 4) the 3-phosphoglycerate group; and 5) the aromatic amino acid group, derived from phosphoenolpyruvate and erythrose-4-phosphate. Superscript numbers next to each AA indicate its categorization, and filled ellipses represent products of the primary biosynthesis pathway. In addition to serving as structural components in proteins, AAs fulfill a wide range of biological roles, functioning as metabolites, energy-yielding substrates, and signaling molecules, as indicated by the descriptions within the rounded rectangles. Abbreviations: Ala, alanine; α-KG, alpha-ketoglutarate; Asn, asparagine; Asp, Asparagine; CBB, Calvin-Benson-Bassham; Cys, cysteine; DAHP, 3-deoxy-D-arabinoheptulosonate 7-phosphate; DMPP, dimethylallyl pyrophosphate; GABA, γ-Aminobutyric acid; Gly, glycine; Gln, glutamine; Glu, glutamic acid; His, histidine; Ile, isoleucine; IPP, Isopentenyl pyrophosphate, Leu. leucine, Lys, lysine; Met, methionine; P5C, 1-pyrroline-5-Carboxylate; Phe, phenylalanine; Pro, proline; PRPP, Phosphoribosylpyrophosphate; RuBisCo, ribulose-1,5-bisphosphate carboxylase-oxygenase; Ser, serine; TCA, tricarboxylic acid; Trp, tryptophan; Tyr, tyrosine; Val, valine. The pathways are based on the KEGG PATHWAY database (https://www.kegg.jp/kegg/pathway.html). The illustration was created with BioRender.com.

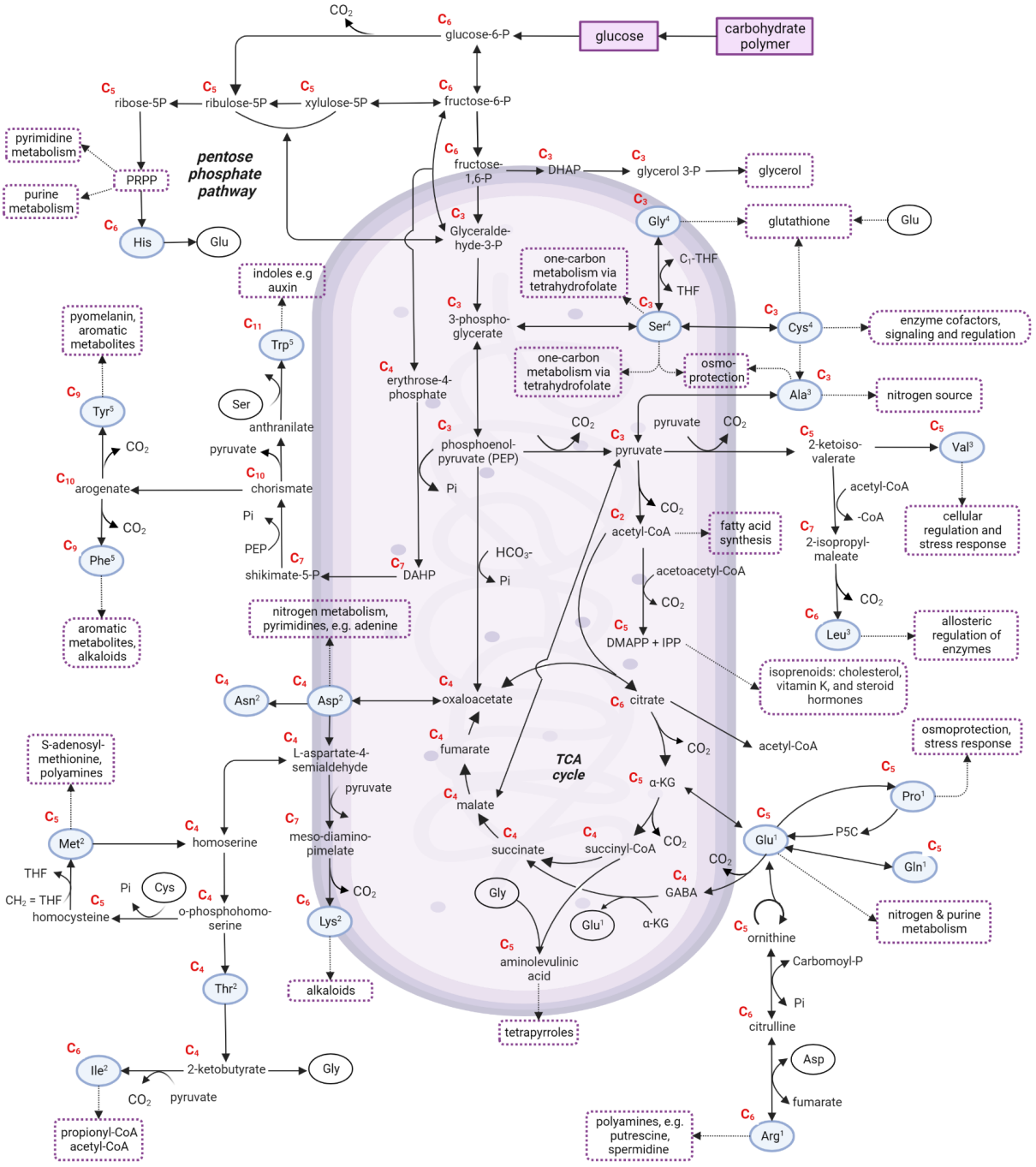

Figure S1B. Amino acid biosynthesis pathways in heterotrophic bacteria. Simplified schematic overview of the anabolic and catabolic amino acid (AA) pathways in heterotrophic bacteria using *Escherichia coli* as a model organism. The superscript number next to each AA indicate its categorization (see Fig. 1 for details) and the filled ellipses indicate that it is a product of the main biosynthesis pathway. The descriptions inside the rounded rectangles exemplify important non-proteinogenic functions of AAs in *E. coli*. Abbreviations: Ala, alanine; α-KG, alpha-ketoglutarate; Asn, asparagine; Asp, Asparagine; CBB, Calvin-Benson-Bassham; Cys, cysteine; DAHP, 3-deoxy-D-arabinoheptulosonate 7-phosphate; DMPP, dimethylallyl pyrophosphate; GABA, γ-Aminobutyric acid; Gly, glycine; Gln, glutamine; Glu, glutamic acid; His, histidine; Ile, isoleucine; IPP, Isopentenyl pyrophosphate, Leu. leucine, Lys, lysine; Met, methionine; P5C, 1-pyrroline-5-Carboxylate; Phe, phenylalanine; Pro, proline; PRPP, Phosphoribosylpyrophosphate; RuBisCo, ribulose-1,5-bisphosphate carboxylase-oxygenase; Ser, serine; TCA, tricarboxylic acid; Trp, tryptophan; Tyr, tyrosine; Val, valine. The pathways are based on the KEGG PATHWAY database (https://www.kegg.jp/kegg/pathway.html). The illustration was created with BioRender.com.

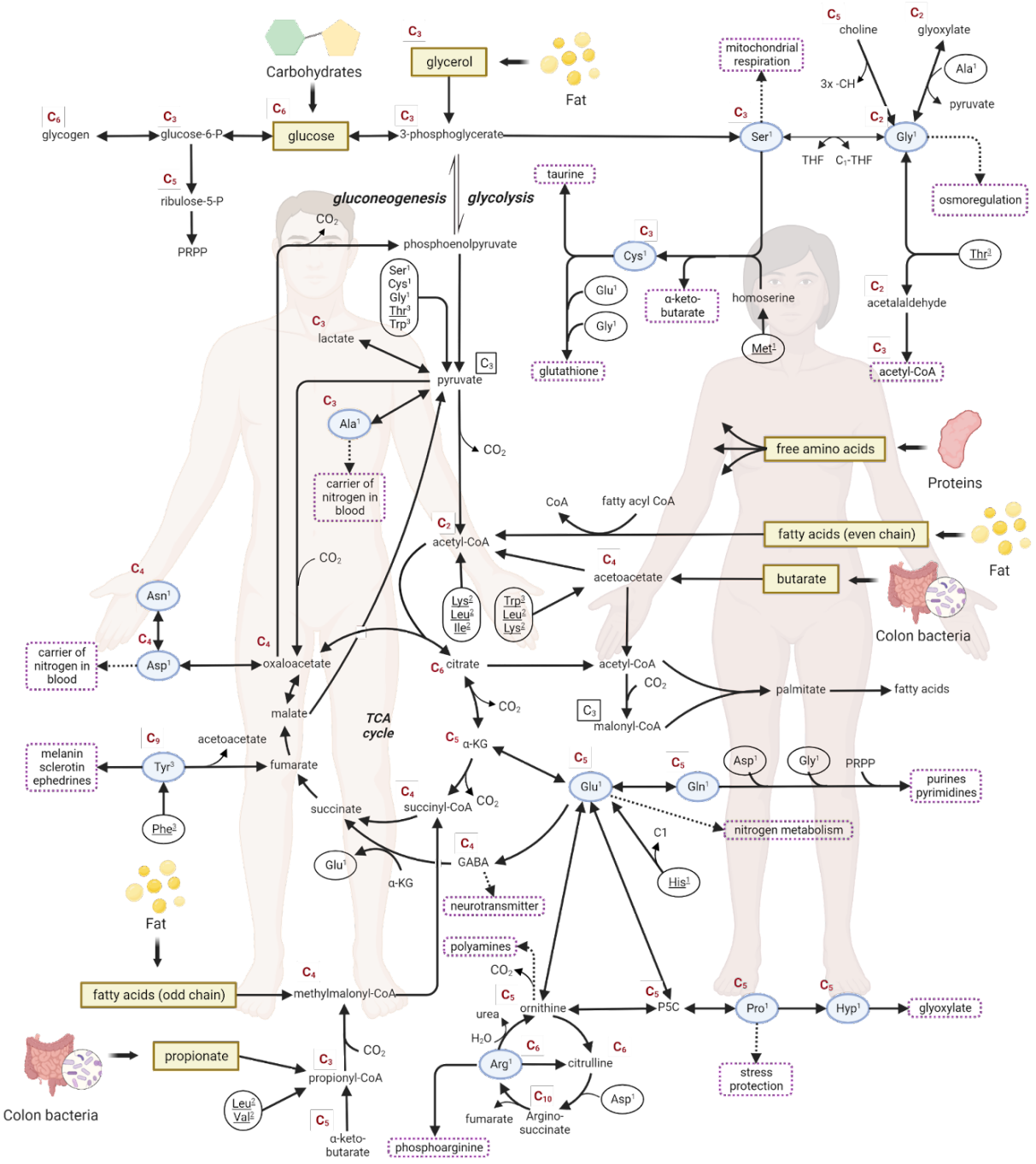

Figure S1C. Anabolic and catabolic amino acid pathways in vertebrates using *Homo sapiens* as a model organism. The non-essential AAs (filled ellipses) can be grouped according to their association with their main biosynthesis pathways: The glycolytic AAs are synthesised from metabolic intermediates (pyruvate, phosphoenolpyruvate) of the glycolytic pathway (in the cytosol) and the tricarboxylic acid (TCA) NEAAs are synthesised from intermediates of the TCA cycle (a-KG, oxaloacetate) (in the mitochondria). Glucose and glycerol are sourced to the glycolytic pathway, and fatty acids (FAs) and short chain fatty acids are sourced to the TCA cycle. The catabolism of excess AAs either occurs via gluconeogenesis or ketogenesis. Gluconeogenesis is the synthesis of glucose from non-carbohydrate precursors such as the glucogenic amino acids (marked with 1) and ketogenesis is the metabolic pathway for producing ketone bodies by breaking down fatty acids and ketogenic amino acids (marked with 2). A large group of AAs can be catabolized by both processes (marked 3). Key roles of the non-essential AAs as precursors in physiological processes other than protein synthesis are indicated within the rounded rectangles. Certain non-proteinogenic amino acids such as citrulline and ornithine are important intermediaries in various pathways involving nitrogenous metabolism.

In terms of the macronutrients, carbohydrates primarily serve as an energy source after being converted to glucose and then to glycolytic intermediates such as 3-phosphoglycerate and pyruvate before entering the TCA cycle. If the supply of carbohydrates exceeds the cell's immediate energy demand, it is stored in the liver as glycogen or, with the help of insulin, converted into fatty acids, circulated to other parts of the body and stored as fat in adipose tissue. Some carbohydrates also become NEAA building blocks. Proteins get converted to AAs in the digestive system before entering the liver. If the AAs are not used to build proteins, they are either catabolised via gluconeogenesis or ketogenesis. Gluconeogenesis is the synthesis of glucose from non-carbohydrate precursors such as the glucogenic amino acids. Ketogenesis is the metabolic pathway for producing ketone bodies by breaking down fatty acids and ketogenic amino acids. A large group of AAs can be catabolized by both processes. Lipids are converted to glycerol, fatty acids and short chain fatty acids. They are able to create energy in a process called beta oxidation that produces acetyl-coA. Some acetyl-coA molecules are used for synthesis of structural and functional lipids, and others are used as an energy source in the TCA cycle. Like the other macronutrients, fatty acids can also be used as NEAA building blocks. The metabolic pathways are summarised based on Frayn and Evans (2016). Other abbreviations: Ala, alanine; Asn, asparagine; Asp, Asparagine; Cys, cysteine; GABA, γ-Aminobutyric acid; Gly, glycine; Gln, glutamine; Glu, glutamic acid; His, histidine; Ile, isoleucine; IPP, Isopentenyl pyrophosphate, Leu. leucine, Lys, lysine; Met, methionine; P5C, 1-pyrroline-5-Carboxylate; Phe, phenylalanine; Pro, proline; PRPP, Phosphoribosylpyrophosphate; Ser, serine; Trp, tryptophan; Tyr, tyrosine; Val, valine. The illustration was created with BioRender.com.

Appendix S2

The power and pitfalls of amino acid carbon stable isotopes for tracing the use and fate of basal resources in food webs

Vane K., Cobain M.R.D., Larsen T.

Literature compilation of basal resource δ^{13}C-EAA data

The overview of individual observations can be found in the Figshare data repository: DOI:10.6084/m9.figshare.22852355

The δ^{13}C-EAA values of basal resources were collected from studies that mentioned having directly measured δ^{13}C-EAA values in basal resources. A Web of Science search was performed until the end of 2022 was based on combined keywords such as 'amino acid', 'carbon isotopes', 'ecology'. Initially, all mentioned δ^{13}C-EAA values in basal resources that were measured directly in the study were compiled, and references therein were additionally screened. We additionally included basal resources from Vane et al. (2023), which was under review at the time. All studies with available δ^{13}C-EAA values either published online or by request were measured with a GC-IRMS. Although the measurements were gained with different derivatization protocols and in different analytical facilities, no corrections were applied to the compiled δ^{13}C-EAA values. This was due to the absence of universally used reference materials with known δ^{13}C values. Some of the variation in δ^{13}C-EAA values between basal resources can thus be attributed to methodological and analytical differences. However, this did not hamper the general observation of discrimination between basal resource groups.

For comparisons between studies, we limited basal resources to those that were measured for five EAAs: leucine, isoleucine, valine, phenylalanine, and threonine. Lysine was not measured in the majority of the studies. Measurements of basal resources that were based on composite samples, such as POM, microbial mats or zooplankton were omitted to ensure that only those basal resources that were directly measured without potential addition of other basal resource traces or detrital materials. This also allowed us to be more precise with the assignment of basal resources to particular groupings, from general groupings of plants, bacteria, and phytoplankton to subgroupings of C_3/C_4/CAM plants, freshwater/marine phytoplankton, diazotrophy in cyanobacteria, brown/red macrophytes, seagrass, and green macrophytes (represented only by *Ulva* sp. plus one measure of *Batophora* sp.). Sample taxonomy was standardised according to the GBIF backbone (the Global Biodiversity Information Facility, GBIF 2022).

The discrimination of the baseline δ^{13}C-EAA values in these basal resources were then visualised by using a linear discrimination analysis (LDA). LDAs were typically limited to only three basal resource groups providing maximal discrimination that can be observed in 2-dimensional plots. In order to estimate the overlap between groups, we calculated the Bayesian posterior distribution of the Bhattacharyya coefficients (BC, Bhattacharyya 1946) of pairwise groups. The BC is a general statistical measure that quantifies the degree of similarity between two multivariate distributions, ranging from 0 (completely dissimilar distributions, i.e. no overlap) to 1 (identical distributions, i.e. complete overlap), regardless of the dimensionality of the data. This makes it highly suitable for δ^{13}C-EAA data, where the dimensionality of the data can vary between studies depending on the number of amino acids that can be measured. This means measures of overlap can be compared either between studies, or contrasted pre- or post-transformations of data (e.g. PCA or LDA dimensionality reduction). In order to estimate the posterior distributions of BC for each pair, and therefore the overlaps, we derived Bayesian posteriors for multivariate normal distributions of basal group δ^{13}C-EAA patterns (post LDA) using an MCMC approach with the "fitMVNdirect" function given in Skinner et al. (2019) with the default settings. This is a generalised, dimension-wise, approach analogous to that implemented in the commonly used SIBER package (Jackson et al. 2011). The BC was then calculated pairwise for each posterior draw using the

"bhattacharyya.matrix" function from the fpc package (Hennig 2023). Analyses were conducted in R statistical software version 4.2.1 (R Core Team 2022).

Table S2.1. Posterior estimates of Bhattacharyya coefficients for group pairs plotted in Fig. 4 of the main manuscript. Q25 and Q75 represent the interquartile range.

ID	pairing	min	q25	median	q75	max
A	Bacteria vs Phytoplankton	0.207	0.345	0.381	0.42	0.594
A	Bacteria vs Plants	0.021	0.061	0.077	0.097	0.208
A	Phytoplankton vs Plants	0.213	0.311	0.338	0.366	0.49
B	Cyanobacteria_D vs Freshwater phytoplankton	0.006	0.194	0.281	0.375	0.917
B	Cyanobacteria_D vs Marine phytoplankton	0	0.02	0.038	0.066	0.407
B	Freshwater phytoplankton vs Marine phytoplankton	0.171	0.322	0.364	0.405	0.555
C	Brown algae vs Green algae	0.32	0.47	0.515	0.56	0.725
C	Brown algae vs Red algae	0.17	0.308	0.349	0.391	0.61
C	Brown algae vs Seagrass	0.018	0.084	0.118	0.169	0.556
C	Green algae vs Red algae	0.446	0.635	0.678	0.723	0.885
C	Green algae vs Seagrass	0.002	0.032	0.058	0.101	0.587
C	Red algae vs Seagrass	0.047	0.184	0.232	0.294	0.674
D	C3 vs C4	0.72	0.885	0.911	0.936	0.989
D	C3 vs CAM	0.144	0.28	0.32	0.366	0.614
D	C4 vs CAM	0.045	0.193	0.248	0.315	0.582

Table S2.2. Posterior estimates of Bhattacharyya coefficients for group pairs plotted in Fig. S2. Q25 and Q75 represent the interquartile range.

Subplot	Pairing	min	q25	median	q75	max
A	Freshwater phytoplankton vs Marine phytoplankton	0.168	0.292	0.332	0.374	0.586
A	Freshwater phytoplankton vs Seagrass	0.042	0.162	0.215	0.288	0.666
A	Marine phytoplankton vs Seagrass	0.02	0.073	0.102	0.143	0.48
B	Bacteria vs Fungi	0.231	0.356	0.396	0.439	0.607
B	Bacteria vs Phytoplankton	0.125	0.23	0.267	0.305	0.48
B	Fungi vs Phytoplankton	0.233	0.349	0.39	0.434	0.643
C	Bacteria vs Macrophytes	0.31	0.449	0.485	0.522	0.682

C	Bacteria vs Plants	0.026	0.068	0.087	0.108	0.244
C	Macrophytes vs Plants	0.255	0.361	0.385	0.411	0.51

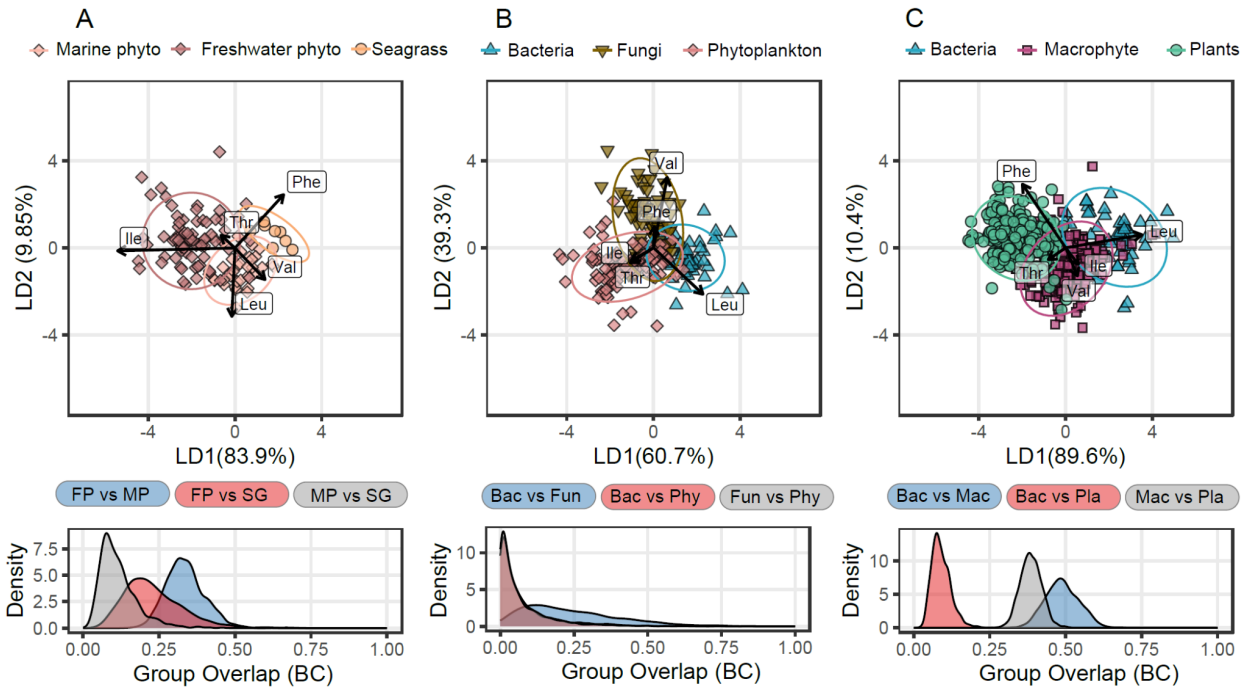

Figure S2: Linear discriminant (LD) analysis of basal resources based on mean-centred δ^{13}C-EAA values compiled from the literature. Upper subplot panel: LD scores for individual samples, with distinct symbols denoting each group. Lower subplot panel: Bhattacharyya coefficients (BC) for group pairs represented as density scores, indicating the degree of overlap in LD scores between groups (0 = no overlap, 1 = identical distributions). EAAs considered: leucine (Leu), isoleucine (Ile), valine (Val), threonine (Thr), and phenylalanine (Phe). Each subplot features the following taxa: A) Bacteria, freshwater phytoplankton, and seagrasses; B) Bacteria, fungi, and phytoplankton; C) Bacteria, macrophytes, and plants (comprising C3, C4, and CAM). For visual clarity, coefficients for each independent variable were multiplied by 8. See sample identities, classifications, and literature sources in Figshare DOI:10.6084/m9.figshare.22852355 and BC values in Table S2.

Compilation References

Arsenault, E. R., J. H. Liew, and J. R. Hopkins. 2022a. "Substrate composition influences amino acid carbon isotope profiles of fungi: Implications for tracing fungal contributions to food webs." *Environmental Microbiology* 24(4): 2089-2097. https://doi.org/10.1111/1462-2920.15961.

Besser, A. C., E. A. Elliott Smith, and S. D. Newsome. 2022. "Assessing the potential of amino acid δ^{13}C and δ^{15}N analysis in terrestrial and freshwater ecosystems." *Journal of Ecology* 110(4): 935-950. https://doi.org/10.1111/1365-2745.13853.

Elliott Smith, E. A., C. Harrod, and S. D. Newsome. 2018. "The importance of kelp to an intertidal ecosystem varies by trophic level: insights from amino acid δ^{13}C analysis." *Ecosphere* 9(11): e02516. https://doi.org/10.1002/ecs2.2516.

Elliott Smith, E. A., C. Harrod, F. Docmac, and S. D. Newsome. 2020. "Intraspecific variation and energy channel coupling within a Chilean kelp forest." *Ecology* 102(1): e03198. https://doi.org/10.1002/ecy.3198.

Elliott Smith, E. A., M. D. Fox, M. L. Fogel, and S. D. Newsome. 2022. “Amino acid $\delta^{13}C$ fingerprints of nearshore marine autotrophs are consistent across broad spatiotemporal scales: An intercontinental isotopic dataset and likely biochemical drivers.” *Functional Ecology* 36(5): 1191-1203. https://doi.org/10.1111/1365-2435.14017.

Fogel, M. L., and N. Tuross. 2002. Extending the limits of paleodietary studies of humans with compound specific carbon isotope analysis of amino acids. *Journal of Archaeological Science* 30(5): 535–545. https://doi.org/10.1016/S0305-4403(02)00199-1.

Jarman, C. L., T. Larsen, T. Hunt, C. Lipo, R. Solsvik, N. Wallsgrove, C. Ka’apu-Lyons, H. G. Close, and B. N. Popp. 2017. “Diet of the prehistoric population of Rapa Nui (Easter Island, Chile) shows environmental adaptation and resilience.” *American Journal of Physical Anthropology* 164(2): 343–361. https://doi.org/10.1002/ajpa.23273.

Manlick, P. J., and S. D. Newsome. 2022. “Stable isotope fingerprinting traces essential amino acid assimilation and multichannel feeding in a vertebrate consumer.” *Methods in Ecology and Evolution* 13(8): 1819–1830. https://doi.org/10.1111/2041-210X.13903.

Larsen, T., D. L. Taylor, M. B. Leigh, and D. M. O’Brien. 2009. “Stable isotope fingerprinting: a novel method for identifying plant, fungal, or bacterial origins of amino acids.” *Ecology* 90(12): 3526–3535. https://doi.org/10.1890/08-1695.1.

Larsen, T., M. Ventura, D. M. O’Brien, J. Magid, B. A. Lomstein, and J. Larsen. 2011. Contrasting effects of nitrogen limitation and amino acid imbalance on carbon and nitrogen turnover in three species of Collembola. *Soil Biology and Biochemistry* 43: 749–759. https://doi.org/10.1016/j.soilbio.2010.12.008.

Larsen, T., M. J. Wooller, M. L. Fogel, and D. M. O’Brien. 2012. “Can amino acid carbon isotope ratios distinguish primary producers in a mangrove ecosystem?” *Rapid Communications in Mass Spectrometry* 26(13): 1541–1548. https://doi.org/10.1002/rcm.6259.

Larsen, T., M. Ventura, N. Andersen, D. M. O’Brien, U. Piatkowski, and M. D. McCarthy. 2013. “Tracing carbon sources through aquatic and terrestrial food webs using amino acid stable isotope fingerprinting.” *PLoS ONE* 8(9): e73441. https://doi.org/10.1371/journal.pone.0073441.

Larsen, T., M. Ventura, K. Maraldo, X. Triadó-Margarit, E. O. Casamayor, Y. V. Wang, N. Andersen, and D. M. O’Brien. 2016. “The dominant detritus-feeding invertebrate in Arctic peat soils derives its essential amino acids from gut symbionts.” *The Journal of animal ecology* 85(5): 1275–1285. https://doi.org/10.1111/1365-2656.12563.

Liew, J. H., K. W. J. Chua, E. R. Arsenault, J. H. Thorp, A. Suvarnaraksha, A. Amirrudin, and D. C. J. Yeo. 2019. “Quantifying terrestrial carbon in freshwater food webs using amino acid isotope analysis: Case study with an endemic cavefish.” *Methods in Ecology and Evolution* 10(9): 1594–1605. https://doi.org/10.1111/2041-210X.13230.

McMahon, K. W., S. R. Thorrold, L. A. Houghton, and M. L. Berumen. 2016. “Tracing carbon flow through coral reef food webs using a compound-specific stable isotope approach.” *Oecologia* 180(3): 809-821. https://doi.org/10.1007/s00442-015-3475-3.

Paolini, M., L. Ziller, K. H. Laursen, and F. Camin. 2015. “Compound-Specific $\delta^{15}N$ and $\delta^{13}C$ Analyses of Amino Acids for Potential Discrimination between Organically and Conventionally Grown Wheat.” *Journal of Agricultural and Food Chemistry* 63: 5841–5850. https://doi.org/10.1021/acs.jafc.5b00662.

Pollierer, M., T. Larsen, A. Potapov, A. Brückner, M. Heethoff, J. Dyckmans, and S. Scheu. 2019. Compound-specific isotope analysis of amino acids as a new tool to uncover trophic chains in soil food webs. *Ecological Monographs* 89(4): e01384. https://doi.org/10.1002/ecm.1384.

Pollierer, M. M., S. Scheu, and A. V. Tiunov. 2020. “Isotope analyses of amino acids in fungi and fungal feeding Diptera larvae allow differentiating ectomycorrhizal and saprotrophic fungi-based food chains.” *Functional Ecology* 34(11): 2375–2388. https://doi.org/10.1111/1365-2435.13654.

Rowe, A. G., K. Iken, A. L. Blanchard, D. M. O'Brien, R. Døving Osvik, M. Uradnikova, and M. J. Wooller. 2019. "Sources of primary production to Arctic bivalves identified using amino acid stable carbon isotope fingerprinting." *Isotopes in Environmental and Health Studies* 55(4): 366–384. https://doi.org/10.1080/10256016.2019.1620742.

Schiff, J. T., F. C. Batista, O. A. Sherwood, T. P. Guilderson, T. M. Hill, A. C. Ravelo, K. W. McMahon, and M. D. McCarthy. 2014. "Compound specific amino acid $\delta^{13}C$ patterns in a deep-sea proteinaceous coral: Implications for reconstructing detailed $\delta^{13}C$ records of exported primary production." *Marine Chemistry* 166: 82–91. https://doi.org/10.1016/j.marchem.2014.09.008.

Scott, J. H., D. M. O'Brien, D. Emerson, H. Sun, G. D. McDonald, A. Salgado, and M. L. Fogel. 2006. "An examination of the carbon isotope effects associated with amino acid biosynthesis." *Astrobiology* 6(6): 867–880. https://doi.org/10.1089/ast.2006.6.867.

Thorp, J. H., and R. E. Bowes. 2017. "Carbon sources in riverine food webs: new evidence from amino acid isotope techniques." *Ecosystems* 20: 1029–1041. https://doi.org/10.1007/s10021-016-0091-y.

Vane, K., T. Larsen, B. M. Scholz-Böttcher, B. Kopke, and W. Ekau. 2018. "Ontogenetic resource utilization and migration reconstruction with $\delta^{13}C$ values of essential amino acids in the *Cynoscion acoupa* otolith." *Ecology and Evolution* 8(19): 9859-9869. https://doi.org/10.1002/ece3.4471.

Vane, K., M. R. D. Cobain, C. N. Trueman, T. R. Vonnahme, S. Rokitta, N. V. C. Polunin, and H. Flores. 2023. "Tracing basal resource use across sea-ice, pelagic, and benthic habitats in the early Arctic spring food web with essential amino acid carbon isotopes." *Limnology and Oceanography* 68(4): 862-877. https://doi.org/10.1002/lno.12315.

Vokhshoori, N. L., T. Larsen, and M. D. McCarthy. 2014. Reconstructing δ13C isoscapes of phytoplankton production in a coastal upwelling system with amino acid isotope values of littoral mussels. *Marine Ecology Progress Series* 504: 59–72. https://doi.org/10.3354/meps10746.

Other Appendix References

Bhattacharyya, A. 1946. "On a measure of divergence between two multinomial populations." *Sankhyā: the indian journal of statistics*, 401-406.

GBIF, 2022. "The Global Biodiversity Information Facility - What is GBIF?." https://www.gbif.org/what-is-gbif.

Hennig C. 2023. "Fpc: Flexible Procedures for Clustering. R package version 2.2-10." https://CRAN.R-project.org/package=fpc

Jackson, A. L., R. Inger, A. C. Parnell, and S Bearhop. 2011. "Comparing isotopic niche widths among and within communities: SIBER–Stable Isotope Bayesian Ellipses in R." *Journal of Animal Ecology*, 80(3), 595-602. https://doi.org/10.1111/j.1365-2656.2011.01806.x

R Core Team. 2022. R: A language and environment for statistical computing. R Foundation for Statistical Computing, Vienna, Austria. https://www.R-project.org/.

Skinner, C., A. C. Mill, S. P. Newman, J. Newton, M. R. D. Cobain and N. V. C. Polunin. 2019. "Novel tri-isotope ellipsoid approach reveals dietary variation in sympatric predators." *Ecology and Evolution,* 9: 13267-13277. https://doi.org/10.1002/ece3.5779

Appendix S3

The power and pitfalls of amino acid carbon stable isotopes for tracing the use and fate of basal resources in food webs

Vane K., Cobain M.R.D., Larsen T.

Phylogeny contributes to variation in δ^{13}C-EAA patterns within vascular plants

As described in Section 2 of the main text, δ^{13}C-EAA patterns are expected to vary with phylogeny due to lineage specific biosynthetic pathways and enzymatic constraints. In addition there are confounding phenotypic expressions observed within taxonomic clades, i.e. clades are on average adapted to live in particular environments, that may also potentially influence δ^{13}C-EAA patterns through phenotypic

expressions that modulate down-stream demands, and therefore isotopic fractionations, of certain EAAs. Although distinctions are apparent across broad taxonomic clades (Section 3), current data are too limited to test widely across basal organisms whether finer scale distinctions are readily quantifiable, although it is suggested in some specific instances (e.g. separation between cultured diatom species, Vane et al. 2023). Here we show however that phylogeny, within the relatively well described phylum of Tracheophyta (vascular plants), partially explains variation in individual δ^{13}C-EAA patterns.

We limited our compilation dataset (in Appendix S2) to only vascular plants. As family was the lowest common taxonomic rank identified across all samples, we defined phylogeny from Tracheophyta down to family for each observation. Initial taxonomic ranks were extracted from GBIF (the Global Biodiversity Information Facility, GBIF 2022). To ensure that residual variation in δ^{13}C-EAA patterns could be adequately estimated, we further restricted the dataset to only those families with at least 3 observations within the dataset, resulting in 18 families in total. Family names were cross referenced against the Open Tree of Life (OTL) and any assigned families that had broken phylogenies (e.g. are paraphyletic) were reassigned to monophyletic subfamily divisions that incorporated all samples from the original family. The phylogenetic subtree of these 18 (sub)families was then extracted from OTL (shown in Fig. S3A, through the R package 'rotl', Michonneau et al. 2016).

To test whether phylogeny explains variation in δ^{13}C-EAA patterns, we constructed a multivariate, phylogenetic mixed effects model in a Bayesian framework, with the five mean-centred EAA δ^{13}C values modelled as a random effect of phylogenetic relatedness based on the topology of the vascular plant family subtree. The model was run in R (version 4.2.1, R Core Team 2022) using the package 'MCMCglmm' (Hadfield, 2010, model specifics are provided in the supplied R code). Trace plots of the chain were checked and showed good model convergence.

The average δ^{13}C-EAA pattern for a vascular plant is shown in Fig. S3. Mean-centred threonine values are relatively enriched in ^{13}C (median 12.1‰) and leucine relatively deplete (median -8.2‰) compared to other EAAs. However, these two EAAs also had the least certainty of their means, shown by the wide credibility intervals (CIs), followed by isoleucine. Average phenylalanine and valine had much higher certainty, with 95% credibility intervals spanning <1‰ (see Fig. S4). Approximately 50% of the total variation in δ^{13}C-EAA patterns was attributed to phylogeny (posterior median = 0.51, 95% CI 0.36 to 0.66). Mean-centred leucine δ^{13}C values varied the most with phylogeny (mean variance of 9.7, 95% CI 3.0 to 18.5), followed by threonine (mean 5.0, 95% CI 0.44 to 11.4) and isoleucine (mean 3.1, 95% CI 0.62 to 6.8), with almost no variation expressed in either phenylalanine (mean 0.15, 95% CI <0.01 to 0.65) or valine (mean 0.31, 95% <0.01 to 1.6), shown in Fig. S3. Qualitatively, it can be observed that some families express similar δ^{13}C-EAA patterns despite being phylogenetically distant from each other. Notably, Fabaceae, the legume plants that typically host nitrogen fixing bacteria in their roots, have relatively deplete threonine values but relatively enriched leucine values. This matches with the distant sister families Posidoniaceae and Hydrocharitaceae, which encompass marine seagrasses and many other aquatic plant species. It can also be seen that the families Agavoideae, Cactaceae and Zygophyllaceae have similar δ^{13}C-EAA patterns marked by relatively deplete leucine but enriched isoleucine and threonine, with representative species typically known for being adapted to dry habitats.

The residual variance - covariance structure is shown in Fig. S4. Threonine expressed the largest individual variation (mean variance 7.35) and negatively co-varied with all other EAAs (all mean correlations < -0.39). These negative correlations intuitively make sense as threonine is relatively the most enriched amino acid (Fig. S3) and the data are mean centred, therefore increasing values in one amino acid will be accompanied by decreases in the other EAAs. Interestingly, valine and phenylalanine, despite showing almost no variation with phylogeny, express considerable individual variances (means of 3.05 and 3.97 respectively). This implies mechanisms at the individual level that result in variation in these EAAs rather than lineage specific mechanisms. Valine and phenylalanine also negatively covary with each other, likely due to the same reasoning as with threonine. Despite having large variations with phylogeny, isoleucine and leucine both have limited individual variances, suggesting that within vascular plants, biosynthetic pathways involving these two amino acids may be less plastic at the individual level.

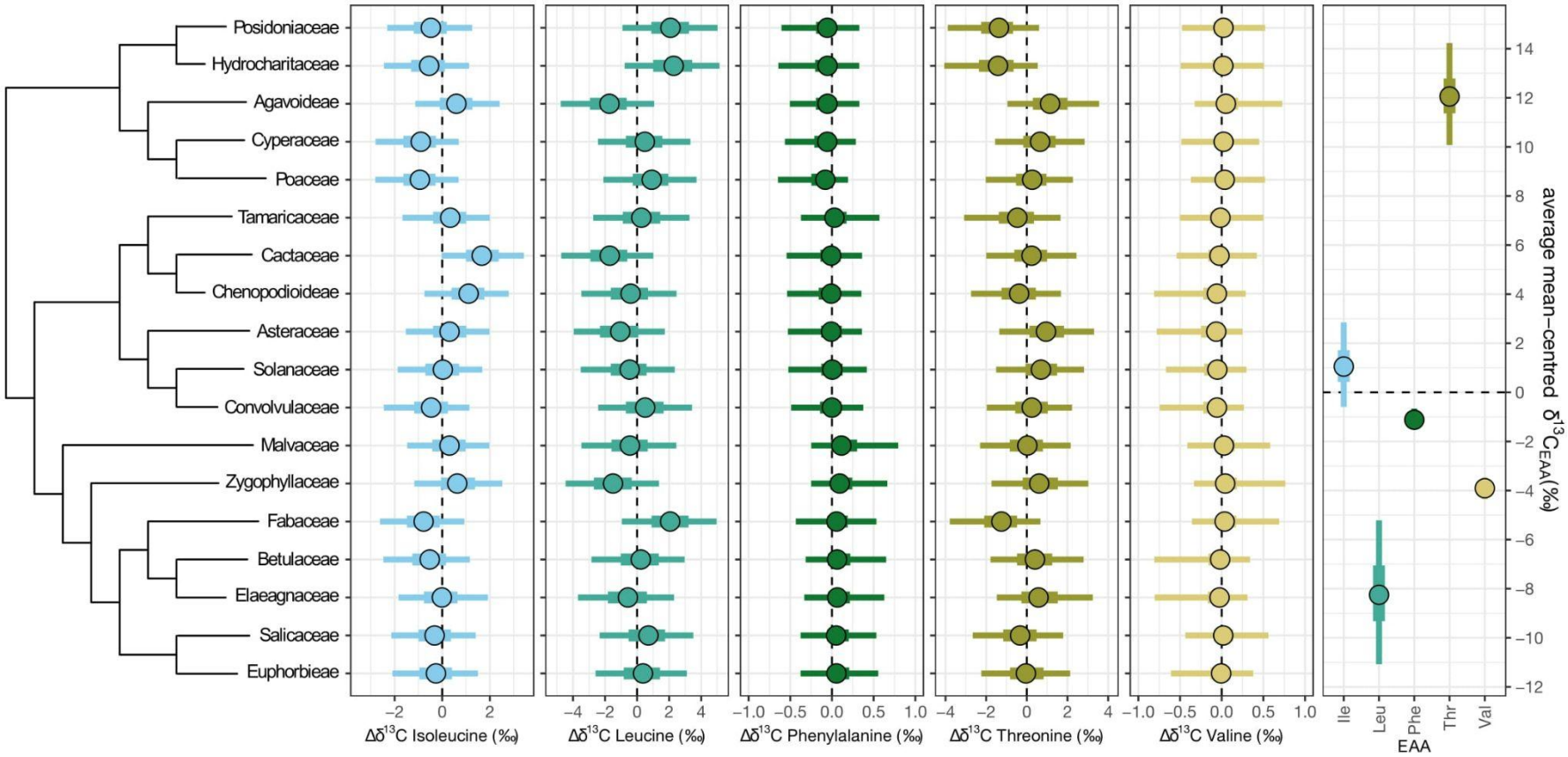

Figure S3A: Modelled mean-centred $\delta^{13}C$ values of five EAAs ($\delta^{13}C$ patterns) of vascular plants. Global average values (right hand panel) and the offsets, $\Delta\delta^{13}C$, for each EAA (first to fifth panels) among the 18 taxonomic (sub)families in the vascular plant dataset. Phylogenetic topology between the 18 families is plotted on the left hand side. Circles indicate median posterior values, thick bars denote the 50% credible intervals (CIs) and thin bars the 95% CIs. Average mean-centred $\delta^{13}C$ CIs for phenylalanine and valine fall within the median circles. Dashed lines are plotted at zero on all panels for clarity.

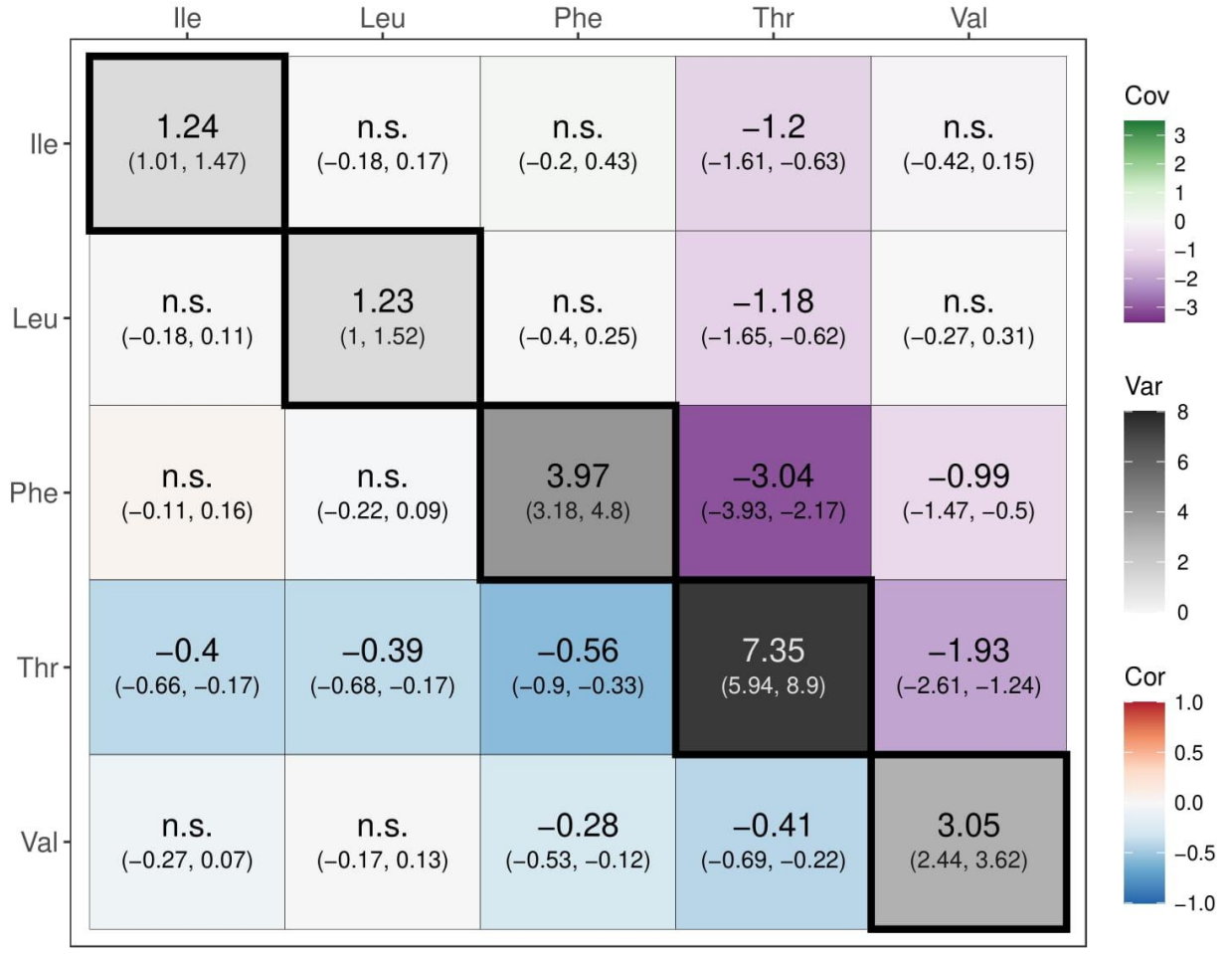

Figure S3B: Residual variance - covariance matrix of modelled vascular plant $\delta^{13}C$ patterns. Variances (Var) of individual EAAs are plotted along the diagonal with thick borders, covariances (Cov) in the upper triangle, and corresponding correlations (Cor) in the lower triangle. Posterior mean values (large text) with 95% credible intervals (smaller text) are given for each EAA pairing. Posterior mean values that are not statistically distinguishable from zero are denoted as n.s.

References

GBIF, 2022. "The Global Biodiversity Information Facility - What is GBIF?." https://www.gbif.org/what-is-gbif.

Hadfield, J. D. 2010. "MCMC Methods for Multi-Response Generalized Linear Mixed Models: The MCMCglmm R Package." *Journal of Statistical Software* 33(2): 1-22.

Michonneau, F., J. W. Brown, and D. J. Winter. 2016. "rotl: an R package to interact with the Open Tree of Life data." *Methods in Ecology and Evolution* 7(12): 1476-1481.

R Core Team. 2022. R: A language and environment for statistical computing. R Foundation for Statistical Computing, Vienna, Austria. https://www.R-project.org/.

Appendix S4

The power and pitfalls of amino acid carbon stable isotopes for tracing the use and fate of basal resources in food webs

Vane K., Cobain M.R.D., Larsen T.

Literature compilation of archaeological human δ^{13}C-AA data

The overview of selected studies can be found in the Figshare data repository: DOI:10.6084/m9.figshare.22852355

We compiled δ^{13}C-AA data from historical and archaeological human populations with diverse subsistence strategies, as reported in eight studies. In two of these studies (Honch et al. 2012 and Colonese et al. 2014), the archaeological and environmental contexts enabled us to select a subset of populations for which we could identify their primary dietary protein sources: freshwater (δ^{13}C-EAA mean: -27.5±1.5‰, n=12), marine (-19.4±1.2‰, n=19), terrestrial C_3 (-27.1±1.0‰, n=12), and terrestrial C4 (-19.1±2.1‰, n=14) proteins. See Table Sx for detailed sample information. The protein sources for the six populations from the remaining six studies were less certain. These populations included individuals from Köpingsvik (bone, Mesolithic and Middle Neolithic; Webb et al. 2018); Nancheng (bone, Proto-Shang; Ma et al. 2021); Nukdo (bone, Late Bronze Age; Choy et al. 2010); Odense rib (bone, Medieval; Brozou et al. 2022); Odense femur (bone, Medieval; Brozou et al. 2022); Pica-8 (hair, Late Intermediate; Mora et al. 2018); Pica-8 (tendon, Late Intermediate; Mora et al. 2018); and Uummannaq (bone, 16th and 17th centuries; Raghavan et al. 2010). Two of the studies reported δ^{13}C-AA values for different tissue types from the same individuals. We compared two types of data preprocessing: measured and EAA mean-centred δ^{13}C-AA data. The former highlights the influence of environmental factors on δ^{13}C-AA variations, while the latter emphasises the effect of metabolic processes on intermolecular δ^{13}C variability. We applied two ordination techniques, PCA and LDA, to assess the relationship between the independent variables (i.e., δ^{13}C-AA values) and the spread of data within and between groups with known primary diet protein sources. We then projected the δ^{13}C-AA values of individuals with unknown protein sources onto the principal component and linear discriminant spaces. To corroborate the correctness of the results, we used mean δ^{13}C-EAA values (phenylalanine and valine), with marine and C_4 protein groups expected to be more ^{13}C enriched than the freshwater and C_3 protein groups. We employed two different methods to assess the similarity of humans to the four protein sources:

1) For both preprocessing datasets, we compared class probability assignments $p\theta(x)$ and likelihood $lx(\theta)$ functions to predict protein sources in the LDA output. While $p\theta(x)$ is best suited for discrete classification to a predefined group because it sums to 1, $lx(\theta)$ is not normalised to 1 and is therefore less prone to false inferences by forcing unlikely classifications.

2) To measure the similarity of the populations to the protein groups across both preprocessing datasets and ordination methods, we calculated Bhattacharyya coefficients, which measure similarity between two multivariate probability distributions (see S2 for statistical details). A coefficient of 0 indicates no overlap between the two distributions, while a coefficient of 1 indicates that they are identical.

PCA captures the direction of maximum variation in the data rather than maximising group separability as is the case for LDA. Therefore, variables contributing to intragroup variation have a greater weight in PCA than LDA. This is particularly apparent when separating the C_3 and freshwater protein groups from the C_4 and marine protein groups based on baseline δ^{13}C-EAA values. In terms of classifying new observations (individuals with unknown protein source), LDA will assign them to the class with the highest likelihood, even if it is small. If the highest likelihood is small, the observation has weak similarities to any of the predefined classes. The Pica 8 hair individuals exemplify this, as the δ^{13}C values of glycine are enriched by ~10‰ compared to glycine in the collagenous Pica 8 samples. This shows that LDA predictions can be misleading when the training data are inadequate or fall outside the boundaries of the training data. Identifying these observations can be achieved through visual inspection of

discriminant scores and likelihood estimates. From visual inspection, it is evident that the Pica-8 hair samples fall outside the predefined C_4 protein group and have much lower likelihoods compared to the tendon samples - see Figs. 6B1 and 6D1 and Table Sx. In contrast to likelihood estimates, which provide values for single observations, Bhattacharyya coefficients (BC) are estimated at the population level, for two compared groups, in this case, a human population versus a protein source. The median BC values of Bayesian posterior estimates reported in Fig. S4 show that PCA ordination generally produces higher median values compared to LDA ordination. This is to be expected as LDA optimises for separation between groups. However, these median BC values have limited value for this case study because populations falling within the 'mixing-space' of the four protein sources but not overlapping with any of them have low BC values. Therefore, it is important to visually inspect the ordination plots when evaluating BC values. Nevertheless, many of the trends reported in likelihood estimates also hold true for the BC values. For instance, both the Odense (both rib and femur) and Nukdo populations exhibit a much greater overlap with C_3 proteins in the PCA than in the LDA techniques, underscoring how sensitive these predictions are to the specific ordination method used.

Out of 64 unknown (predicted) individuals, 18 were categorised differently between the two data set representations (measured vs. mean-centred) due to the slight structural differences. According to the LDA output, most of these individuals likely consumed mixed diets, e.g. Nukdo individuals on C3/marine protein (δ^{13}C-EAA mean: -25.9±1.1‰, n=9), or on brackish resources, e.g. the Köpingsvik (-22.1±0.5‰, n=5) and Uummannaq (-20.4±0.5‰, n=6) individuals. The measured values for the Uummannaq individuals have a marine protein bias, while the mean-centred values have a freshwater protein bias (Fig. 6). For the Odense individuals (femur: -26.3±0.7‰, n=10; rib: -26.2±1.2‰, n=10), the measured values categorised all but one femur sample as C3, while the mean-centred data categorized 11 in C_3, 3 in marine, and 6 in C_4 group. The mean δ^{13}C-EAA values and contextual information support the predictions based on measured values for the Uummannaq individuals and non-C_3 predictions of the Odense individuals. The prediction of individuals from the remaining populations (Nancheng, -15.4±2.2‰, n=12; Pica 8 tendon, -19.3±3.8‰, n=6; Pica 8 hair, -16.4±1.3‰, n=6) are consistent between the two data sets with all but one individual clustering with the C4 protein group. The prediction of the outlier individual (SE-T3) with the C_3 protein group is corroborated by its mean δ^{13}C-EAA value (-26.8‰). A visual inspection shows that predictions based on measured δ^{13}C-EAA values are more accurate, as seen in Figs. $6B_1$ and $6D_1$. For example, the individual (M70) with a mean δ^{13}C-EAA value of -22.1‰ is a clear outlier in Fig. $6B_1$, trending towards the C_3 group, while a similar trend is less obvious in Fig. $6D_1$.

The data compilation comprises two populations, Pica-8 and Odense, from which it is possible to infer dietary histories from the same individuals thanks to analyses of different tissue types. The earlier dietary history of the Pica-8 individuals represented by the tendon samples indicates that the individuals relied on different subsistence strategies: Terrestrial C_4 (n=4), marine C_4 (SI-T74; n=1), and possibly a mixture of terrestrial C_3 and C_4 (SE-T3; n=1). The comparatively higher mean δ^{13}C-EAA values of the hair than tendon samples, typically between 1 and 2‰, support that the population became more reliant on C_4 protein sources. This is particularly true for the SE-T3 whose hair samples were ^{13}C enriched by 8.6‰ compared to the tendon samples, which had a mean δ^{13}C-EAA value typical of the terrestrial protein

group. We are also questioning whether the classification of the SI-T74 and SE-T3 tendon samples to the C_4 group is correct in part because of their mean δ^{13}C-EAA values are depleted by ~3‰ compared to the the remaining Pica-8 individuals and most of the C_4 Nancheng individuals. Thus, it appears that the ordination and mean δ^{13}C-EAA results do not fully corroborate one another. In terms of inferring dietary histories based on collagen only, the ribs of the Odense individuals most likely represent the period after they were admitted to a leprosy hospital and the femurs represent earlier periods. As noted by the authors of the study, it appears that several individuals increased marine protein consumption after hospitalisation (Brozou et al. 2022). For individuals relying on proteins from brackish waters, the predictions of the Uummannaq (Raghavan et al. 2010) and Köpingsvik (Webb et al. 2018) populations are in line with modern salinity observations showing brackish waters in both locations, but with the protein sources of the Uummannaq individuals being more marine-based compared to the Köpingsvik individuals (Holinde and Zielinski 2016, Kniebusch et al. 2019). Most Nukdo individuals relied more on marine than C_3 proteins (Choy et al. 2010).

Regardless of the preprocessing and ordination methods, both datasets have many similar features in terms of the weight and direction of independent variables (Fig. 6B2 vs. Fig. 6D2): Alanine, aspartate, and glutamate generally contribute to maximising intragroup variation (Fig. 6C2), and phenylalanine, valine, proline, and glycine contribute to maximising intergroup variation (Fig. 6B2 and 6D2). Our study confirmed that δ^{13}C of phenylalanine vs. valine separate terrestrial and aquatic resources (Honch et al. 2012, Larsen et al. 2013). Like previous studies, we found that phenylalanine relative to valine is more ^{13}C enriched in terrestrial than in aquatic protein groups. Among the NEAAs, proline is important for separating the C_3 from the other protein groups. Our analysis could not determine the cause of the ^{13}C enrichment in the C_3 protein group compared to other groups. However, according to Liu et al. (2018), copepods on a high-carbohydrate diet exhibited a higher trophic ^{13}C enrichment of proline than anchovies on a high-protein diet. The ^{13}C enrichment of glycine is highest in the freshwater protein group and lowest in the C_4 protein group (Fig. 6B2). The cause of these isotopic effects remains unclear, as they could result from either metabolic processes in the food sources or post-ingestive processes. Factors contributing to these effects may include the conversion of excess dietary protein into fat and energy, as well as the de novo synthesis of glycine. Although alanine and glutamate are relatively uninformative amino acids, the terrestrial protein groups were significantly more ^{13}C enriched than the aquatic protein groups ($P < 0.001$). This difference may arise from higher carbohydrate consumption in terrestrial protein groups compared to aquatic protein groups. Epidemiological studies investigating the δ^{13}C-AA response to high-fructose corn syrup-sweetened beverage intake have identified alanine and glutamate as potential markers of carbohydrate intake (Choy et al. 2013, Yun et al. 2018, 2020, Johnson et al. 2021). Both NEAAs use pyruvate, a glycolytic intermediate, as a precursor, and acetyl-CoA, a product of beta-oxidation, acts as a precursor for glutamate but not glycine (Fig. S1C). The distinct response of alanine and glutamate to carbohydrate intake is likely influenced by the balance of dietary fat to carbohydrate.

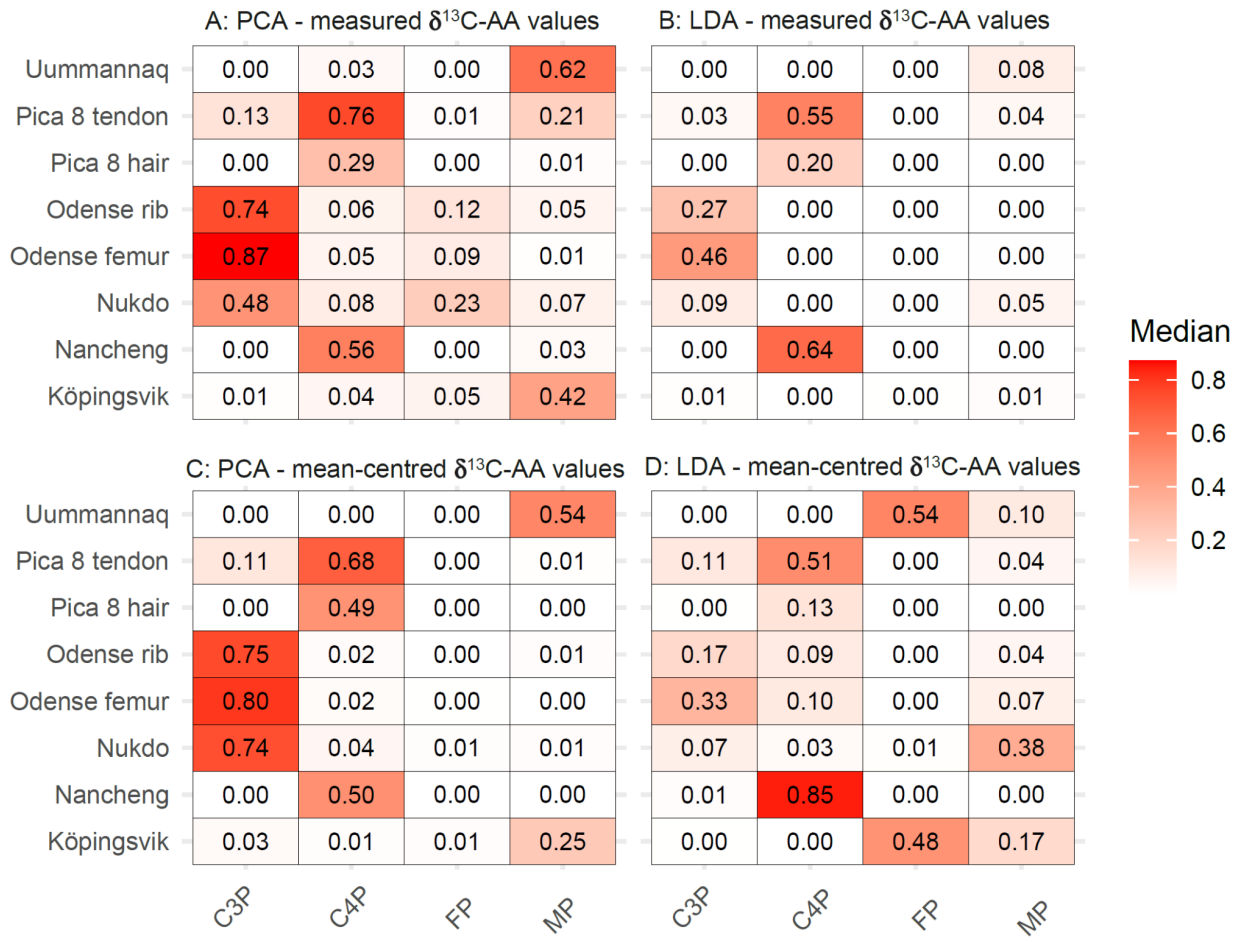

Figure S4: Comparison of human populations of known diets with those with uncertain diets. The matrix plots show the median Bhattacharyya coefficients (0 = no overlap, 1 = identical distributions) indicating the degree of overlap in PC (left hand side) or LD (right hand side) scores between human groups (see Fig. 6) and their potential dietary protein sources (FP, freshwater protein; MP, marine protein, C3P, terrestrial C_3 protein; C4P, terrestrial C_4 protein). Top panels are based on measured δ^{13}C-AA data whereas bottom panels are EAA (phenylalanine and valine) mean-centred δ^{13}C-AA values .

Compilation References

Brozou, A., B. T. Fuller, V. Grimes, G. Van Biesen, Y. Ma, J. L. Boldsen, and M. A. Mannino. 2022. "Aquatic resource consumption at the Odense leprosarium: Advancing the limits of palaeodiet reconstruction with amino acid δ^{13}C measurements." *Journal of Archaeological Science* 141: 105578. https://doi.org/10.1016/j.jas.2022.105578.

Choy, K., C. I. Smith, B. T. Fuller, and M. P. Richards. 2010. "Investigation of amino acid δ^{13}C signatures in bone collagen to reconstruct human palaeodiets using liquid chromatography-isotope ratio mass spectrometry." *Geochimica et Cosmochimica Acta* 74: 6093-6111. https://doi.org/10.1016/j.gca.2010.07.025.

Colonese, A. C., M. Collins, A. Lucquin, M. Eustace, Y. Hancock, R. de Almeida Rocha Ponzoni, A. Mora, C. Smith et al. 2014. Long-term resilience of late Holocene coastal subsistence system in southeastern

South America. Plos ONE 9(4): e93854. https://doi.org/10.1371/journal.pone.0093854.

Honch, N. V., J. S. O. McCullagh, and R. E. M. Hedges. 2012. "Variation of bone collagen amino acid δ13C values in archaeological humans and fauna with different dietary regimes: Developing frameworks of dietary discrimination." American Journal of Physical Anthropology 148(4): 495–511. https://doi.org/10.1002/ajpa.22065.

Ma, Y., V. Grimes, G. Van Biesen, L. Shi, K. Chen, M. A. Mannino, and B. T. Fuller. 2021. "Aminoisoscapes and palaeodiet reconstruction: New perspectives on millet-based diets in China using amino acid $\delta^{13}C$ values." *Journal of Archaeological Science* 125: 105289. https://doi.org/10.1016/j.jas.2020.105289.

Mora, A., A. Pacheco, C. Roberts, and C. Smith. 2018. "Pica 8: Refining dietary reconstruction through amino acid $\delta^{13}C$ analysis of tendon collagen and hair keratin." *Journal of Archaeological Science* 93: 94–109. https://doi.org/10.1016/j.quaint.2016.10.018.

Raghavan, M., J. S. O. McCullagh, N. Lynnerup, and R. E. M. Hedges. 2010. "Amino acid $\delta^{13}C$ analysis of hair proteins and bone collagen using liquid chromatography/isotope ratio mass spectrometry: paleodietary implications from intra-individual comparisons." *Rapid Communications in Mass Spectrometry* 24(5): 541–548. https://doi.org/10.1002/rcm.4398.

Webb, E. C., N. V Honch, P. J. H. Dunn, A. Linderholm, G. Eriksson, K. Lidén, and R. P. Evershed. 2018. "Compound-specific amino acid isotopic proxies for distinguishing between terrestrial and aquatic resource consumption." *Archaeological and Anthropological Science* 10: 1–18. https://doi.org/10.1007/s12520-015-0309-5.

Other Appendix References

Choy, K., S. H. Nash, A. R. Kristal, S. Hopkins, B. B. Boyer, and D. M. O'Brien. 2013. "The carbon isotope ratio of alanine in red blood cells is a new candidate biomarker of sugar-sweetened beverage intake." *Journal of Nutrition* 143: 878–884. https://doi.org/10.3945/jn.112.172999.

Johnson, J. J., P. A. Shaw, E. J. Oh, M. J. Wooller, S. Merriman, H. Y. Yun, T. Larsen, J. Krakoff, S. B. Votruba, and D. M. O'Brien. 2021. "The carbon isotope ratios of nonessential amino acids identify sugar-sweetened beverage (SSB) consumers in a 12-wk inpatient feeding study of 32 men with varying SSB and meat exposures." *The American journal of clinical nutrition* 113(5): 1256–1264. https://doi.org/10.1093/ajcn/nqaa374.

Holinde, L., and O. Zielinski. 2016. "Bio-optical characterization and light availability parameterization in Uummannaq Fjord and Vaigat–Disko Bay (West Greenland)." *Ocean Science*, 12(1): 117-128. https://doi.org/10.5194/os-12-117-2016

Kniebusch, M., H. M. Meier, and H. Radtke. 2019. "Changing salinity gradients in the Baltic Sea as a consequence of altered freshwater budgets." *Geophysical Research Letters*, 46(16): 9739-9747. https://doi.org/10.1029/2019GL083902

Larsen, T., M. Ventura, N. Andersen, D. M. O'Brien, U. Piatkowski, and M. D. McCarthy. 2013. "Tracing carbon sources through aquatic and terrestrial food webs using amino acid stable isotope fingerprinting." PLoS ONE 8(9): e73441. https://doi.org/10.1371/journal.pone.0073441.

Liu, H. Z., L. Luo, and D. L. Cai. 2018. "Stable carbon isotopic analysis of amino acids in a simplified food chain consisting of the green alga Chlorella spp., the calanoid copepod Calanus sinicus, and the japanese anchovy (Engraulis japonicus)." Canadian Journal of Zoology 96: 23–30. https://doi.org/10.1139/cjz-2016-0170.

Yun, H. Y., J. W. Lampe, L. F. Tinker, M. L. Neuhouser, S. A. A. Beresford, K. R. Niles, Y. Mossavar-Rahmani Yasmin, L. G. Snetselaar, L. Van Horn, R. L. Prentice, D. M. O'Brien. 2018. "Serum Nitrogen and Carbon Stable Isotope Ratios Meet Biomarker Criteria for Fish and Animal Protein Intake in a Controlled Feeding Study of a Women's Health Initiative Cohort." *The Journal of Nutrition* 148:

1931-1937. https://doi.org/10.1093/jn/nxy168.

Yun, H. Y., L. F. Tinker, M. L. Neuhouser, D. A. Schoeller, Y. Mossavar-Rahmani, L. G. Snetselaar, L. V. van Horn, C. B. Eaton, R. L. Prentice, J. W. Lampe, and D. M. O'Brien. 2020. "The carbon isotope ratios of serum amino acids in combination with participant characteristics can be used to estimate added sugar intake in a controlled feeding study of US postmenopausal women." *Journal of Nutrition* 150(10): 2764–2771. https://doi.org/10.1093/jn/nxaa195.

Appendix S5

The power and pitfalls of amino acid carbon stable isotopes for tracing the use and fate of basal resources in food webs

Vane K., Cobain M.R.D., Larsen T.

The compilation of dietary offsets between $\delta^{13}C_{EAA}$ values in diet and metazoan tissues

The methodology overview of each study can be found in the Figshare data repository: DOI:10.6084/m9.figshare.22852355

To investigate the differences in offsets between δ^{13}C-EAA values between diet and metazoan tissues, δ^{13}C-EAA values from controlled feeding studies that aimed to study the routing of AAs from different dietary compositions to animal tissues with δ^{13}C-AA values were compiled. We searched Web of Science for articles published from the beginning of online records until May 2022 using the terms “amino acid”, “carbon isotopes”, “fractionation”. While not all feeding experiments aiming to qualify the routing of AAs with carbon isotopes could be found with these search terms, references within publications mentioning trophic discrimination of EAAs were additionally screened.

As a result, 17 publications were found that described the measured δ^{13}C-EAA values between animal tissue and their specific diet. Analytical and methodological information was extracted from each publication and compiled. Extracted analytical information included instrumentation (e.g. GC-IRMS or LC-IRMS) derivatisation method in case of GC-IRMS measurements, description of the chemical pretreatments of both consumer and diet tissues. Methodology descriptions encompassed consumer species, type of tissue, dietary type or variations, amount of days that the diet was fed to the consumer, and how many individual replicate consumer tissues were measured. δ^{13}C-EAA values were mainly acquired from tables in the publication, online supplementary materials and data repositories, or direct requests to the corresponding author. However, offsets in δ^{13}C-EAA values were gained from a graph in Howland et al. (2003) as the request for raw data was unanswered. No corrections to the δ^{13}C-EAA values between the studies were necessary due to the interest in the offsets in δ^{13}C-EAA values between diet and tissue that were measured in the same analytical facility. As not all offsets were presented in a similar manner between publications (e.g. $\delta^{13}C\text{-}EAA_{diet}$ - $\delta^{13}C\text{-}EAA_{tissue}$), some offsets were calculated directly from study data.

References

Hare, P. E., M. L. Fogel, T. W. Stafford, A. D. Mitchell, and T. C. Hoering. 1991. “The isotopic composition of carbon and nitrogen in individual amino acids isolated from modern and fossil proteins.” *Journal of Archaeological Science* 79(5): 512–515. https://doi.org/10.1001/archderm.1959.01560170010002.

Johnson, B. J., M. L. Fogel, and G. H. Miller. 1998. “Stable isotopes in modern ostrich eggshell: A calibration for paleoenvironmental applications in semi-arid regions of southern Africa.” *Geochimica et Cosmochimica Acta* 62(14): 2451–2461.

Howland, M. R., L. T. Corr, S. M. M. Young, V. Jones, S. Jim, N. J. Van Der Merwe, A. D. Mitchell, and R. P. Evershed. 2003. “Expression of the dietary isotope signal in the compound-specific δ^{13}C values of pig bone lipids and amino acids.” *International Journal of Osteoarchaeology* 13(1-2): 54–65. https://doi.org/10.1002/oa.658.

Jim, S., V. Jones, S. H. Ambrose, and R. P. Evershed. 2006. “Quantifying dietary macronutrient sources of carbon for bone collagen biosynthesis using natural abundance stable carbon isotope analysis.” *British Journal of Nutrition* 95(6): 1055. https://doi.org/10.1079/BJN20051685.

Newsome, S. D., M. L. Fogel, L. Kelly, and C. M. Del Rio. 2011. “Contributions of direct incorporation from diet and microbial amino acids to protein synthesis in Nile tilapia.” *Functional Ecology* 25(5): 1051–1062. https://doi.org/10.1111/j.1365-2435.2011.01866.x.

Newsome, S. D., N. Wolf, J. Peters, and M. L. Fogel. 2014. “Amino acid δ^{13}C analysis shows flexibility in the routing of dietary protein and lipids to the tissue of an omnivore.” *Integrative and comparative biology* 54(5): 890–902. https://doi.org/10.1093/icb/icu106.

Newsome, S. D., K. L. Feeser, C. J. Bradley, C. Wolf, C. Takacs-Vesbach, and M. L. Fogel. 2020. Isotopic and genetic methods reveal the role of the gut microbiome in mammalian host essential amino acid metabolism. *Proceedings of the Royal Society B* 287(1922): 20192995. https://doi.org/10.1098/rspb.2019.2995.

Whiteman, J. P., S. L. Kim, K. W. Mcmahon, P. L. Koch, and S. D. Newsome. 2018. "Amino acid isotope discrimination factors for a carnivore: physiological insights from leopard sharks and their diet." *Oecologia* 188(4): 977–989. https://doi.org/10.1007/s00442-018-4276-2.

Huneau, J. F., O. L. Mantha, D. Hermier, V. Mathé, G. Galmiche, F. Mariotti, and H. Fouillet. 2019. "Natural isotope abundances of carbon and nitrogen in tissue proteins and amino acids as biomarkers of the decreased carbohydrate oxidation and increased amino acid oxidation induced by caloric restriction under a maintained protein intake in obese rats." *Nutrients* 11(5): 1–16. https://doi.org/10.3390/nu11051087.

Webb, E. C., J. Lewis, A. Shain, E. Kastrisianaki-Guyton, N. V. Honch, A. Stewart, B. Miller, J. Tarlton, and R. P. Evershed. 2017. "The influence of varying proportions of terrestrial and marine dietary protein on the stable carbon-isotope compositions of pig tissues from a controlled feeding experiment." *STAR: Science & Technology of Archaeological Research* 3: 36–52. https://doi.org/10.1080/20548923.2016.1275477.

McMahon, K. W., M. L. Fogel, T. S. Elsdon, and S. R. Thorrold. 2010. "Carbon isotope fractionation of amino acids in fish muscle reflects biosynthesis and isotopic routing from dietary protein." *Journal of Animal Ecology* 79(5): 1132–1141. https://doi.org/10.1111/j.1365-2656.2010.01722.x.

McMahon, K. W., M. J. Polito, S. Abel, M. D. Mccarthy, and S. R. Thorrold. 2015b. "Carbon and nitrogen isotope fractionation of amino acids in an avian marine predator, the gentoo penguin (*Pygoscelis papua*)." *Ecology and Evolution* 5(6): 1278-1290. https://doi.org/10.1002/ece3.1437.

Wang, Y. V, A. H. L. Wan, Å. Krogdahl, M. Johnson, and T. Larsen. 2019a. "^{13}C values of glycolytic amino acids as indicators of carbohydrate utilization in carnivorous fish." *PeerJ* 7: e7701. https://doi.org/10.7717/peerj.7701.

Barreto-Curiel, F., U. Focken, L. R. D'Abramo, J. Mata-Sotres, and M. T. Viana. 2019. "Assessment of amino acid requirements for *Totoaba macdonaldi* at different levels of protein using stable isotopes and a non-digestible protein source as a filler." *Aquaculture* 503: 550–561. https://doi.org/10.1016/j.aquaculture.2019.01.038.

Liu, H. Z., L. Luo, and D. L. Cai. 2018. "Stable carbon isotopic analysis of amino acids in a simplified food chain consisting of the green alga *Chlorella* spp., the calanoid copepod *Calanus sinicus*, and the japanese anchovy (*Engraulis japonicus*)." *Canadian Journal of Zoology* 96: 23–30. https://doi.org/10.1139/cjz-2016-0170.

Takizawa, Y., Y. Takano, B. Choi, P. S. Dharampal, S. A. Steffan, N. O. Ogawa, N. Ohkouchi, and Y. Chikaraishi. 2020. "A new insight into isotopic fractionation associated with decarboxylation in organisms: implications for amino acid isotope approaches in biogeoscience." *Progress in Earth and Planetary Science* 7: 50. https://doi.org/10.1186/s40645-020-00364-w.